Mathematical Modelling of Weld Phenomena, eds H. Cerjak, K. E. Easterling, Institute of Materials, London, 1993, pp. 109–182

Modelling the Evolution of Microstructure in Steel Weld Metal

H. K. D. H. Bhadeshia and *L.–E. Svensson

University of Cambridge
Materials Science and Metallurgy
Pembroke Street, Cambridge CB2 3QZ, U. K.
www.msm.cam.ac.uk/phase–trans

.

*ESAB AB, Gothenburg, Sweden

Abstract. Physical models for the development of microstructure have the potential of revealing new phenomena and properties. They can also help identify the controlling variables. The ability to model weld metal microstructure relies on a deep understanding of the phase transformation theory governing the changes which occur as the weld solidifies and cools to ambient temperature. Considerable progress has been made with the help of thermodynamic and kinetic theory which accounts for the variety of alloying additions, non–equilibrium cooling conditions and other many other variables necessary to fully specify the welded component. These aspects are reviewed with the aim of presenting a reasonably detailed account of the methods involved, and of some important, outstanding difficulties.

It is now well established that extremely small concentrations of certain elements can significantly influence the transformation behaviour of weld metals. Some of these elements are identical to those used in the manufacture of wrought microalloyed steels, whereas others enter the fusion zone as an unavoidable consequence of the welding process. The theory available to cope with such effects is as yet inadequate. Methods for incorporating the influence of trace elements such as oxygen, aluminium, boron, nitrogen, titanium and the rare earth elements into schemes for the prediction of microstructure are discussed. The very high sensitivity of modern microalloyed steels to carbon concentration is also assessed. Some basic ideas on how the approximate relationships between weld microstructure and mechanical properties can be included in computer models are discussed.

INTRODUCTION

Welding procedures have in the past been developed empirically, with some assessment of mechanical properties, and by drawing on accumulated experience. This method has been very successful, as evident in the popularity of the process in virtually all structural engineering applications. It is usually as an afterthought that the macrostructure and microstructure are examined with a view to developing a deeper understanding of the weld, at a more gentle pace when compared against the demands of commercial timetables. This pragmatic approach is hardly surprising in view of the complexity of the microstructural phenomena associated with weld deposits and their heat affected zones. Nevertheless, in an ideal world, the microstructure

should take early prominence in the research, especially when there are clear indications that it limits the achievable properties of the weld.

A rational approach towards the design of welding alloys and procedures, can benefit from the development of quantitative and reliable models capable of relating the large number of variables involved (such as chemical composition, heat input and joint design) to the details of the microstructure (*e.g.,* volume fractions, phase chemistries, particle sizes and distribution). It is for this reason that the subject of microstructure modelling in steel welds has mushroomed to a point where it is now possible to obtain reasonable estimates of the influence of variables such as chemical composition on the deposit characteristics [1].

A number of reviews have recently been compiled on the subject addressed here (Bhadeshia, 1987; 1990). Space limitations have, however, limited these reviews to rather cursory treatments. The opportunity is taken here to present an updated, and more comprehensive assessment of the research on the modelling of weld metal microstructures. Our aim is to make the article useful for learning, especially for those who do not wish to consult and coordinate the information to be found in the large number of research papers on the subject. Although the paper deals specifically with weld metals, most of the phase transformations concepts should also be applicable to wrought alloys.

SOLIDIFICATION

Pure iron is an exciting element: in its solid state, it has three allotropic forms called austenite (γ), ferrite and ϵ–iron. The latter has a hexagonal close–packed crystal structure, is the highest density state of iron, and is only stable at very large pressures. At ambient pressures, ferrite is stable at temperatures just below the equilibrium melting temperature (in which case it is called δ) and at relatively low temperatures as the α form. Austenite is the stable form in the intervening temperature range between the δ and α. As was recognised a long time ago by Zener and others, this complicated (but useful) behaviour is related to electronic and magnetic changes as a function of temperature.

The phase behaviour of pure iron does not change radically with the addition of small amounts of solute, *i.e.,* for low–alloy steels. Lightly alloyed steel weld deposits begin solidification with the epitaxial growth of delta–ferrite (δ) from the hot grain structure of the parent plate at the fusion boundary (Davies & Garland, 1975; Savage *et al.*, 1965; Savage & Aaronson, 1966). The large temperature gradients at the solid/liquid interface ensure that solidification proceeds with a cellular front (Calvo *et al.*, 1963), so that the final δ–grains are columnar in shape, the major axes of the grains lying roughly along the direction of maximum heat flow (Fig. 1a). On further cooling, austenite allotriomorphs nucleate at the δ–ferrite grain boundaries, and their higher rate of growth along the δ–δ boundaries (and presumably, along temperature gradients) leads to the formation of columnar austenite grains whose shape resembles that of the original solidification structure. Since welding involves a moving heat source, the orientation of the temperature isotherms alters with time. Consequently, the major growth direction of the austenite is found to be somewhat different from that of the δ–grains (Dadian, 1986).

[1] Alberry & Jones, 1979, 1982; Ashby & Easterling, 1982; Alberry *et al.*, 1983; Goldak *et al.*, 1984; Ion *et al.*, 1984; Bhadeshia *et al.*, 1985; Mehrotra *et al.*, 1985; Goldak *et al.*, 1986; Akselsen *et al.*, 1986; Buchmayer & Cerjak, 1988.

If the cooling rate is large enough, then the liquid can be induced to solidify as metastable austenite instead, Fig. 1b. This could happen even when δ–ferrite is the thermodynamically favoured phase in low–alloy steels (Fredriksson, 1976; 1983). It has been suggested that this is especially likely when the partition coefficient $k = c_S/c_L$ is closer to unity for austenite than for ferrite. c_S and c_L are the solute solubilities in the solid and liquid phases respectively (Fredriksson, 1976). The austenite growth rate can in those circumstances exceed that of δ–ferrite when the liquid is sufficiently undercooled. Solidification with austenite as the primary phase becomes more feasible as the steel is alloyed with austenite stabilising elements, until the γ eventually becomes the thermodynamically stable phase.

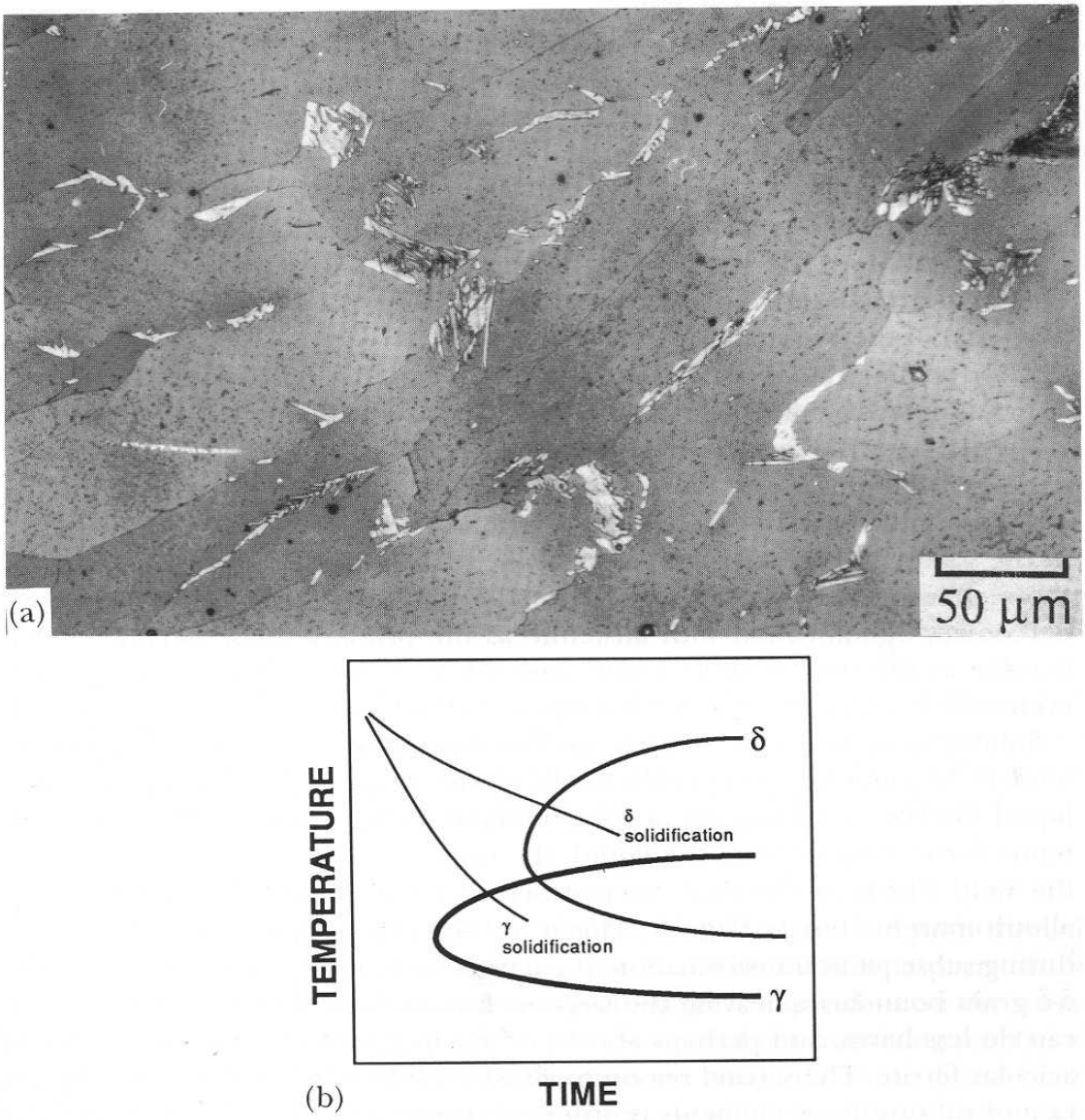

Fig. 1: (a) Columnar δ–ferrite grains, with austenite (light phase) allotriomorphs growing at the δ–grain boundaries. (b) Schematic continuous–cooling–transformation diagram illustrating the solidification mode in low–alloy steels, as a function of the cooling rate. Faster cooling rates can in principle lead to solidification to metastable austenite.

Solidification to austenite can be undesirable for two reasons; large inclusions tend to become trapped preferentially at the cusps in the advancing solid/liquid interface and end up at the columnar grain boundaries (Sugden & Bhadeshia, 1988a). When austenite forms directly from the liquid, the inclusions are located in the part of the weld which in the final microstructure corresponds to relatively brittle allotriomorphic ferrite (Fig. 2). This is not the case with δ solidification since during subsequent transformation, the daughter austenite grains cut across the δ/δ grain boundaries, leaving the large inclusions inside the grains where they can do less harm, and perhaps also be of use in stimulating the nucleation of acicular ferrite. The second reason to avoid γ solidification diffusion rate of substitutional elements is orders of magnitude larger in ferrite than in austenite, so that any segregation is less likely to persist when the liquid transforms to ferrite (Fredriksson, 1976, 1983).

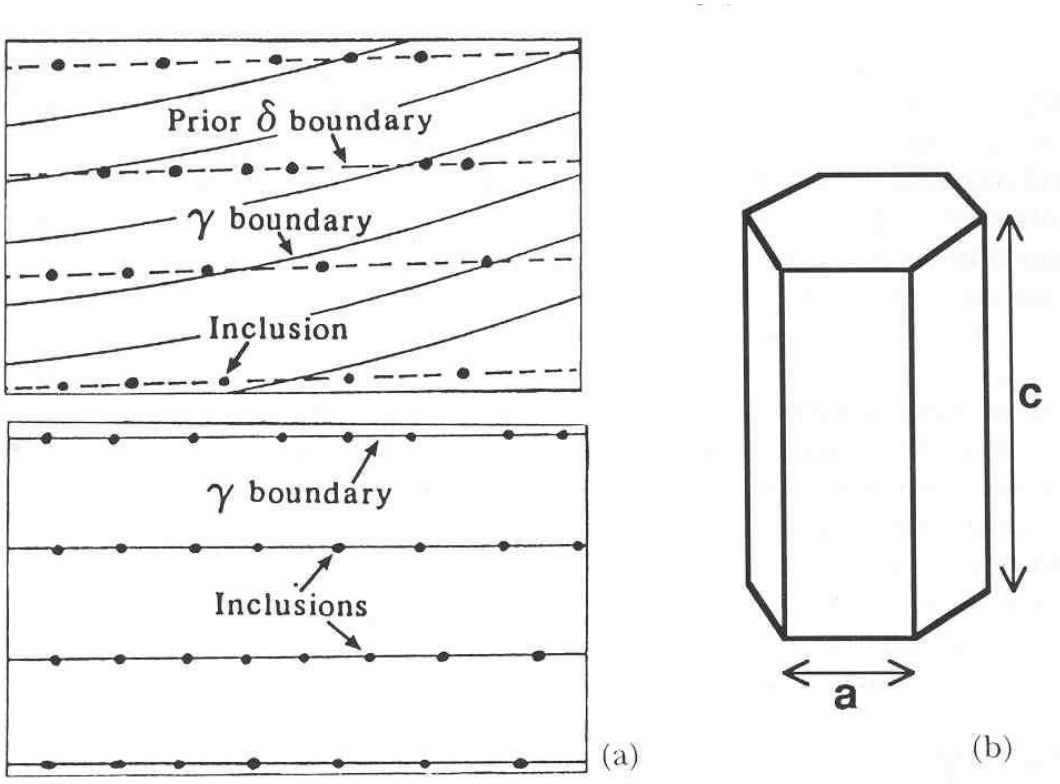

Fig. 2: (a) Location of large inclusions for solidification as δ–ferrite and as austenite. (b) A hexagonal prism model for the columnar austenite grains typical of the microstructure of steel weld metals.

EVOLUTION OF THE AUSTENITE GRAIN STRUCTURE

Stereology Both the shape and size of the austenite grains is of importance in the evolution of the final microstructure. The effect of the austenite grain size is two fold: there is firstly the usual phenomenon in which the number density of austenite grain boundary heterogeneous nucleation sites increases with the total grain boundary area per unit volume of sample. This amounts to the classical and well established hardenability variation with austenite grain size. The second,

and more subtle effect, arises from the grain–shape anisotropy. Although the columnar grains of austenite are very long, the evolution of many aspects of the microstructure within an individual austenite grain is dependent on the mean lineal intercept within that grain. Since the chances of test lines lying parallel to the longest dimension of the columnar grain are small, the mean lineal intercept depends mainly on the width of the grain. As will be seen later, this means that the grain length can often be excluded as a factor in the calculation of microstructure.

The anisotropy of grain structure causes certain complications in representing the grain parameters in any microstructure model. The morphology can be described approximately by a uniform, space–filling array of hexagonal prisms,Fig. 2b (Bhadeshia *et al.*, 1986a). An approximation is that the elongated austenite grains curve as they grow into the weld pool, in response to the changing orientation of the isotherms. The actual grains are also not of uniform size. Each hexagonal prism can be represented by its length c and cross–sectional side length a. With these approximations, the mean lineal intercept $\underline{L}$ and mean areal intercept $\underline{A}$, as measured from several *differently oriented sections* are given by (Underwood, 1970):

$$\underline{L} = 12^{0.5}ac/(3^{0.5}a + 2c) \simeq 3^{0.5}a \tag{1}$$

$$\underline{A} = 27^{0.5}a^2c/(3a + c) \simeq 27^{0.5}a^2 \tag{2}$$

the approximations being valid when $c \gg a$, as is generally the case for weld deposits. By measuring these quantities, the parameters c and a can be determined. This is unfortunately, difficult to do, and is not completely necessary for microstructure modelling if some further reasonable approximations are made (Bhadeshia *et al.*, 1985a; 1986a). The most important parameter is the quantity a if $c \gg a$.The mean lineal intercept measured at random on a longitudinal section (which reveals equiaxed austenite grain sections) of the weld, is given by

$$\underline{L_l} = \pi a \; cos\{30^o\}/2. \tag{3}$$

On the other hand, it has been common practice to define the austenite grain size from the transverse section of a weld, with the size being measured not at random, but by aligning the test lines normal to the larger dimension of the grain sections. If it is assumed that the c–axes of the austenite grains lie in the plane of the transverse section, then the mean lineal intercept $\underline{L_{tn}}$ measure in the *t*ransverse section in a direction *n*ormal to the major axes of the grain sections turns out to be identical to $\underline{L_l}$, and is a relatively easy quantity to measure.

The approximations involved in the determination of a from $\underline{L_{tn}}$ are valid when the weld is deposited in the flat position. For vertical–up welds, the austenite grains adopt an orientation in which they do not present very anisotropic shapes in the transverse section, often tending instead to acquire an equiaxed shape (Evans, 1981; Svensson, 1986). The c–axes of the hexagonal prisms are then inclined at a relatively shallow angle ϕ, estimated to be $\simeq 66^\circ$ for manual metal arc welds by Evans (1981), to the welding direction and hence to the plate surface. Consequently, for vertical–up welds, it can be demonstrated that the mean lineal intercept measured on the transverse section (with the test lines oriented at random with respect to the grain structure) is given by

$$\underline{L_t} = \frac{3\pi\beta a}{2 + 4(0.25 + \beta^2)^{0.5}} \tag{4}$$

where $\beta = 2cos\{30^o\}/cos\{\phi\}$ (Bhadeshia and Svensson, 1989a,b).

From the above discussion, it appears that the current methods of measuring the columnar austenite grain structure via $\underline{L}_{tn}$ provide adequate information for microstructure modelling. It is however anticipated, that as the phase transformation models increase in sophistication, it will be necessary to think more in terms of the total austenite grain surface per unit volume of sample (S_V). This parameter will in general require measurements to be made on several differently orientated planes of section relative to the columnar grains. For a typical weld microstructure, an approximation of S_V based on just $\underline{L}_{tn}$ is likely to lead to an error of about 30% (see for example, Bhadeshia *et al.*, 1986a).

Another assumption usually made in specifying the austenite grain structure of welds is that it is uniform. In fact, because growth begins epitaxially from the fusion surface, the grain structure changes with distance. Those grains whose fast–growth directions are favourably orientated with respect to the heat–flow tend to stifle the others as directional solidification proceeds.

Factors Influencing Size It is not possible as yet to predict the austenite grain size (*e.g.,* $\underline{L}_{tn}$) of steel welds; even the factors controlling this grain size are far from clear. It has naturally been assumed, by extrapolation from grain growth theory, that the nonmetallic inclusions which are common in steel welds control the grain size by Zener pinning the boundaries. This analogy is however, not justified since the austenite grains form by the *transformation* of δ–ferrite, whereas Zener pinning deals with the hindrance of grain boundaries during grain growth. The driving force for grain growth typically amounts to just a few Joules per mole, whereas that for transformation from δ–ferrite to austenite increases indefinitely with undercooling below the equilibrium transformation temperature. Pinning of δ/γ interfaces cannot then be effective. A mechanism in which inclusions pin the columnar austenite grain boundaries is also inconsistent with the *shape* of these grains, since the motion of the δ/γ interfaces along the steepest temperature gradients is clearly not restricted; if pinning were effective, the austenite grains that evolve should be isotropic.

There is some evidence to support the conclusion that the columnar austenite grain size is not influenced by for example, the oxygen content of the weld (Bhadeshia *et al.*, 1985a, 1986a). Experiments to the contrary (Harrison & Farrar, 1981) really refer to the *reheated* weld metal, where the grain size is related to a coarsening reaction driven by γ/γ surface energy. On the other hand, there are data which indicate that low weld oxygen concentrations correlate with large columnar austenite grain sizes (Fleck *et al.*, 1986). There is a possible explanation for these contradictory results. If it is assumed that in some cases, *e.g.,* when the initial austenite grain size is extremely fine, the columnar austenite grain structure coarsens during cooling after solidification. North *et al.* (1990) have presented evidence to reveal such coarsening. Further work is needed urgently to clarify these issues.

The columnar austenite grain size must to some extent correlate with the grain size in the parent plate at the fusion boundary, since solidification occurs by the epitaxial growth of those grains (Davies & Garland, 1975). However, the relationship cannot be simple, since during solidification, those grains with their $< 1\,0\,0 >$ directions most parallel to the direction of steepest temperature gradient grow rapidly, stifling the grains which are not suitably oriented. Consequently, the crystallographic texture of the parent plate, and the plane of that plate on which the weld is deposited, must influence the final austenite grain structure. Clear differences

in the austenite grain structure were found between three welds deposited on mutually perpendicular faces of the same sample, in a recent experiment designed to illustrate the influence of crystallographic texture on the grain size (Babu *et al.*, 1991). More systematic work is now called for. A corollary is that particles in the parent plate (*e.g.,* carbo–nitrides) may limit the coarsening of the plate grains at the fusion boundary, and therefore lead ultimately to a smaller grain size in the fusion zone.

Regression equations are currently used in making crude estimates of the columnar austenite grain size:

$$\overline{\mathrm{L}}_{\mathrm{tn}}(\mu\mathrm{m}) = 64.5 - 445.8(\mathrm{wt.\%C}) + 139(\mathrm{wt.\%Si}) - 7.6(\mathrm{wt.\%Mn}) \\ +16(\text{heat input, kJ mm}^{-1}) \qquad (5)$$

If these are to be believed, then the alloy chemistry itself has a significant effect on grain structure, perhaps by influencing the thermodynamics and kinetics of the $\delta \rightarrow \gamma$ transformation (Fig. 2b).

THE AS–DEPOSITED MICROSTRUCTURE

A *calculation* of microstructure requires a detailed description of each phase. For example, the growth rate of a particle cannot be estimated without a knowledge of the compositions of the parent and product phases at the interface. The simplest assumption would be to assume diffusion–controlled growth, in which case, the compositions are, for a binary alloy at least, given by a tie–line of the equilibrium phase diagram. The formation of the particle may be associated with the development of elastic strains, especially if the mechanism of transformation is displacive. These strains lead to a modification of the phase diagram, and might alter the particle–shape in an effort to minimise the strain energy.

Work on weld metal microstructures has evolved along different lines when compared against the mainstream of steel research. In an effort to develop microstructure–property relationships, there has been an exaggerated emphasis on purely microstructural observations. There are some difficulties with the notation, which is derived largely from morphological observations rather than from the details of the mechanism of transformation, which are also essential for quantitative work.

The microstructure obtained as the weld cools from the liquid phase to ambient temperature is called the *as–deposited* or *primary* microstructure. It consists of allotriomorphic ferrite α, Widmanstätten ferrite α_w, acicular ferrite α_a, and the so-called microphases, which might include small amounts of martensite, retained austenite or degenerate pearlite (Fig. 3). Bainite is also found in some weld deposits, particularly of the type used in the power generation industry (Lundin *et al.*, 1986). Allotriomorphic ferrite is sometimes called "polygonal" ferrite or "proeutectoid" ferrite, but polygonal simply means many sided (like all ferrite morphologies) and Widmanstätten ferrite can also be proeutectoid. Widmanstätten ferrite is sometimes included under the general description "ferrite with aligned MAC", the abbreviation referring to martensite, austenite and carbide. However, bainite plates can also form in a similar shape, although their thermodynamic and kinetic characteristics are quite different. From a phase

transformations point of view, the Dubé classification of ferrite grains remains the most useful to this day (Dubé *et al.*, 1958; Heckel & Paxton, 1961).

The above description is incomplete for multirun welds, in which some of the regions of original primary microstructure are reheated to temperatures high enough to cause reverse transformation into austenite, which during the cooling part of the thermal cycle retransforms into a variety of somewhat different products. Other regions may simply be tempered by the deposition of subsequent runs. The microstructure of the reheated regions is called the *reheated* or *secondary* microstructure.

A detailed classification of microstructure, based on the kind of knowledge needed in its calculation, is presented in Appendix 1.

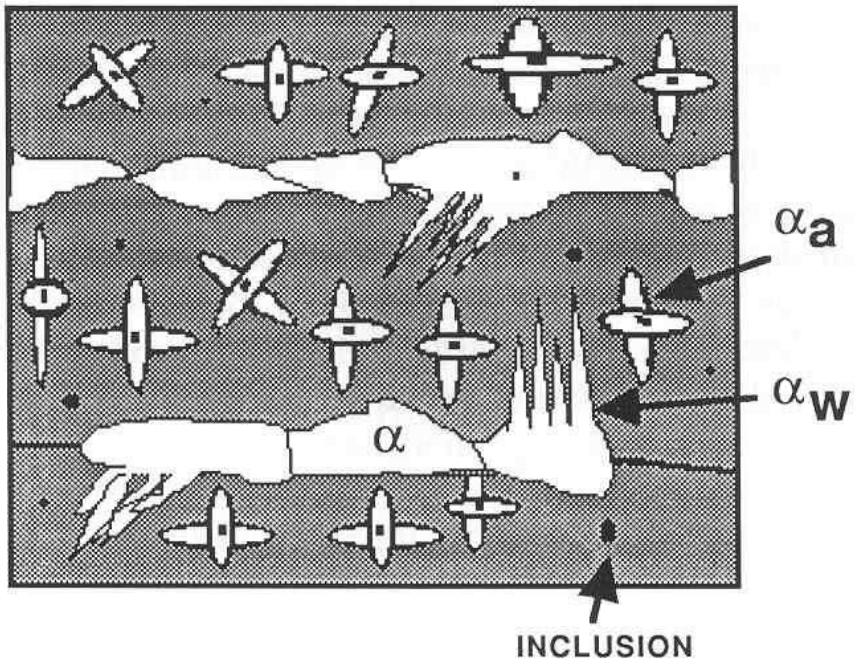

Fig. 3: An illustration of the essential constituents of the primary microstructure of a steel weld deposit. The diagram is inaccurate in one respect, that inclusions cannot be expected to be visible in all of the acicular ferrite plates on a planar section of the microstructure. This is because the inclusion size is much smaller than that of an acicular ferrite plate, so that the chances of sectioning an inclusion and plate together are very small indeed.

ALLOTRIOMORPHIC FERRITE

Kinetics Allotriomorphic ferrite (α) is the first phase to form on cooling below the Ae_3 temperature and nucleates heterogeneously at the boundaries of the columnar austenite grains. The fundamental aspects of allotriomorphic ferrite have been reviewed in detail (Bhadeshia, 1985a), where many of the original references can also be found. In low alloy steel welds, the boundaries rapidly become decorated with virtually continuous layers of ferrite, so that subsequent transformation simply involves the reconstructive thickening of these layers, a process which

can be modelled in terms of the normal migration of planar α/γ interfaces. The assumption involved implies that the initial formation of a thin, continuous layer of allotriomorphic ferrite takes a much smaller time when compared with its subsequent thickening to the final size. The assumption is supported, at least for low–alloy steel welds, by the fact that the volume fraction of allotriomorphic ferrite correlates strongly with its *growth* kinetics Fig. 4. Dallum and Olson (1989) have demonstrated that the *thickness* of the allotriomorphic ferrite layer is insensitive to the initial austenite grain size, at least for the low–alloy steel and heat–treatment conditions they utilised. A result like this can only be justified if it is assumed that nucleation does not have a great influence on the overall transformation kinetics.

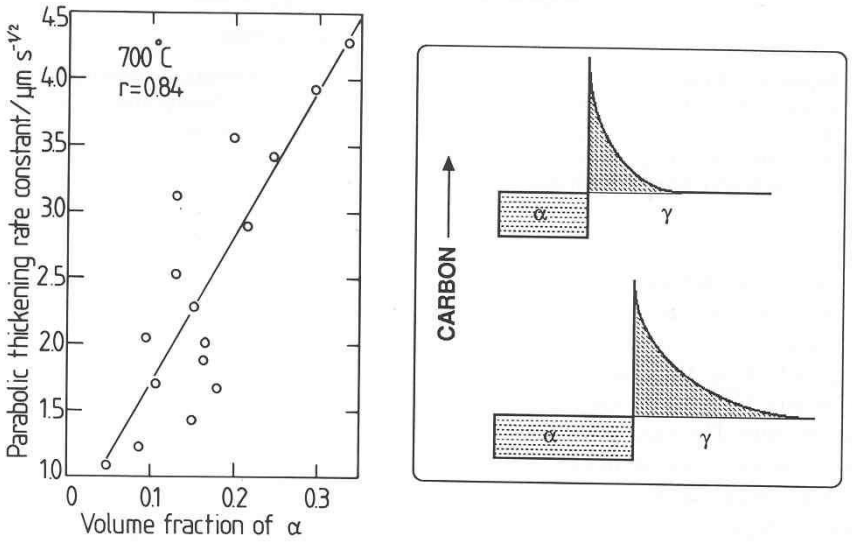

Fig. 4: (a) Diagram showing the correlation between the calculated parabolic thickening rate constant (a variable related to the growth rate) and the volume fraction of allotriomorphic ferrite obtained in a series of manual metal arc weld deposits (Bhadeshia *et al.*, 1985b), fabricated using similar welding parameters but with different final weld chemistries. Each point on the diagram therefore represents a different alloy composition. (b) An illustration of how the diffusion distance increases with ferrite layer thickness, this being the root cause of the parabolic thickening kinetics. The shaded regions represent carbon depletion and enrichment (when compared against the average carbon concentration in the steel) in the ferrite and austenite respectively. The extent of depletion in the ferrite must exactly equal the enrichment in the austenite, so that it is inevitable that the diffusion field increases as the ferrite grows, and the reaction slows down (parabolically).

Given these facts, and assuming that the growth of allotriomorphic ferrite occurs under paraequilibrium conditions, then the half–thickness q of the layer during isothermal growth is given by:

$$q = \alpha_1 t^{1/2} \tag{6}$$

where α_1 is the one–dimensional parabolic thickening rate constant, and t is the time defined to begin from the initiation of growth. The parabolic relation implies that the growth rate slows down as the ferrite grows. It originates from the fact that the total amount of solute partitioned

during growth increases with time. Consequently, the diffusion distance increases with time, thereby reducing the growth rate (Fig. 4b).

Paraequilibrium is a constrained equilibrium in which the ratio of iron to substitutional solute concentration remains constant everywhere, but subject to that constraint, the carbon achieves equality of chemical potential (Hultgren, 1951; Hillert, 1952; Rudberg, 1952). It seems a reasonable assumption given that welds generally cool at a rapid rate. The parabolic rate constant is obtained by solving the equation:

$$\frac{x^{\gamma\alpha} - \overline{x}}{x^{\gamma\alpha} - x^{\alpha\gamma}} = \sqrt{\frac{\pi}{4\underline{D}}}\,\alpha_1 \exp\left\{\frac{\alpha_1^2}{4\underline{D}}\right\}\mathrm{erfc}\left\{\frac{\alpha_1}{2\underline{D}^{1/2}}\right\} \tag{7}$$

where $x^{\gamma\alpha}$ and $x^{\alpha\gamma}$ are the paraequilibrium carbon concentrations in austenite and ferrite respectively at the interface, $\overline{x}$ is the average carbon concentration in the alloy and $\underline{D}$ is a weighted average diffusivity (Trivedi & Pound, 1969; Bhadeshia, 1981b) of carbon in austenite, given by:

$$\underline{D} = \int_{x^{\gamma\alpha}}^{\overline{x}} \frac{D\{x\}\,dx}{\overline{x} - x^{\gamma\alpha}} \tag{8}$$

where D is the diffusivity of carbon in austenite at a particular concentration of carbon (Fig. 5a). This equation is strictly valid only for steady–state growth, but Coates (1973) has suggested that it should be a reasonable approximation for parabolic growth as well, although he did not justify this. The approximation has recently been verified (Bhadeshia *et al.*, 1986c) for steels of the type used for welding, by comparing calculations of the parabolic rate constant done using the $\underline{D}$ approximation against a more rigorous numerical analysis of the diffusion equation for one–dimensional diffusion–controlled growth (Atkinson, 1967). A comparison of the rate constants shows that the two methods lead essentially to the same results (Fig. 5b).

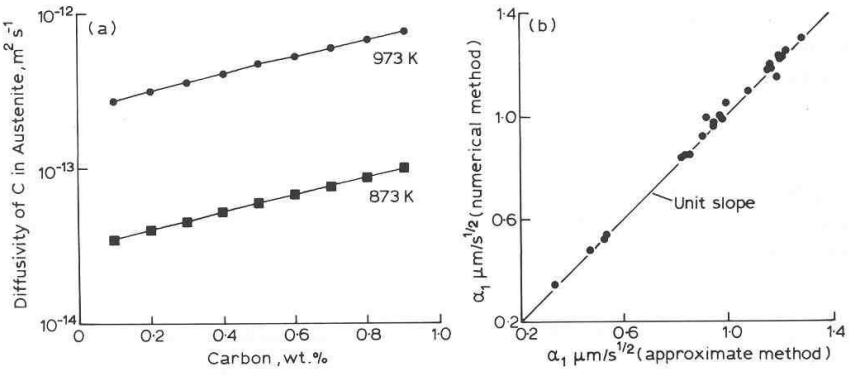

Fig. 5: (a) An illustration of the concentration dependence of the diffusivity of carbon in austenite. (b) Comparison of the parabolic rate constants calculated using a weighted average carbon diffusivity (approximate method) and a numerical method which properly accounts for the concentration dependence of diffusivity during non–steady–state growth (Bhadeshia *et al.*, 1986c)

The calculation of the parabolic rate constants also requires a knowledge of the chemical compositions of the phases at the transformation interfaces, and for diffusion–controlled growth,

these compositions can be deduced approximately using the phase diagram which can nowadays easily be computed, even for multicomponent steels (*e.g.,* Bhadeshia & Edmonds, 1980). Some typical kinetic data for allotriomorphic ferrite are presented in Fig. 6. Note that none of these calculations take account of *soft–impingement* effects, *i.e.,* the retardation in growth kinetics due to the overlap of concentration fields of particles growing from different positions, or because the concentration in the austenite at its furthest point from the ferrite becomes enriched. It is known (Vandermeer *et al.*, 1989) that soft–impingement has a large influence on the growth kinetics, and further work is needed to incorporate it into the current weld microstructure models. The effects should become more prominent as the volume fraction of ferrite increases, or as the austenite grain size decreases.

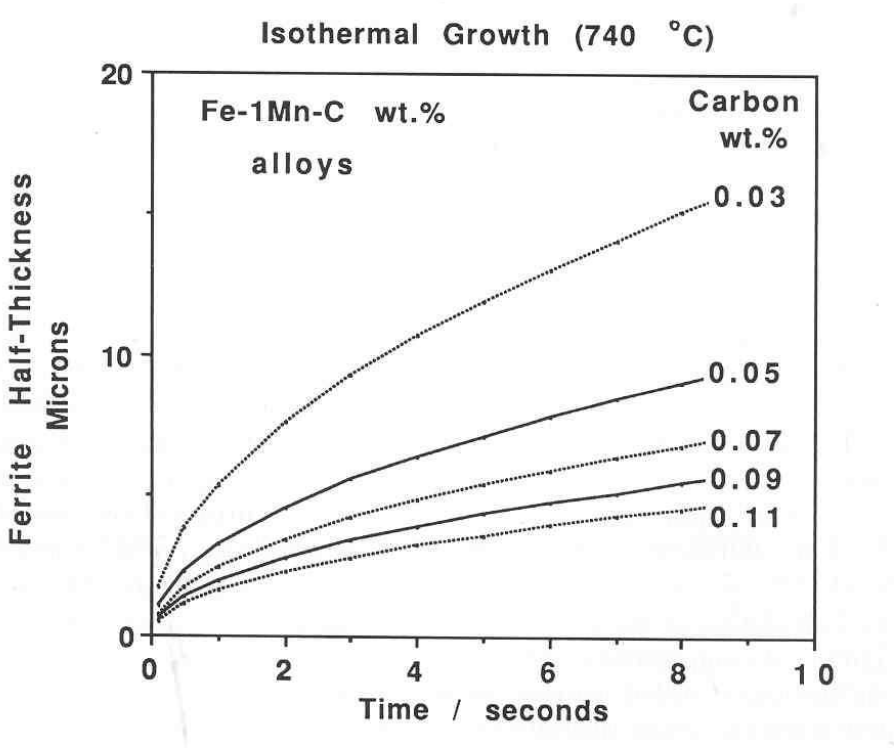

Fig. 6: Diagram illustrating how the calculated thickness of an allotriomorphic ferrite layer increases during isothermal transformation, in the absence of soft–impingement effects. Each curve represents a Fe–1Mn–C wt.% steel with the carbon concentration as indicated on the diagram.

That the formation of allotriomorphic ferrite in most welds is dependent largely on the rate of growth is apparent from the good correlation between α_1 and the volume fraction of α obtained (Bhadeshia *et al.*, 1985b). A better understanding of the role of alloy elements requires a method for estimating the volume fraction of allotriomorphic ferrite. This can be done by integrating the thickening of the layers over a temperature range T_h to T_l. Allotriomorphic ferrite growth begins at T_h, a temperature which can be estimated using a calculated TTT curve (Bhadeshia, 1982; 1988a), and Scheil's rule (Christian, 1975) to allow for the fact that the process involves continuous cooling transformation. It "finishes" at T_l, the temperature where the reconstructive

and displacive C–curves of the TTT diagram intersect (*i.e.,* where displacive transformations have a kinetic advantage). Thus

$$q = \int_{t=0}^{t_1} 0.5\alpha_1 t^{-0.5} + \frac{\partial \alpha_1}{\partial t} t^{0.5} \; dt \tag{9}$$

where $t = 0$ at T_h and $t = t_1$ at T_l. The second term on the right hand side of this expression has been neglected in previous analyses – its significance has yet to be determined.

Notice that the expression also relies on the unverified assumption that the compositions of the phases at the interface instantaneously adjust themselves to the phase diagram as the temperature is lowered. The volume fraction of ferrite is then given by

$$v_\alpha = \frac{2q \; \tan\{30°\}[2a - 2q \; \tan\{30°\}]}{a^2} \tag{10}$$

so that the dependence on austenite grain size becomes obvious. This equation is found to represent the volume fraction of allotriomorphic ferrite extremely well, but only after an empirical correction by a factor of about 2 – the fraction is always underestimated. There are clearly a lot of difficulties with the way in which the allotriomorphic ferrite content is at present calculated, and more work is needed to resolve the difficulties already mentioned before commenting further. A part of the problem might be related to the assumption that a uniform layer of α is instantaneously established at T_h; a more elaborate theory capable of dealing with discontinuous layers of ferrite is available, which for isothermal transformation gives:

$$-\ln\{1 - i\} = 2S_V \Omega^{-1} \alpha_1 t^{0.5} f\{\eta\alpha_1, \; I_B, \; t\} \tag{11}$$

where i is the volume fraction of ferrite divided by its equilibrium volume fraction at the transformation temperature concerned (Bhadeshia *et al.*, 1987a). Ω is a normalised supersaturation given by the ratio $(x^{\gamma\alpha} - \overline{x})/(x^{\gamma\alpha} - x^{\alpha\gamma})$, S_V is the total quantity of austenite grain surface per unit volume, η it the aspect ratio of ferrite allotriomorphs formed at the austenite grain surfaces and f is a function described by Bhadeshia *et al.* (1987a). Although this expression should be a better representation of allotriomorphic ferrite kinetics, the grain boundary nucleation rate I_B needed to evaluated the function is not yet available with sufficient accuracy. More work is necessary in this area of research and generally on the subject of nucleation kinetics.

Fleck *et al.* (1986) have adopted a different approach based on an Avrami type equation:

$$v_\alpha = 1 - \exp\{-2S_V G t\} \tag{12}$$

where S_V is the austenite grain boundary surface per unit volume and G is the growth rate of the ferrite. The form of the equation is not correct for α since it implies that the v_α can be unity, but their conclusion that

$$\ln\{1 - v_\alpha\} \propto 1/d, \tag{13}$$

where d is the austenite grain size, becomes identical to that of Bhadeshia *et al.* (1987a) if d is multiplied by a factor which is the equilibrium volume fraction of α, to take account of the fact that solute partitions during the growth of ferrite.

Effect of Solidification–Induced Segregation There are two major causes of chemical segregation in welds, the relatively large cooling rates involved and variations in process parameters during welding. The latter cannot in general be accurately predicted, but the extent of segregation due to nonequilibrium solidification can be estimated from the partition coefficient k_i which is the ratio of the concentration of element i in the δ–ferrite to that in the liquid phase. The coefficient can be calculated for the liquidus temperature, and the minimum concentration to be found in a heterogeneous solid weld is then taken to be $k_i\overline{x}$. This is the composition of the solute–depleted region of the weld, since it is assumed that diffusion during cooling to ambient temperatures does not lead to significant homogenisation (Gretoft *et al.*, 1986). Carbon, which diffuses much more rapidly than substitutional solutes, is assumed to be homogeneously distributed in the austenite prior to transformation.

The method for incorporating the effect of substitutional solute segregation into weld microstructure calculations, is via the influence on the temperature at which the allotriomorphic ferrite begins to grow (T_h). In general, it is the solute depleted regions which should transform first to ferrite. Thus, the TTT diagram used for estimating T_h should be calculated not from the average composition of the steel, but using the composition of the solute depleted regions.

This procedure seems to work well, presumably because the major effect of substitutional solute segregation during the welding of low–alloy steels is on enhancing the nucleation of allotriomorphic ferrite, and hence on the temperature range $T_h \rightarrow T_l$ (Gretoft *et al.*, 1986; Strangwood & Bhadeshia, 1987b). The effect of chemical segregation becomes more pronounced as the level of alloying additions rises.

Allotriomorphic Ferrite – Mechanical Properties It has in the past been accepted that allotriomorphic ferrite is bad for weld metal toughness because it offers little resistance to cleavage crack propagation. However, it is a reconstructive transformation involving the diffusion of all atoms, so that grains of α can grow freely across γ grain boundaries, into all of the adjacent grains. Displacive transformations (Widmanstätten ferrite, bainite, acicular ferrite, martensite) involve the coordinated movement of atoms, and such movements cannot be sustained across grain boundaries. Hence, a vestige of the γ grain boundary remains when the transformation products are all displacive, and in the presence of impurities, can lead to intergranular failure with respect to the prior austenite grain boundaries. With allotriomorphic ferrite, the original γ boundaries are entirely disrupted, removing the site for the segregation of impurities. This conclusion is supported by observations reported in the literature. Abson (1988) examined a large set of weld deposits. Of these, a particular weld which had no allotriomorphic ferrite content and a particularly high concentration of phosphorus exhibited brittle failure at the prior columnar austenite grain boundaries in the manner illustrated in Fig. 7.

It is well known that the post–weld heat treatment (600 °C) of titanium and boron containing welds leads to embrittlement with failure at the columnar austenite grain boundaries (Still and Rogerson, 1978, 1980; Kluken and Grong, 1992). Phosphorus has been shown to segregate to these prior austenite boundaries and cause a deterioration in the toughness. The titanium and boron make the welds sensitive to post–weld heat treatment because they prevent allotriomorphic ferrite, and hence expose the remains of the austenite grain boundaries to impurity segregation.

Kayali *et al.* (1984) and Lazor and Kerr (1980) have reported such failure, again in welds containing a microstructure which consisted only of acicular ferrite. Sneider and Kerr (1984) have noted that such fracture appears to be encouraged by excessive alloying. Boron is important in this respect because it can lead to an elimination of austenite grain boundary nucleated phases; recent observations on intergranular fracture at the prior austenite boundaries (Kluken *et al.*, 1994) can be interpreted in this way. This is consistent with our hypothesis, since large austenite–stabilising solute concentrations tend to reduce the allotriomorphic ferrite content.

It must be emphasised that it is not the reduction in allotriomorphic ferrite content *per se* which worsens the properties; the important factor is the degree of coverage (and hence disruption) of the prior austenite grain surfaces. In addition, the impurity content has to be high enough relative to the amount of prior austenite grain surface, to cause embrittlement. Classical temper embrittlement theory suggests that additions of elements like molybdenum should mitigate the effects of impurity controlled embrittlement, although such ideas need to be tested for the as–deposited microstructure of steel welds. To summarise, it is likely that α should not entirely be designed out of weld microstructures, especially if the weld metal is likely to contain a significant impurity concentration.

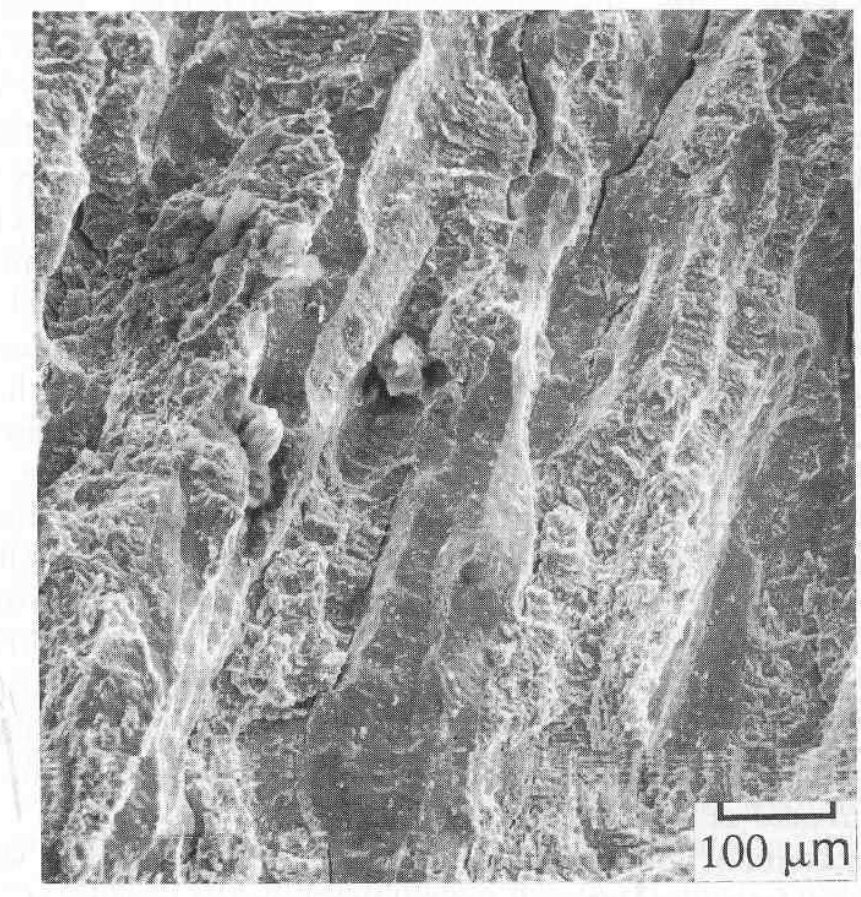

Fig. 7: Fracture along the prior columnar austenite grain boundaries in a weld with zero allotriomorphic ferrite content.

Recent work reinforces the conclusion that some allotriomorphic ferrite should be retained in the weld microstructure in order to improve its high temperature mechanical properties. Ichikawa *et al.* (1994b) examined the mechanical properties of large heat input submerged arc welds designed for fire–resistant steels. They demonstrated that the high temperature ductility and the creep rupture life of the welds deteriorated sharply in the absence of allotriomorphic ferrite (Fig. 8). The associated intergranular fracture, with respect to the prior austenite grain boundaries, became intragranular when some allotriomorphic ferrite was introduced into the microstructure.

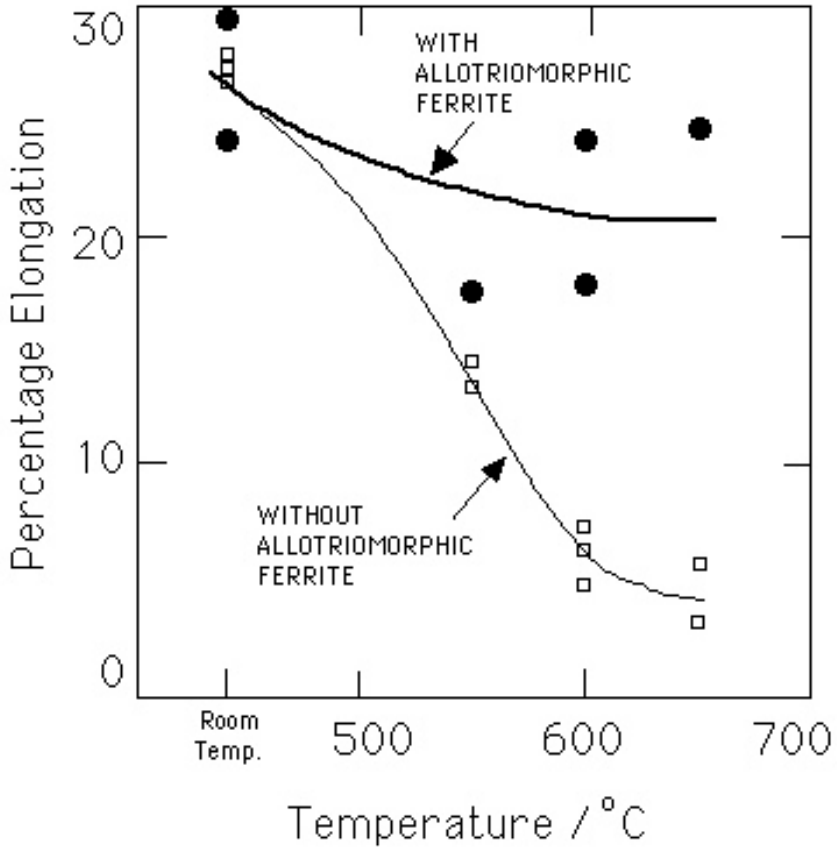

Fig. 8: The elevated temperature tensile elongation of submerged arc steel welds, in which the small amount of allotriomorphic ferrite was controlled using boron additions (Ichikawa *et al.*, 1994b).

Steel can be infiltrated at the prior austenite grain boundaries by liquid zinc. In a study of the heat–affected zone of steel welds, Iezawa *et al.* (1993) demonstrated that their susceptibility to liquid zinc embrittlement depended on the allotriomorphic ferrite content, which in turn varied with the boron concentration (Fig. 8). The absence of allotriomorphs at the prior austenite grain boundaries clearly made them more sensitive to zinc infiltration, proving again that these boundaries have a high–energy structure which is susceptible to wetting and impurity segregation.

The rutile based electrode systems currently under development generally lead to phosphorus concentrations of about 0.010–0.015 wt.%, and the popular use of titanium and boron gives a weld deposit without allotriomorphic ferrite. The welds have therefore been found to be

extremely susceptible to stress relief embrittlement with fracture along the prior austenite grain boundaries. Possible solutions include:

(a) Reduction in the phosphorus concentration, although this might entail cost penalties.

(b) Introduction of between 0.2–0.5 wt.% of molybdenum. Molybednum is an element frequently added to wrought steels in order to prevent impurity induced embrittlement (*e.g.,* Briant and Banerji, 1978). Molybdenum has been shown to retard temper embrittlement (Schulz and McMahon, 1972; McMahon *et al.*, 1977; Yu and McMahon, 1980) and retardation is greatly increased when vanadium is also added (McMahon and Zhe, 1983). It was believed at one time that molybdenum scavanges phosphorus, but experiments have failed to confirm this mechanism (Krauss and McMahon, 1992). Elements such as molybdenum and vanadium must be used cautiously in weld deposits, because their addition leads to a considerable increase in strength, which can in turn trigger a reduction in toughness. Their use must therefore be compensated by appropriate adjustments in the concentrations of other elements.

(c) Manganese has long been known to make steels more sensitive to impurity induced temper embrittlement (Steven and Balajiva, 1959), even in pure iron (Yu–Qing and McMahon, 1986). Nickel has a similar effect when silicon is also present. This suggests that both manganese and nickel concentrations should be kept to a minimum.

(d) Carbon is known to be beneficial for intergranular cohesion (Briant and Banerji, 1978; McMahon, 1987). Many cored wire electrodes have been developed to give very low carbon concentrations (0.03 wt.%) in the weld deposits. From work in the general area of welding, a carbon concentration in the range 0.10–0.12 wt.% may in fact be acceptable.

(e) The composition of the weld should be adjusted to permit the formation of a thin layer of allotriomorphic ferrite.

Nature of Prior Austenite Grain Boundaries It was argued above that with displacive transformations (which cannot cross austenite grain boundaries), a "vestige" of the austenite grain boundary structure is left in the microstructure. The following evidence suggests that these prior austenite grain boundaries are high–energy boundaries:

(a) The prior austenite grain boundaries are sites for the reversible segregation of misfitting impurity atoms such as phophorus (Briant and Banerji, 1978). The extent of segregation is larger than that at martensite lath boundaries.

(b) Carbides nucleate preferentially at the prior austenite grain boundaries during the tempering of martensite or bainite. This applies to both cementite (Hyam and Nutting, 1956) and to those alloy carbides such as $M_{23}C_6$ which find it difficult to nucleate (Baker and Nutting, 1959). A consequence of this is that the carbides located at the prior boundaries are coarser. Some carbides such as cementite are brittle and hence assist the propagation of fracture at the prior austenite grain boundaries.

(c) Prior austenite grain boundaries can be revealed by etching, often with great clarity, in microstructures where they have not been destroyed by transformation products which

grow across austenite grains (Vander Vroot, 1984). In a successfully etched sample, it is the prior boundaries which are etched, but grain contrast is obviously not obtained because the original austenite is no longer there.

Why then is the misfit present at austenite grain boundaries inherited in fully transformed specimens when the mechanism of transformation is displacive? The answer to this lies in the fact that the displacive transformation of austenite involves a minimal movement of atoms. The Bain Strain, which is the pure component of the deformation which converts the austenite lattice into that of ferrite, does not rotate any plane or direction by more than about 11°. Furthermore, the change in volume during transformation is a few percent. The excellent registry between the parent and product lattices is illustrated by the electron diffraction pattern of Fig. 9.

Consequently, the detailed arrangement of atoms at an austenite grain boundary is unlikely to be influenced greatly by displacive phase transformation.

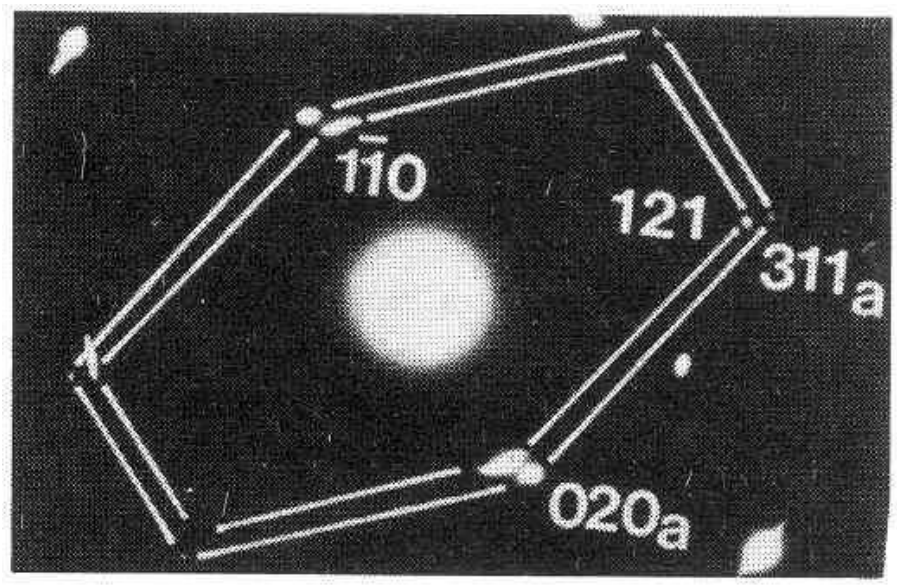

Fig. 9: Electron diffraction pattern from martensite and austenite in steel (Bhadeshia, 1987). The austenite reflections are labelled "a".

WIDMANSTÄTTEN FERRITE

The paraequilibrium formation of α_w can occur at relatively small driving forces (Bhadeshia, 1981a, 1985b, 1988b), and the strain energy due to its displacive transformation mechanism is mitigated by the cooperative, back–to–back growth of self–accommodating crystallographic variants (leading to a small strain energy term of $\sim 50\,\mathrm{J\,mol^{-1}}$). The α_w seen using a light microscope can be visualised as consisting of two mutually accommodating plates with slightly different habit plane indices, giving the characteristic thin wedge morphology of α_w. The shape of the plate can be approximated by a thin wedge of length z in the major growth direction, growth in the other two dimensions soon becoming stifled by impingement with the diffusion fields of nearby plates in a packet. The details of this model, particularly the fact that it

predicts that the volume fraction of Widmanstätten ferrite should be proportional to the plate length, need to be verified further. At first sight, such a dependence could only arise if the Widmanstätten ferrite developed into a lath rather than a plate shape.

The lengthening rate G of Widmanstätten ferrite can be estimated using the Trivedi (1970) theory for the diffusion–controlled growth of parabolic cylinders (Bhadeshia, 1985b). Because of its shape, and unlike allotriomorphic ferrite, Widmanstätten ferrite grows at a constant rate as long as soft–impingement (overlap of diffusion fields) does not occur. The calculated growth rates are found to be so large for typical weld deposits, that the formation of Widmanstätten ferrite is usually complete within a fraction of a second. Hence, for all practical purposes, the transformation can be treated as being isothermal (Fig. 10a).

Transformation to Widmanstätten ferrite is taken to begin when that of allotriomorphic ferrite ceases at T_l; the volume fraction is given by

$$v_W = C_4 G(2a - 4q\ \tan\{30^\circ\})t_2^2/(2a)^2 \tag{14}$$

where C_4 is a constant independent of alloy composition and t_2 is the time *available* for the formation of Widmanstätten ferrite. Note that the v_W depends not only on the austenite grain size but also on the thickness of the layer of allotriomorphic ferrite which formed earlier. In fact the situation is more complex, as indicated by the fact that v_W hardly correlates with G (Fig. 10b). Hard impingement with intragranularly nucleated acicular ferrite has to be taken into account (Fig. 11); this depends on the time t_c, which is the time between the cessation of allotriomorphic ferrite and the onset of acicular ferrite. If the time interval $t_3 = (2a\ \sin\{60^o\} - 2q)/G$ required for an α_w plate to grow unhindered across the austenite grain is less than t_c, α_w plates can grow unhindered across the austenite grain (*i.e.,* $t_2 = t_3$), but if not, then $t_2 = t_c$. When an algorithm is included to account for all this, the calculated volume fraction v_W is found to be in good agreement with experiments (Bhadeshia *et al.*, 1985a, 1986b, 1987b; Gretoft *et al.*, 1986; Bhadeshia & Svensson, 1989a,b).

THE NATURE OF ACICULAR FERRITE

"Acicular ferrite" α_a is a phase most commonly observed as austenite transforms during the cooling of low–alloy steel weld deposits (see for example, the reviews by Grong and Matlock, 1986; Abson and Pargeter, 1986; and Bhadeshia, 1988b). It is of considerable commercial importance because it provides a relatively tough and strong microstructure. It forms in a temperature range where reconstructive transformations become relatively sluggish and give way to displacive reactions such as Widmanstätten ferrite, bainite and martensite.

The transformation has not been studied from a fundamental point of view in any great depth, and so there are as yet no models which allow the volume fraction v_a of acicular ferrite to be calculated from first principles. For this reason, the mechanism of transformation is reviewed below in some detail. Note that in spite of the dirth of basic work in this area, for many welds it is nevertheless possible to estimate v_a via the equation

$$v_a = 1 - v_\alpha - v_W - v_m \tag{15}$$

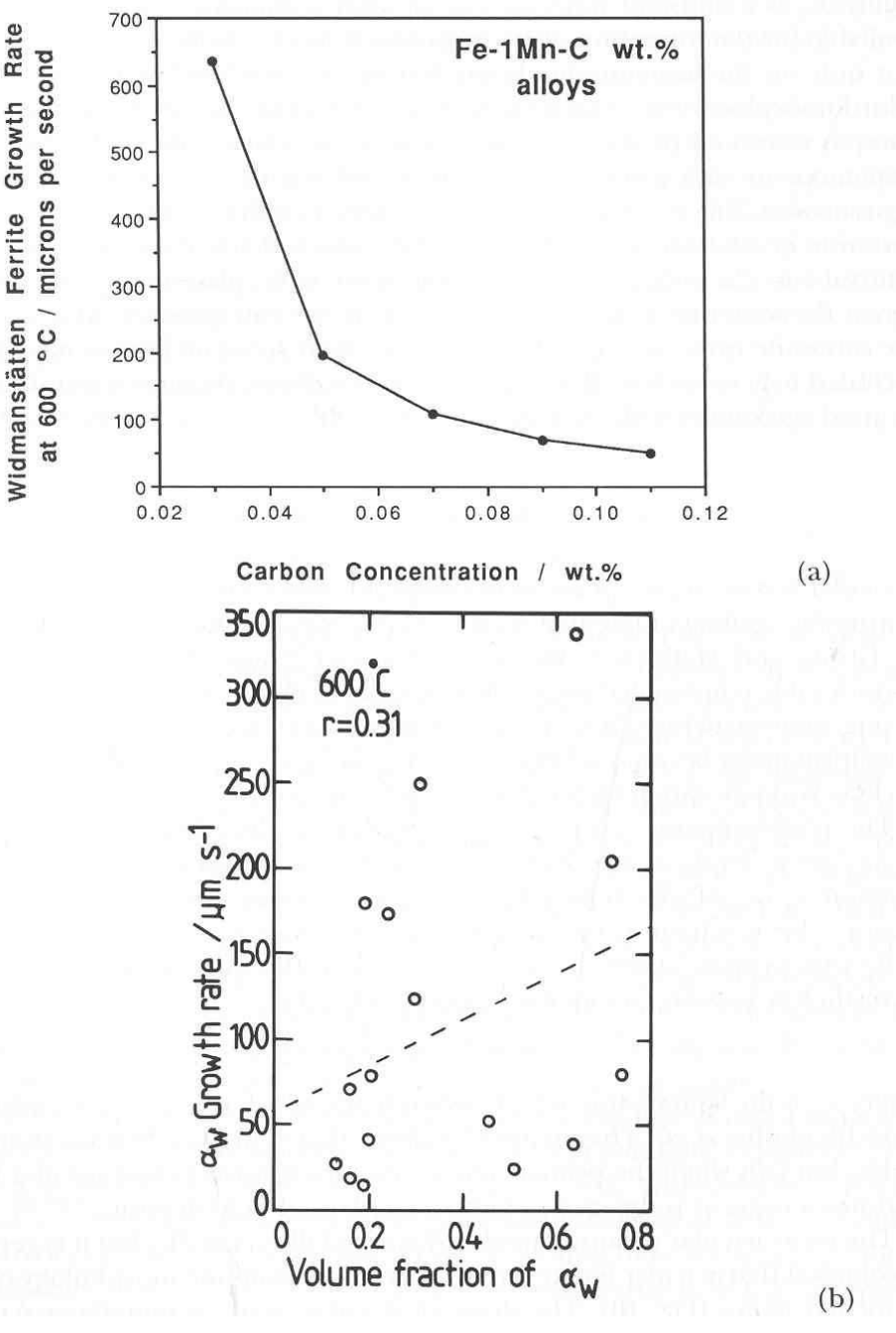

Fig. 10: (a) The calculated isothermal growth rates of Widmanstätten ferrite in a series of Fe–1Mn–C wt.% alloys as a function of carbon concentration. Notice that the growth rates are so large, that the plates could grow right across typical austenite grains within a fraction of a second. (b) Calculated growth rates of Widmanstätten ferrite for a series of low–alloy steel weld deposits, illustrating the poor correlation against the volume fraction of Widmanstätten ferrite.

where v_m is the volume fraction of microphases, which in turn can be estimated as in (Bhadeshia *et al.*, 1985a). The method has been shown to work well for numerous welds, but fails when the primary microstructure consists of just acicular ferrite and martensite, as is the case in

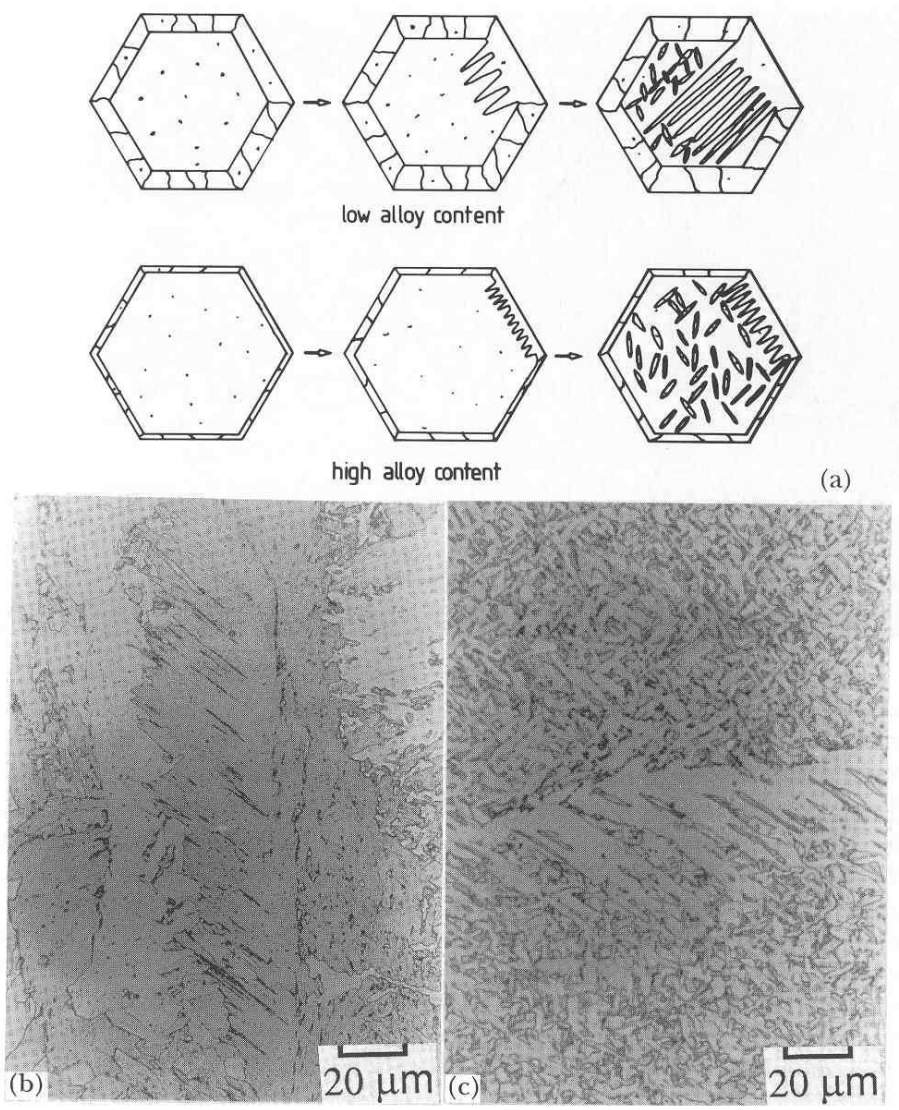

Fig. 11: (a) Schematic diagrams illustrating the development of microstructure in weld deposits. The hexagons represent cross–sections of columnar austenite grains whose boundaries first become decorated with uniform, polycrystalline layers of allotriomorphic ferrite, followed by the formation of Widmanstätten ferrite. Depending on the relative transformation rates of Widmanstätten ferrite and acicular ferrite, the former can grow entirely across the austenite grains or become stifled by the intragranularly nucleated plates of acicular ferrite. This diagram takes no account of the influence of alloying additions on the austenite grain structure. (b) Actual optical micrograph illustrating the unhindered growth of Widmanstätten ferrite in a weld deposit. (c) Optical micrograph showing how the growth of Widmanstätten ferrite is stifled by the formation of acicular ferrite.

high strength steel weld deposits (Deb *et al.*, 1987; Svensson & Bhadeshia, 1988; Bhadeshia & Svensson, 1989c).

The term *acicular* means shaped and pointed like a needle, but it is generally recognised that acicular ferrite has in three–dimensions the morphology of thin, lenticular plates (Fig. 12). The

shape of acicular ferrite is sometimes stated to be rod–like, but there is no evidence to support this. In two–dimensional sections, the acicular ferrite always appears like a section of a plate rather than of a rod. The true aspect ratio of such plates has never been measured but in random planar sections, the plates are typically about $10\,\mu$m long and $\sim 1\,\mu$m wide, so that the true aspect ratio is likely to be much smaller than 0.1.

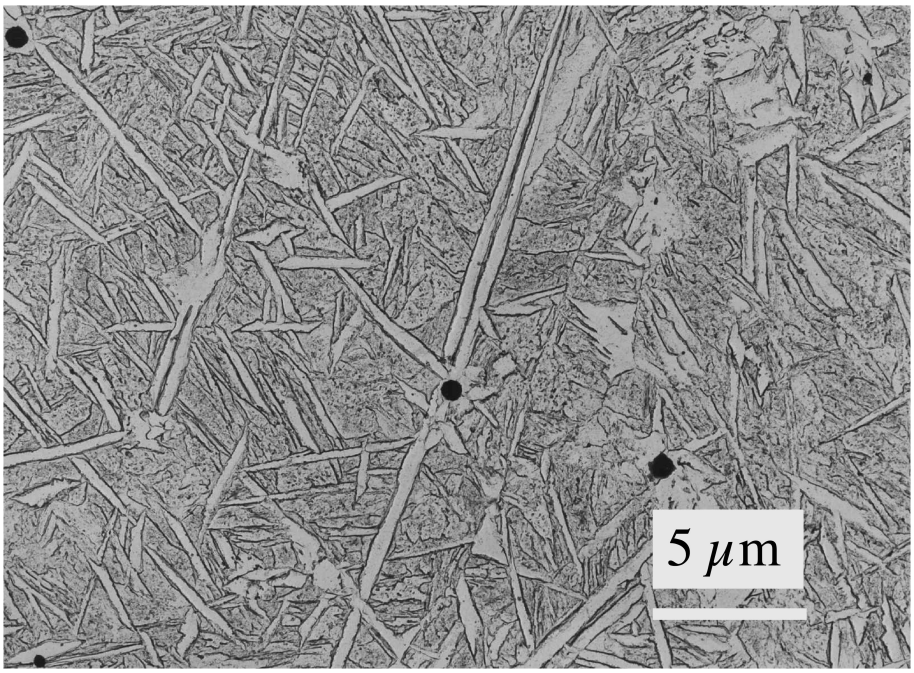

Fig. 12: Replica transmission electron micrograph of acicular ferrite plates in a steel weld deposit (after Barritte).

As the liquid weld pool cools, its solubility of dissolved gasses decreases. Reactions between these gases and other elements causes the formation of solid particles such as oxides. Those particles formed in the very hot and turbulent region immediately beneath the arc are mostly swept out of the pool (Kluken and Grong, 1989). It is the precipitates that form in the lower, relatively cold region of the pool that become trapped into the solid weld. An arc–weld deposit typically contains some $10^{18}\,\mathrm{m}^{-3}$ inclusions of a size greater than $0.05\,\mu$m, distributed throughout the microstructure, although there is a tendency for some of the larger particles to be pushed towards, and consequently trapped along the solidification–cell boundaries during the advance of the solid–liquid interface (Sugden and Bhadeshia, 1988a). The mean particle size of the inclusions important in influencing the microstructure is of the order of $0.4\,\mu$m. It is the interaction of the liquid weld metal with any surrounding gases, together with the use of strong deoxidising elements such as silicon, aluminium and titanium, and protective slag–forming compounds which causes the entrapment of complex multiphase nonmetallic inclusions in the solid at the advancing δ–ferrite/liquid interface. The inclusions have two major effects on the steel: they serve the desirable role of promoting the intragranular nucleation of acicular ferrite plates, leading to an improvement in toughness without a loss of strength. But they also are responsible for the nucleation of voids during ductile fracture, or the nucleation of cleavage cracks during brittle fracture. Achieving a proper balance between these conflicting factors is very difficult without a basic understanding of the mechanisms controlling these interactions.

There are now many results which prove that the inclusions responsible for the heterogeneous nucleation of acicular ferrite are themselves inhomogeneous, as illustrated in Fig. 13 (Ito and Nakanishi, 1976; Mori *et al.*, 1981; Kayali *et al.*, 1983; Dowling *et al.*, 1986; Mills *et al.*, 1987; Thewlis, 1989a,b) The microstructure of the *inclusions* is particularly important from the point of view of developing a clear understanding of their role in stimulating the nucleation of ferrite. As an example, it has been reported that the nonmetallic particles found in some submerged arc weld deposits consist of titanium nitride cores, surrounded by a glassy phase containing manganese, silicon and aluminium oxides, with a thin layer of manganese sulphide (and possibly, titanium oxide) partly covering the surface of the inclusions (Barbaro *et al.*, 1988). This detailed sequence of inclusion formation is not understood and seems to contradict (admittedly simplistic) thermodynamic arguments. For example, titanium oxide is supposed to be thermodynamically more stable than titanium nitride, and yet the latter is the first to form from the liquid phase.

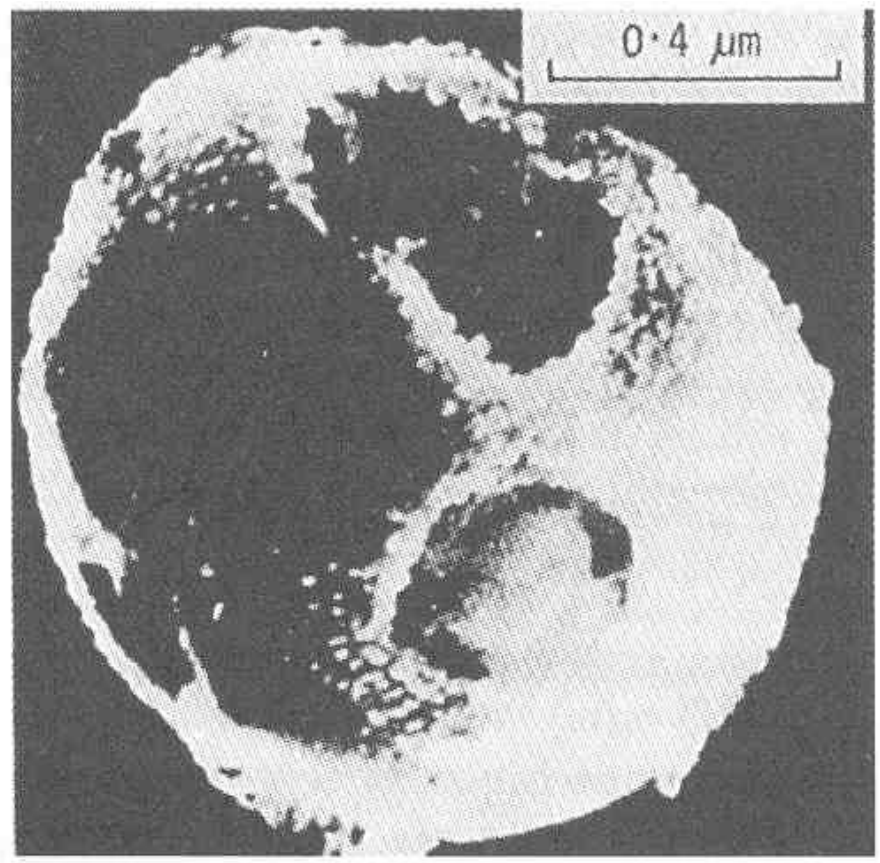

Fig. 13: Scanning transmission electron micrograph of a nonmetallic inclusion in a steel weld metal. The inclusion surface is very irregular, and it features many phases (after Barritte).

The inclusions may therefore be oxides or other compounds but they can under some circumstances influence the subsequent development of microstructure during cooling of the weld deposit. Acicular ferrite plates, during the early stages of transformation nucleate on inclusions present in the large columnar austenite grains which are typical of weld deposits (Ito and Nakanishi, 1976). Subsequent plates may nucleate autocatalytically, so that a one-to-one

correspondence between the number of active inclusions and the number of α_a plates is not expected (Ricks *et al.*, 1982).

The shape change accompanying the growth of acicular ferrite plates has been characterised qualitatively as an invariant-plane strain (Fig. 14). Other measurements imply that the stored energy of acicular ferrite is $\sim 400\,\mathrm{J\,mol^{-1}}$ (Strangwood & Bhadeshia, 1987a; Yang & Bhadeshia, 1987a). Consistent with the observed surface relief effect, microanalysis experiments indicate that there is no bulk partitioning of substitutional alloying elements during the formation of acicular ferrite (Strangwood, 1987). A recent study using an atomic resolution microanalytical technique (field–ion microscopy/atom–probe) has demonstrated unambiguously that manganese and silicon do not partition at all between acicular ferrite and its adjacent austenite (Chandrasekharaiah *et al.*, 1994).

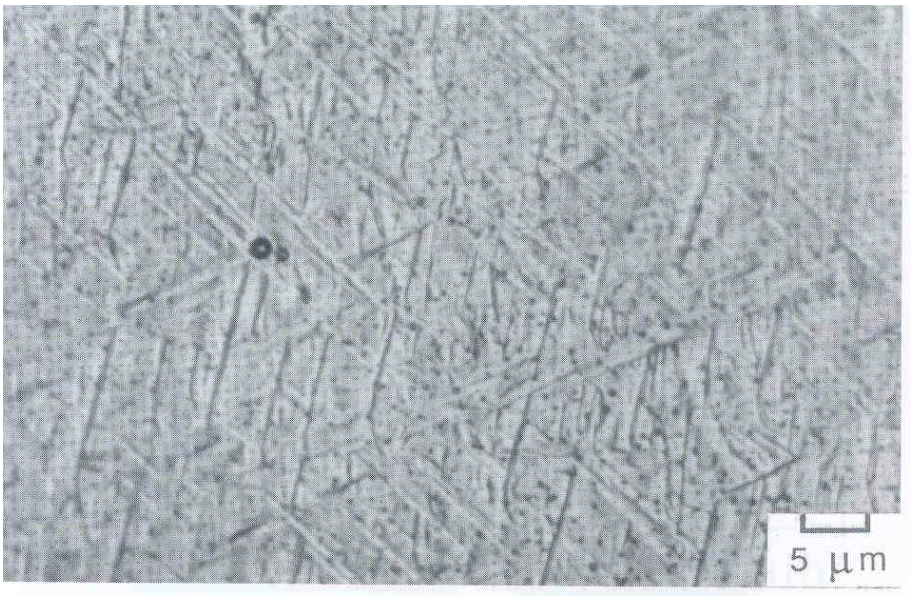

Fig. 14: Nomarski interference contrast micrograph from a surface relief experiment in which a sample was metallographically polished and then transformed to acicular ferrite in an inert protective atmosphere (Strangwood and Bhadeshia, 1987).

Plates of α_a have never been found to cross austenite grain boundaries and the orientation relationship between α_a and the austenite grain in which it grows is *always* such that a close–packed plane of the austenite is parallel or nearly parallel to a closest–packed plane of α_a, and corresponding close–packed directions within these planes are within a few degrees of each other (Strangwood & Bhadeshia, 1987a).

As stated earlier, the growth of acicular ferrite is accompanied by an invariant–plane strain shape deformation. Since the transformation occurs at fairly high temperatures where the yield strengths of the phases concerned are relatively low, the shape change may to some extent be plastically accommodated. This plastic deformation would in turn cause the dislocation density of the acicular ferrite and of any residual austenite to increase. A recent review on acicular ferrite (Farrar and Harrison, 1987) has quoted a dislocation density in the range $10^{12} - 10^{14}\,\mathrm{m^{-2}}$ based on the work of Tuliani (1973) and Watson (1980), although the details of the measurements were not mentioned. A study by Yang and Bhadeshia (1990) found the dislocation density

of acicular ferrite in a high–strength steel weld deposit to be about $5 \times 10^{14}\,\mathrm{m}^{-2}$, making a contribution of approximately 145 MPa to the strength of the phase.

ACICULAR FERRITE: MECHANISM OF GROWTH

The equilibrium volume fraction of transformation expected as an alloy is cooled from the austenite phase field into the $\alpha + \gamma$ phase field is given by the application of the lever rule to a tie line of the phase diagram. When transformation terminates before this equilibrium fraction is achieved, the reaction is said to be incomplete. This " incomplete–reaction phenomenon" can be taken to be a consequence of the nonequilibrium character of the transformation product.

The acicular ferrite transformation obeys the incomplete–reaction phenomenon, the degree of reaction tending to zero as the transformation temperature rises towards the bainite–start (B_S) temperature (Bhadeshia & Christian, 1990). At a given temperature, the transformation stops as x_γ reaches the T_o' curve (Fig. 15). The T_o' curve is the locus of all points where the free energies of austenite and ferrite (with a certain amount of stored energy) of the same composition are identical. The evidence all indicates that the growth of acicular ferrite is diffusionless, with carbon partitioning into austenite *after* the transformation event.

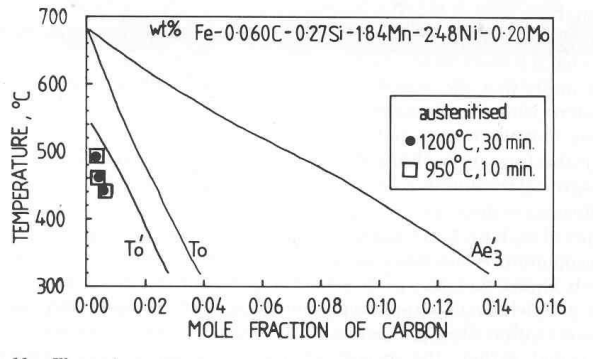

Fig. 15: Illustration of the incomplete–reaction phenomenon for acicular ferrite formed by isothermal transformation of a reheated a low–alloy steel weld deposit. The reaction always stops well before the austenite reaches its equilibrium or paraequilibrium carbon concentration (after Yang and Bhadeshia, 1987a).

The experimental data to date indicate that acicular ferrite is essentially identical to bainite. Its detailed morphology differs from that of conventional bainite because the former nucleates intragranularly at inclusions within large γ grains whereas in wrought steels which are relatively free of nonmetallic inclusions, bainite nucleates initially at γ/γ grain surfaces and continues growth by the repeated formation of subunits, to generate the classical sheaf morphology. Acicular ferrite does not normally grow in sheaves because the development of sheaves is stifled by hard impingement between plates nucleated independently at adjacent sites. Indeed, conventional bainite or acicular ferrite can be obtained under identical isothermal transformation conditions in the same (inclusion rich) steel. In the former case, the austenite grain size has to be small in order that nucleation from grain surfaces dominates and subsequent growth then swamps the interiors of the γ grains. For a larger γ grain size, intragranular nucleation on

inclusions dominates, so that α_a is obtained (Fig. 16). Hence, the reason why α_a in not usually obtained in wrought steels is because they are relatively free of inclusions and because most commercial heat treatments aim at a small austenite grain size. It is ironic that bainite when it was first discovered was referred to as acicular ferrite (Davenport & Bain, 1930), and that the terms acicular ferrite and bainite were often used interchangeably for many years after 1930; see for example, Bailey (1954).

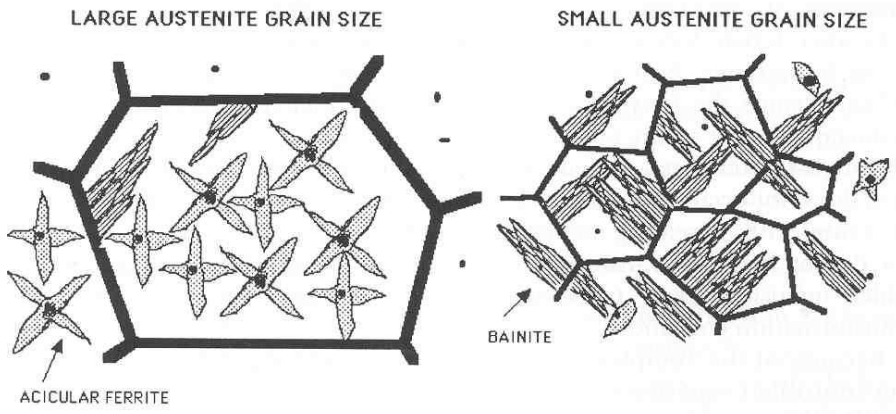

Fig. 16: An illustration of the effect of austenite grain size in determining whether the microstructure is predominantly acicular ferrite or bainite. A small grain sized sample has a relatively large number density of grain boundary nucleation sites and hence bainite dominates, whereas a relatively large number density of intragranular nucleation sites leads to a microstructure consisting mainly of acicular ferrite.

There is in addition, a lot of circumstantial evidence which suggests that a reduction in austenite grain size leads to a replacement of acicular ferrite with bainite (*e.g.,* Imagumbai *et al.*, 1985). When steels are welded, the austenite grains in the heat affected zone coarsen, the degree of coarsening depending on the amount of heat input during welding. It follows that when steels containing appropriate inclusions are welded, the amount of acicular ferrite that forms in the heat affected zone increases at the expense of bainite, as the heat input and hence the austenite grain size is increased (Fig. 17a). Eventually, at very large heat inputs, the cooling rate decreases so much that larger quantities of Widmanstätten ferrite are obtained and there ia a corresponding reduction in the amount of acicular ferrite. Without the inclusions, the acicular ferrite content is always very small (Fig. 17b).

Acicular ferrite is sometimes considered to be intragranularly nucleated Widmanstätten ferrite, on the basis of the observation of macroscopic "steps" at the transformation interface, which are taken to imply a ledge growth mechanism (Ricks *et al.*, 1982). This kind of evidence is, however, tenuous in the sense that a step mechanism is a mechanism for interface motion, and carries no implication about the mechanism of transformation. Even martensite may grow by the movement of coherent atomic steps (Christian & Edmonds, 1984; Bhadeshia & Christian, 1990). Furthermore, the reported observations are weak in the sense that perturbations of various kinds can always be seen on transformation interfaces between ferrite and austenite. Such perturbations do not however necessarily imply a step mechanism of growth. Evidence that the residual austenite is enriched in carbon is also quoted in support of the contention

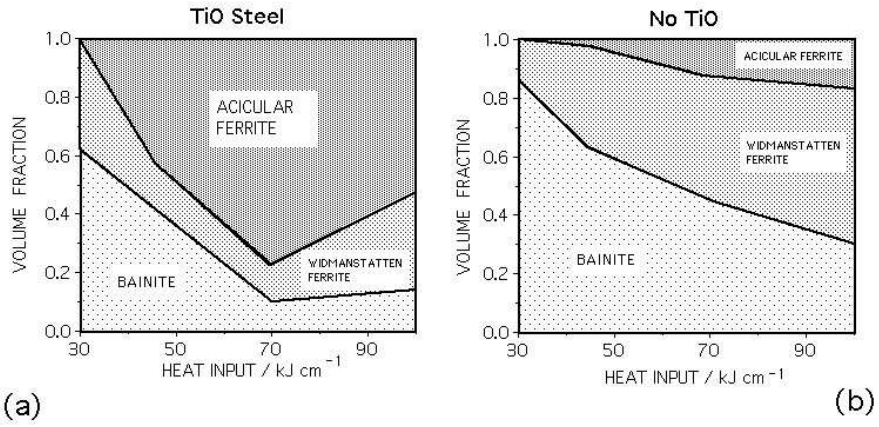

Fig. 17: Changes in the microstructure of the heat affected zone of welds, as a function of the heat input during welding. (a) Steel containing titanium oxide particles. (b) Ordinary steel without inclusion inoculation. After Chijiiwa *et al.* (1988).

that α_a is Widmanstätten ferrite (Ricks *et al.*, 1982) but as pointed out above, the enrichment can occur during or after the transformation event is completed.

NUCLEATION OF ACICULAR FERRITE

It has been demonstrated, assuming classical nucleation theory, that inclusions are less effective in nucleating ferrite when compared with austenite grain surfaces (Ricks *et al.*, 1982). The primary reason why this turns out to be the case is that with inclusions, the ferrite/inclusion interfacial energy is assumed to be large (similar to the austenite/inclusion energy), whereas with austenite grain boundary nucleation, the ferrite can in principle adopt an orientation relationship which minimises its interfacial energy. Experiments in general confirm this conclusion since ferrite formation in most weld deposits first begins at the austenite grain boundaries. Furthermore, larger inclusions are expected to be more effective since the curvature of the inclusion/nucleus interface will then be reduced. This is again generally consistent with experimental observations, although the tendency to state a minimum particle size below which nucleation does not occur is incorrect. It is the activation energy for nucleation which decreases with increasing inclusion size. The activation energy also depends on the driving force for transformation, so that for any specific steel, the size below which inclusions cease to be significant nucleation sites must vary with the transformation conditions.

Lattice Matching Theory Because of the complexity of the inclusions, and the difficulty in conducting controlled experiments with welds, the nucleation potency of inclusions is not clearly understood. A popular idea is that those inclusions which show the best "lattice matching" with ferrite are most effective in nucleating the ferrite (Mori *et al.*, 1980; 1981).

The lattice matching is expressed in terms of a mean percentage planar misfit κ. To calculate κ, it is assumed that the inclusion is facetted on a plane $(h\ k\ l)_I$, and that the ferrite deposits epitaxially with its plane $(h\ k\ l)_\alpha || (h\ k\ l)_I$, with the corresponding rational directions $[u\ v\ w]_I$

and $[u\ v\ w]_\alpha$ being inclined at an angle ϕ to each other. The interatomic spacings d along three such directions within the plane of epitaxy are examined to obtain (Bramfitt, 1970):

$$\kappa = \frac{100}{3} \sum_{j=1}^{3} \mid d_j^I \cos\phi - d_j^\alpha \mid / d_j^\alpha. \tag{16}$$

Data calculated in this manner, for a variety of inclusion phases are presented in Table 1. A description of the relationship between two crystals with cubic lattices requires five degrees of freedom, three of which are needed to specify the relative orientation relationship, and a further two in order to identify the interface plane, *i.e.,* the plane of contact between the two crystals. As far as the interface plane is concerned, Mills *et al.* considered nine different kinds of epitaxy, confined to planes of low crystallographic indices: $\{0\,0\,1\}$, $\{0\,1\,1\}$ & $\{1\,1\,1\}$. The orientation relationships considered are listed in Table 1. The Bain orientation implies $\{1\,0\,0\}_\alpha || \{1\,0\,0\}_I$ and $< 1\,0\,0 >_\alpha \ || \ < 0\,1\,1 >_I$. The cube orientation occurs when the cell edges of the two crystals are parallel (*i.e.,* they are in an identical orientation in space).

Table 1: Some misfit values between different substrates and ferrite. The data are from a more detailed set published by Mills *et al.* (1987), and include all cases where the misfit is found to be less than 5%. The inclusions all have a cubic–F lattice and the ferrite is body–centered cubic (cubic–I).

Inclusion	Orientation	Plane of Epitaxy	Misfit %
TiO	Bain	$\{1\,0\,0\}$	3.0
TiN	Bain	$\{1\,0\,0\}$	4.6
γ–alumina	Bain	$\{1\,0\,0\}$	3.2
Galaxite	Bain	$\{1\,0\,0\}$	1.8
CuS	Cube	$\{1\,1\,1\}$	2.8

To enable the lattice matching concept to be compared with experiments, it is necessary not only to obtain the right orientation relationship, but the inclusion must also be facetted on the correct plane of epitaxy.

The idea of lattice matching stems originally from work on the solidification of aluminium melts inoculated with particles in order to produce grain refinement (see for example, Chart *et al.*, 1975); as will be seen later, the extrapolation of this concept to solid state transformations is not entirely justified. It has even been suggested (Mills *et al.*, 1987) that there may exist reproducible orientation relationships between inclusions and the ferrite plates that they nucleate. Experiments however, demonstrate the absence of a reproducible ferrite/inclusion orientation relationship (Dowling *et al.*, 1986).

In boron–containing welds, Oh *et al.* (1991) found that titanium and zirconium additions both gave similar variations in microstructure as their respective concentrations were increased. This is in spite of the fact that the titanium oxide is supposed to have a better crystallographic match when compared with the large misfit with zirconium oxide. Unfortunately, it had to be *assumed* that the titanium oxide was TiO and the zirconium oxide ZrO_2; futhermore, their zirconium containing welds also had substantial quantities of titanium, between 51 and 73 parts per

million. Nevertheless, the basic idea is worth investigating further, but with a characterisation of the inclusions and with better control over the weld chemistry.

The fact that the inclusions, which form in the liquid steel, are randomly orientated in space, and that the orientation relationship of acicular ferrite with the parent austenite is always found to be of the KS/NW type, necessarily implies that the inclusion/ferrite orientation relation also has to be random Fig. 18. A contrary view is due to Kluken *et al.* (1991), who claim that the δ–ferrite grains sometimes nucleate epitaxially with inclusions. In those circumstances, the acicular ferrite will also bear an orientation relationship with the inclusions since it will be related to the δ–ferrite via the austenite. Textural measurements have been cited in support of this hypothesis (Kluken *et al.* 1990).

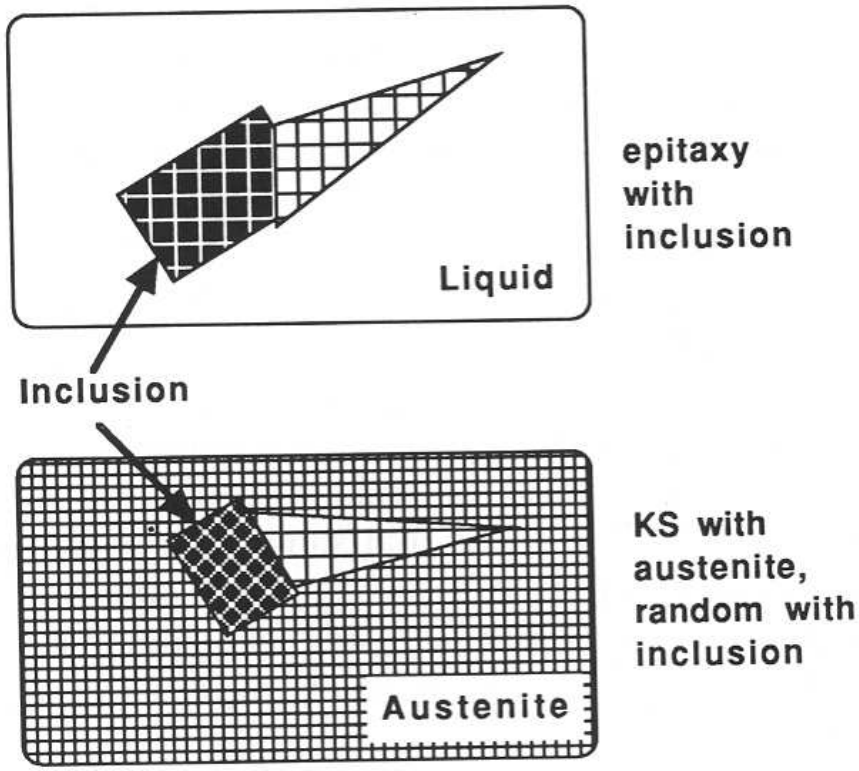

Fig. 18: Schematic illustration of the orientation relationship that develops between ferrite and inclusions. The inclusion must be randomly orientated to the austenite, since it nucleates in the liquid, whereas the austenite grows from the fusion boundary. Consequently, the ferrite (which has an orientation relationship with the austenite) must also be randomly orientated with respect to the inclusion.

Other Possibilities Other ways in which inclusions may assist the formation of acicular ferrite include stimulation by thermal strains or by the presence of chemical heterogeneities in the vicinity of the inclusion/matrix interface; see review by Farrar and Harrison (1987). Alternatively, the inclusions may simply act as inert sites for heterogeneous nucleation (Ricks *et al.*, 1982; Barritte and Edmonds, 1982; Dowling *et al.*, 1986). Chemical reactions are also possible at the inclusion matrix interface, as revealed by experiments in which pure ceramics were

diffusion bonded to steels (Strangwood & Bhadeshia, 1988). The diffusion bonded composite samples were then subjected to heat treatments in which the steel transforms from austenite to ferrite. By comparing ferrite formation events at the ceramic/steel interface with those within the bulk of the steel, it was possible to identify the mechanism by which the ceramics influence ferrite nucleation. Chemical reactions, the details of which depended on the particular ceramic tested, were found to be powerful stimulants for ferrite nucleation (Table 2). Although these experiments reveal a possible mechanism for the interaction between nonmetallic particles and ferrite nucleation, only allotriomorphic ferrite (rather than acicular ferrite) could be studied because of the high alloy content of the steels used. The results may not therefore be directly applicable to weld deposits. For example, Ti_2O_3 is widely believed to be a good nucleant for acicular ferrite, but is found in the context of the diffusion bonding experiments to be chemically inert.

Table 2: List of ceramics which were found to be chemically active in experiments designed to test for ferrite nucleation at ceramic/steel pressure bonds.

Chemically Active	Chemically Inactive
TiO_2	TiO, Ti_2O_3, TiC, TiB_2, TiN
$Al_2Si_2O_7$	Al_2O_3
MnO_2	MnO
SiC, Si	Si_3N_4, SiO_2
CoO, V_2O_5	ZrO_2, FeS, Y_2O_3

Correspondence Between Inclusions and Plates Although the plates of acicular ferrite which form first nucleate heterogeneously on the nonmetallic inclusions, subsequent plates can form autocatalytically. As pointed out earlier, it follows that a one-to-one correspondence between plates of acicular ferrite and inclusions is not to be expected. However, it is difficult to establish this using metallography. By analogy with the procedure used by Chart *et al.* (1975) for aluminium alloys, if the volume of a typical plate of acicular ferrite is taken to be $10^{-16}\mathrm{m}^3$, and that of a spherical inclusion $4 \times 10^{-20}\mathrm{m}^3$, then of all the grains examined, only 7.4% can be expected to display the nucleating particle. Furthermore, the intercept of the particle in the section concerned may be much smaller then its diameter. The calculation presented by Chart *et al.* is valid when the grains of the major phase are approximately spherical. It is necessary to allow for the anisotropy of shape in the case of acicular ferrite. If the acicular ferrite which contains an inclusion of radius $r = 0.2$ μm, is assumed to be of the shape of a square plate of side 10μm and thickness $t = 1$ μm, then the ratio of the mean linear intercepts of the two phases is given by $4r/6t$ (Myers, 1953; Mack, 1956). This means that about 13% of all the plates observed may be expected to show the nucleating particles, assuming that the entire section of the acicular ferrite plate is observed in the sample. The calculation also assumes that each plate contains just one inclusion, and more importantly, that each observed–inclusion is responsible for nucleating the plate in which it is found (*i.e.,* it has not been circumstantially incorporated into the plate).

If the volume fraction of acicular ferrite in the sample examined is large then it is not safe to assume that the observation of a particle in the plate implies that the particle is a nucleating

centre. Recent work by Barbaro *et al.* (1990) claims that many of the acicular ferrite plates nucleate autocatalytically, since the number of nucleating inclusions in any acicular ferrite "colony" was found to be less than the number of plates in that colony. The conclusion is however not safe since the percentage of plates containing inclusions was around 7-11%. On the other hand, given that there is an invariant-plane strain shape deformation accompanying transformation, it is very likely that some degree of autocatalysis does occur during the acicular ferrite transformation. By examining the orientation relationships between adjacent plates in clusters of acicular ferrite plates, it has been possible to demonstrate that such plates have a similar orientation in space (Yang & Bhadeshia, 1989a). Furthermore, the proportion of plates having similar orientations is found to be larger than expected from a knowledge of the austenite/ferrite orientation relationship. This could be taken as evidence for autocatalytic nucleation.

ALUMINIUM AND TITANIUM OXIDES

While the theory capable of ranking different kinds of nonmetallic inclusions in terms of their effectiveness in nucleating acicular ferrite does not exist, there is considerable circumstantial evidence that titanium oxides (TiO, Ti_2O_3, TiO_2) are very potent in this respect, and that Al_2O_3 is not. Titanium nitride also appears to be effective in nucleating acicular ferrite, but is less stable at high temperatures when compared with titanium oxide. The problem is complicated by the fact that most welds, and indeed, wrought steels, contain aluminium which in general is a stronger oxide former than titanium. Consequently, it is the alumina which forms first in the melt, followed by titania, which often grows as a thin coating on the alumina particles. Thus, there has to be available sufficient oxygen to first tie up the aluminium, and then to combine with the titanium (Horii *et al.*, 1986; 1988). The concentration of oxygen required therefore depends on the level of aluminium, which should be minimal in steels designated for acicular ferrite microstructures. This is the reason why Ringer *et al.* (1990) were unable to detect titanium oxides in titanium containing steels which had low oxygen concentrations and enough aluminium to combine with that oxygen.

In order to simplify the problem of oxide (or nitride) formation, it is usual to assume that the stronger oxide forming element is the first to react with oxygen, followed by the weaker oxide forming element. This assumption is based on the magnitude of the free energy change accompanying the oxidation of the free element. It can lead to difficulties. As emphasised earlier, titanium oxide is supposed to be thermodynamically more stable than the titanium nitride, and yet the latter is often the first to grow from the liquid phase:

$$\mathrm{Ti} + \mathrm{O_2} \rightleftharpoons \mathrm{TiO_2} \qquad \Delta \mathrm{G^O} = -9.2 \times 10^5 - 50.2\,\mathrm{T} \quad \mathrm{J\,mol^{-1}} \tag{17}$$

$$\mathrm{Ti} + \mathrm{N} \rightleftharpoons \mathrm{TiN} \qquad \Delta \mathrm{G^O} = -3.4 \times 10^5 - 30.1\,\mathrm{T} \quad \mathrm{J\,mol^{-1}} \tag{18}$$

where $\Delta \mathrm{G^O}$ is the standard free energy of formation (Kubaschewski and Evans, 1950).

These apparent contradictions could be attributed to kinetic effects, but they could also arise because the stabilities of the oxides are assessed using free energy data which are standardised for the reaction of each metallic element with one mole of oxygen, the oxide and the pure

element having unit activities. It is unlikely that this method correctly represents the real situation where all the reactants and products activities are far from unity. The ranking of the oxide stabilities can change as a function of the actual concentrations of the reactants. Nevertheless, in the absence of any suitable model capable of predicting the reactivities of the variety of elements in liquid solution with oxygen, the best working hypothesis must assume that they react in accordance with an intuitive order of oxidising potential. For welds, this usually means that aluminium has the first 'bite' at the available oxygen, followed by titanium, as was assumed by Horii *et al.* (1986; 1988) in their study of submerged arc weld deposits.

As stated earlier, excessive aluminium can tie up the available oxygen and prevent the titanium from forming oxides. A further advantage of minimising the aluminium content is that a smaller oxygen concentration can then be used to achieve the same titanium effect, thereby reducing the inclusion content in the steel. Any free nitrogen, which may combine with the titanium to form a nitride, should also be controlled, perhaps by adding boron as a nitrogen getering agent. Experiments have revealed that trace elements like calcium, and rare earth elements like cerium, at the concentrations used typically for inclusion shape control in wrought alloys, have no detectable influence on the development of the acicular ferrite microstructure (Horii *et al.*, 1986; 1988). Such elements may be incorporated from the fused base plate into the weld deposit, especially during high heat input welding which leads to considerable dilution effects (Fig. 19). Continuously cast steels which are aluminium killed are a potent source of aluminium for welds in which the degree of dilution is large.

One difficulty as far as welds are concerned, is that the small amount of aluminium that remains in solid solution, as opposed to that which combines with oxygen, does not seem to correlate well with the total aluminium or oxygen concentration (Thewlis, 1989a, b). For reasons which are not clear, small concentrations of dissolved aluminium seem to promote the formation of Widmanstätten ferrite, which is a nuisance when attempts are being made to design microstructures which are essentially acicular ferrite. The effect manifests itself particularly in the as–deposited microstructure of self–shielded arc welds (SSAW) which usually exhibits a small volume fraction of acicular ferrite but an exaggerated amount of Widmanstätten ferrite (Abson, 1987b; Grong *et al.*, 1988). In the SSAW process, the pool has little or no protection by any shielding gas; it is instead, deoxidised by the large aluminium concentration in the electrode, the deposit ending up with more than 0.5 wt.% of aluminium and only about 120 p.p.m. of oxygen. The lack of acicular ferrite has been attributed to the low oxygen concentration, but on the other hand, it is the Widmanstätten ferrite which forms first, leaving little residual austenite available for subsequent transformation to acicular ferrite. The propensity to form Widmanstätten ferrite in self–shielded arc welds correlates with their large concentration of aluminium in solid solution. [2]

It has been reported that the mean size of nonmetallic inclusions in welds increases with the overall aluminium concentration (Thewlis, 1989a), but the observed variations are in fact rather small and Evans (1990) has demonstrated that very large changes in aluminium concentration at constant oxygen concentration cause negligible variations in the mean inclusion diameter.

[2] A possible mechanism for the effect of dissolved aluminium in promoting Widmanstätten ferrite is as follows. A large concentration of soluble aluminium is only possible when the overall aluminium concentration is large, in which case the aluminium oxide will be in the form of γ–alumina rather than galaxite. They will not then be effective in nucleating acicular ferrite, so that grain boundary nucleated Widmanstätten ferrite growth can occur without hinderance.

The factors influencing inclusion size are not understood in detail, and although inclusions are sometimes regarded as a panacea for improved weld microstructure, their ability to nucleate cleavage and ductile failure must also be appreciated. These contradicting requirements call for a compromise level of inclusions, but it seems likely that current weld deposits contain excessive oxygen concentrations, well beyond the levels needed to induce the intragranular nucleation of ferrite. For example, oxygen concentrations less than 120 p.p.m. are established to be adequate in producing an acicular ferrite microstructure in wrought alloys. The problem is likely to become more prominent in the near future, as strength levels increase and toughness therefore becomes more sensitive to the presence of nonmetallic particles.

The character of inclusions also alters as the aluminium concentration rises, the oxide particles being predominantly $MnOSiO_2$ at low Al content, and then changing to a mixed spinel oxide (Al_2O_3MnO) and finally to γ–Al_2O_3 (Thewlis, 1990). It is believed that the aluminium to oxygen ratio should be such as to favour the formation of galaxite, although the ratio itself is difficult to estimate for multicomponent systems containing strong deoxidisers other than aluminium and because the soluble concentration of Al etc. cannot be calculated.

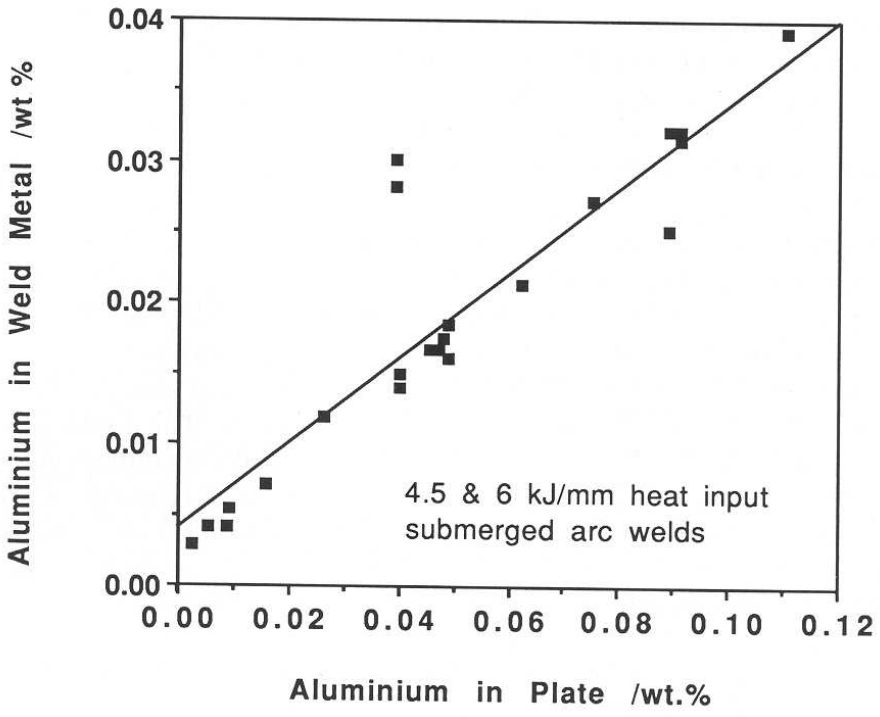

Fig. 19: A plot of the aluminium concentration in the weld metal versus that in the steel, illustrating the incorporation of trace elements from the base plate into the weld fusion zone during high heat input welding (Horii *et al.*, 1986; 1988).

It is sometimes argued that manganese sulphide (MnS) is a prerequisite for the intragranular nucleation of ferrite, but recent experiments (Ringer *et al.*, 1990) reveal that Ti_2O_3 particles are effective even in the absence of MnS surface films, or of any detectable manganese depletion in the austenite near the particles.

Naturally, any manganese depletion caused by the precipitation of its sulphide can only help the nucleation of ferrite. It has been demonstrated conclusively that depletion zones are indeed

to be found in the vicinity of MnS which precipitates from austenite, but that the zones are rapidly homogenised soon after the precipitation is completed (Mabuchi *et al.*, 1996). The MnS is therefore only active in stimulating ferrite nucleation if the latter occurs shortly after MnS formation. Any prolonged holding in the austenite phase field homogenises the manganese concentration. For the same reason, MnS particles might be active as heterogeneous nucleation sites on the first occasion that they precipitate, but their potency is reduced if the sample is then reheated into the austenite phase field. This has significant implications for the large number of experiments based on reheated weld metals.

Although this review is concerned largely with weld deposits, there is a lot to be learned from recent advances in the production of wrought acicular ferrite steels with controlled oxide additions. The oxide particles in wrought acicular ferrite steels have a diameter of about $2\,\mu$m, and are introduced during steel making. The oxide particles thought to be effective in nucleating acicular ferrite are believed to be Ti_2O_3, although each inclusion is usually a complex combination of the titanium compounds and phases such as MnS, Al_2O_3, (Mn,Si)O, etc., in both crystalline and amorphous conditions. The aluminium concentration of the steel has to be minimal (< 30 p.p.m.) during steelmaking since the formation of Ti–oxides is otherwise prevented (Nishioka and Tamehiro, 1988). This is confirmed by the detailed studies of Imagumbai *et al.* (1985), who measured the microstructure of a large number of wrought steels together with the soluble aluminium concentration and the oxide particle densities. They demonstrated that there is a strong effect of dissolved aluminium on the microstructure, with the volume fraction of acicular ferrite obtained decreasing rapidly at concentrations greater than about 70 p.p.m. (Fig. 20a). An interesting result from their work is that the effect of inclusions in enhancing the formation of acicular ferrite was found to saturate at about 120 p.p.m. of oxygen, although this limiting value must also depend on the heat treatment and the details of the other phases present in the steel (Fig. 20b). For example, it is obvious from their work, that the austenite grain size has to be large in order to favour the formation of substantial amounts of acicular ferrite, consistent with the results of Yang and Bhadeshia (1987b). The most critical region of the heat affected zone of welds is the region nearest the fusion zone, where the austenite grain structure is very coarse, and in this respect, the inoculated steels are ideal since the coarse grains transform readily to acicular ferrite. It is interesting to note (as pointed out by Imagumbai *et al.*) that the oxygen concentration of these steels ($\simeq 120$ p.p.m.) is comparable with that of normal fully killed steel (which usually contains aluminium oxides), so that any detrimental effect of inclusions in helping fracture is not exaggerated for the inoculated steels.

Experimental measurements indicate that the procedure is very successful in enhancing the toughness of the critical regions of the HAZ's of welds under both laboratory and commercial conditions. It is worth emphasising that the design of such steels also requires that the alloy chemistry be adjusted to avoid the prior formation of excessive quantities of phases such as allotriomorphic ferrite, Widmanstätten ferrite, etc., so as to leave enough untransformed austenite available for the formation of an effective quantity of intragranularly nucleated acicular ferrite. As discussed by Nishioka and Tamehiro (1988), this can be accomplished by the careful use of microalloying elements such as Nb, Mo and B, thereby avoiding a large rise in the carbon equivalent of the steel. Boron should be avoided for critical applications, since its effects are sometimes difficult to control.

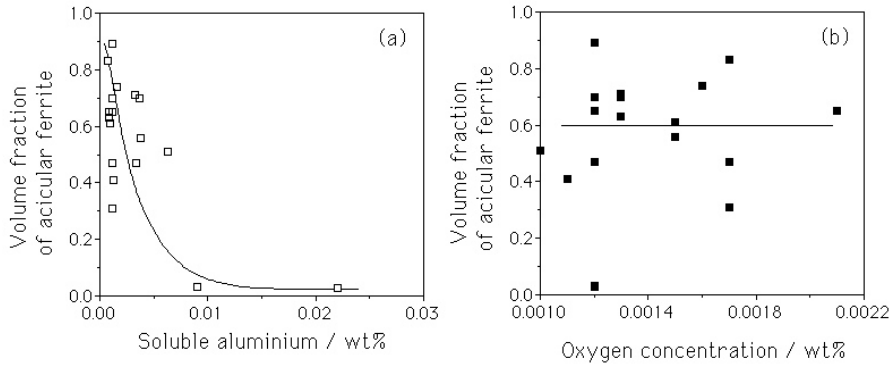

Fig. 20: (a) The volume fraction of acicular ferrite as a function of the soluble aluminium concentration; a level exceeding about 0.007 wt.% is clearly undesirable. (b) The volume fraction of acicular ferrite as a function of the total oxygen concentration; oxygen beyond 0.012 wt.% makes little difference to the microstructure (data from Imagumbai *et al.*, 1985).

Titanium at Very Small Concentrations It is known that in some circumstances, very small concentrations of titanium (< 50 p.p.m.) can be a stimulus for acicular ferrite. Some elegant experiments by Ichikawa *et al.* (1994a) have revealed that the role of titanium in these cases is not to provide titanium oxide or nitride substrates, but more to foster a transition from glassy Si/Mn rich oxides to crystalline manganese and aluminium rich galaxite (Al_2O_3.MnO). The small amount of titanium shows up when the inclusions are microanalysed, but not as a separate phase.

Effect of Silicon We have seen that the aluminium concentration influences the formation of titanium oxides because of its stronger affinity for oxygen. Although silicon has a weaker affinity for oxygen than aluminium, it still has a significant bearing on the amount of oxygen available to form titanium oxide (Lee and Pan, 1992a). It is found that in wrought steels, an increase in the silicon concentration in the molten steel leads to a decreased in the available oxygen concentration, and consequently promotes the formation of titanium nitrides at the expense of titanium oxides. This in turn leads to a deterioration of the microstructure (a reduction in the acicular ferrite content) since TiN particles are effective in preventing austenite grain growth in the heat affected zone.

SULPHUR AND THE RARE EARTH ELEMENTS

It is of interest to examine a recent attempt at inducing the intragranular nucleation of allotriomorphic ferrite using nonmetallic inclusions (Ochi *et al.*, 1988). The steel concerned had a relatively high sulphur concentration (~ 0.07 wt.%) in order to precipitate a fine dispersion of MnS particles. A small vanadium addition (0.1 wt.%) then led to the precipitation of vanadium nitride on the sulphides, which in turn provided the sites for the subsequent formation of vanadium carbides. The carbides were then found to act as substrates for the intragranular nucleation sites for ferrite. This particular sequence of events seems tortuous and remarkable, but has been demonstrated rigorously by Ochi *et al.*, although the reason why vanadium car-

bide is effective in nucleating ferrite is not obvious. Whether a similar sequence can be of use in nucleating acicular ferrite remains to be seen, although high levels of sulphur are usually not tolerated in steel weld deposits.

Yamamoto *et al.* (1987) have made the claim that it is the MnS, which grows on the titanium oxide long after solidification, that is really responsible for the nucleation of acicular ferrite. Consistent with this, their microanalysis data indicated that the oxide particles usually contain about 10 wt.% of manganese, and that the lack of sulphur (< 0.001 wt.%) in the steel reduced the fraction of acicular ferrite that formed. A contradictory result has been reported by Chijiiwa *et al.* (1988), that a reduction of sulphur concentration from 0.005 to 0.001 wt.% tends to decrease the amount of allotriomorphic ferrite and promote the formation of acicular ferrite. Furthermore, Evans (1986) found that an increase in the amount of MnS in nonmetallic inclusions entrapped in steel weld metals leads to a decrease in the volume fraction of acicular ferrite. Ringer *et al.* (1990) also found that Ti_2O_3 particles without any surrounding MnS films can nevertheless be effective in the intragranular nucleation of ferrite. Following an assessment of the literature on inclusions in weld deposits, Abson (1987a) considered that the presence of MnS at the surface of oxide particles inhibits the nucleation of ferrite, and furthermore, that the addition of elements which getter sulphur makes the inclusions more effective. Ichikawa *et al.* (1994a) in careful experiments have shown minute manganese sulphides on nonmetallic inclusions are ineffective as ferrite nucleants.

An interesting study by Umemoto *et al.* (1986) has revealed that quite small concentrations of sulphur ($\simeq 0.005$ wt.%) can in some circumstances lead to an enhancement in the nucleation rate of bainite. It seems that when the austenitising temperature is sufficiently low, the sulphur tends to precipitate at the austenite grain boundaries in the form of iron rich sulphides. These in turn promote the nucleation of bainite. Umemoto *et al.* noted that steels austenitised at an elevated temperature, and subsequently held at a lower temperature (apparently still in the austenite phase field), precipitate a very small volume fraction of cementite particles at the austenite grain boundaries. They also stimulate the nucleation of bainite. These results are difficult to understand if the two austenitisation heat treatments are confined strictly to the single phase austenite fields. For example, the cementite particles were found at the austenite grain boundaries of a Fe–0.61C wt.% alloy, after quenching from 1200°C.

There are evidently, major problems in reaching any conclusions about the role of sulphur in inducing the formation of acicular ferrite. Nevertheless, the notion that manganese sulphide is potent in nucleating ferrite is attractive from a commercial point of view, because it is in any case a common impurity in steels. However, in normal circumstances it precipitates in the solute–enriched interdendritic regions of the solidification microstructure, regions which are rich in manganese and hence have a relatively low tendency to transform to ferrite. The ability of any MnS to act as the heterogeneous nucleation site for ferrite is then reduced by the locally large concentration of austenite stabilising elements in the interdendritic regions. To overcome this difficulty, Ueshima *et al.* (1989) systematically studied methods of producing more uniform distributions of MnS particles, by inducing the sulphide particles to nucleate on oxide particles which grow in the liquid phase and are trapped more or less uniformly by the advancing solidification front. High purity melts, each containing 0.004 wt.% of sulphur, were deoxidised using one of Al, Ti, Zr, La, Ce, Hf or Y. Of these, aluminium and titanium additions were found to be the most uniformly dispersed and insensitive to the killing time within the range 30–600 s (Fig. 21). All of the deoxidising elements studied were able to promote MnS

nucleation (Fig. 21), but Ti_2O_3 and zirconia were particularly effective, with aluminium being the least potent in this respect. The MnS precipitated during solid–state transformation over a temperature range estimated to be 1050–1400 °C. Whilst these results do not help clarify the role of sulphides in stimulating ferrite nucleation, they establish the methods of controlling the sulphide precipitation. Ueshima *et al.* did estimate using diffusion theory that the formation of MnS would lead to a manganese depleted zone in its close proximity of the precipitate, a zone in which the tendency to form ferrite would be enhanced. There are however, contradictory experimental data which suggest the absence of such zones (Barritte *et al.*, 1982; Lee and Pan, 1992b). Direct confirmation of the role of sulphides as ferrite nucleating agents is now needed, but even if the role is found to be positive, great care will have to be exercised to avoid the potent grain boundary embrittling effect of sulphur.

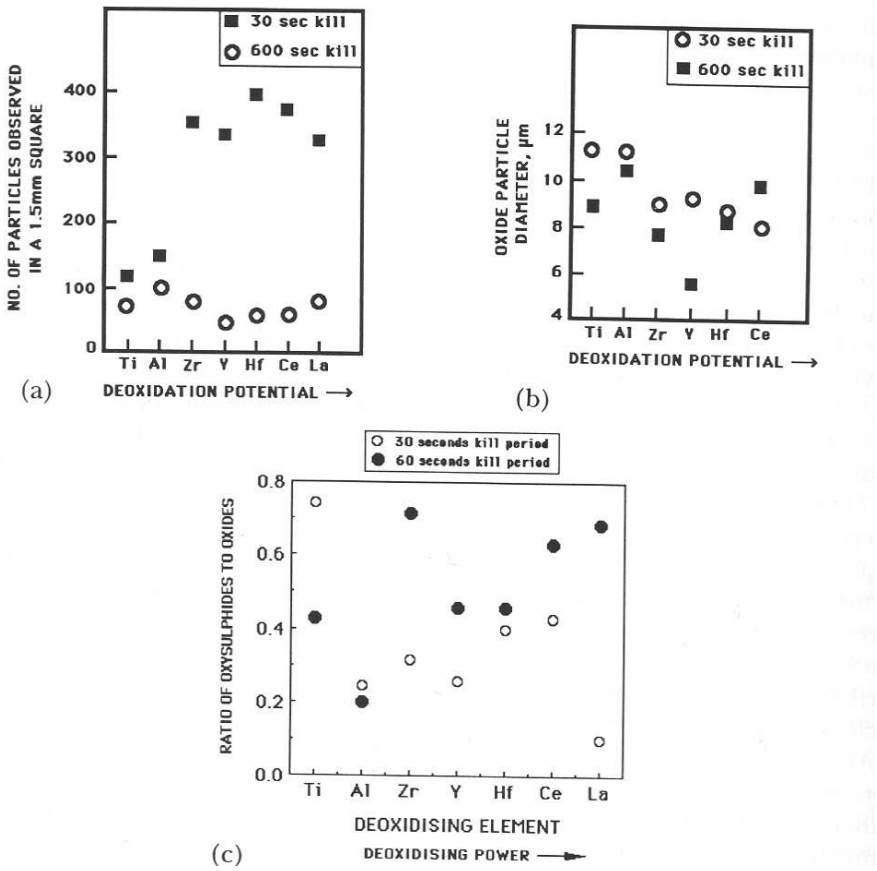

Fig. 21: The effects of a variety of deoxidising elements on the nature of oxide and oxysulphide precipitation in steel (Ueshima *et al.*, 1989). (a) Number density of oxide particles; (b) size of oxide particles; (c) propensity of the oxide to stimulate the solid–state nucleation of sulphide.

Finally, it is worth mentioning the research by Nakanishi *et al.* (1983) on role of oxysulphides in wrought steels. In the heat–affected zone of steels containing titanium nitride, the nitride dissolves in the immediate proximity of the fusion boundary, leading to a detrimental coarse austenite grain structure. Nakanishi *et al.* demonstrated that a combined treatment with titanium nitride and calcium oxysulphides prevents the heat–affected zone grain coarsening because the oxysulphides are stable to very high temperatures.

There has been considerable recent interest in the addition of traces of the rare–earth elements (cerium, neodymium, lanthanum and yttrium) to steels in order to enhance their hardenability (Jingsheng *et al.*, 1988). Attention has been focused on cerium additions of up to 0.15 wt.%, where it is found that the transformation kinetics for allotriomorphic ferrite formation are retarded to a greater extent than for bainite formation. The mechanism is believed to be similar to that of boron, involving segregation to the austenite grain boundaries. The analogy with boron is reinforced by the observation that cerium has little effect on the acicular ferrite transformation (Horii *et al.*, 1986; 1988). Thus, it appears that cerium and boron both retard the allotriomorphic ferrite reaction to a much greater extent than the bainite reaction. The effect of cerium is reduced drastically if the phosphorus content exceeds 0.02 wt.%, although the mechanism of this interaction has yet to be established.

A further indirect role of elements such as yttrium arises from their ability to getter sulphur, especially if the presence of sulphides influences the nucleation frequency of ferrite (Abson, 1987a).

Dissolved Sulphur Caution is obviously necessary in using sulphur as an alloying addition, because of its well established role in embrittling steels. At the same time, it is possible to envisage circumstances where the embrittlement could be more than compensated by a general improvement in microstructure. Thus, Lee and Pan (1992b) have reported an improvement in toughness as the sulphur concentration is raised from 0.0005 to within the range 0.005–0.01 wt.%, due to its effect on increasing the acicular ferrite content of the microstructure. Their experiments established that some of the sulphur segregates to the austenite grain boundaries and hence increases the hardenability of the steel, since segregation must reduce the grain boundary energy. Consequently, the amount of allotriomorphic ferrite is reduced and there is a corresponding increase in the acicular ferrite content, together with an improvement in toughness.

Further increases in sulphur concentration caused an increase in the precipitation of sulphides at the austenite grain boundaries. The precipitates enhanced the nucleation rate of allotriomorphic ferrite at the austenite grain surfaces and hence led to a deterioration of mechanical properties. There is therefore an optimum sulphur concentration.

It is probable that this mechanism of property improvement is only useful in steels which contain inclusions suitable for acicular ferrite nucleation. The mechanism of microstructure improvement is after all based on the relative potency of austenite grain surface and intragranular nucleation sites. Consistent with this, variations in sulphur concentration in the range 0.002–0.006 wt.% do not appear to have any effect on the properties of the heat affected zone of steels without acicular ferrite (Konkol, 1987).

NITROGEN, TITANIUM, BORON

Nitrogen is not usually a deliberate alloying addition in most low–alloy steel weld deposits. It is picked up from the environment and from impurities in the consumables used in the welding process. In situations where the weld is diluted by the parent plate, the composition of the plate must also influence the nitrogen concentration in the weld. Although the concentration

of nitrogen is generally kept rather small ($\simeq$ 40–120 p.p.m.) it is known to have a potent detrimental effect on the toughness of the weld. The mechanism of embrittlement is believed to be associated with strain age–hardening (Lancaster, 1987; Keown *et al.*, 1976; Judson and McKeown, 1982; Oldland, 1985). This, combined with solid–solution hardening causes an increase the yield stress of the weld without modifying the microstructure, and consequently cause a decrease in the toughness.

Nitrogen is a diatomic gas, so that its activity in liquid steel (a_N) varies according to Sievert's law, with the square root of the partial pressure of nitrogen (p_N) in the gas which is in equilibrium with the liquid steel (Phelke and Eliott, 1960):

$$a_N = K p_N^{0.5} \tag{19}$$

where K is a proportionality constant which depends on temperature. The concentration of nitrogen (x_N) is related to the activity by the relation:

$$a_N = f x_N \tag{20}$$

where f is the activity coefficient given by (Wagner, 1952):

$$\log\{f\} = \sum_i x_i e_i \tag{21}$$

where x_i is the concentration in weight per cent of an element i in the liquid steel, and e_i is the corresponding Wagner interaction parameter between the element concerned and nitrogen, for diluted solutions.

If it is assumed that the amount of nitrogen found in the weld at ambient temperature is to some extent related directly to its solubility in liquid steel, then the above method should provide a crude way of rationalising the effect of *weld chemistry* on the nitrogen content of the welds. An approach like this has been used successfully for gas metal arc welding of steels in a nitrogen atmosphere (Kobayanshi *et al.*, 1972). It has recently been applied with moderate success to manual metal arc (including iron–powder electrodes) and submerged arc welds, Fig. 22 (Bhadeshia *et al.*, 1988). The accuracy of relating weld nitrogen concentration to the weld pool chemistry and to the nitrogen content of the consumables and parent plate must of course be limited. For example, variations in arc length, during manual metal arc welding, can easily lead to substantial corresponding variations in the weld nitrogen content. The method for estimating the nitrogen concentration is nonetheless useful in indicating overall trends.

The effect of nitrogen on the development of microstructure in low–alloy steel welds has until recently been difficult to understand, especially in the context of welds containing titanium and boron as deliberate alloying additions. Some studies (Mori *et al.*, 1981; Kawabata *et al.*, 1986) indicated that nitrogen has no detectable influence on the acicular ferrite content of welds, whereas others (Okabe *et al.*, 1983; Ito and Nakanishi, 1975) indicated alterations in microstructure as a function of the nitrogen concentration. Given that weld nitrogen concentrations are rarely out of the range 0.004–0.020 wt.%, nitrogen is hardly expected to have any significant thermodynamic effect on the stability of the the parent and product phases. Any

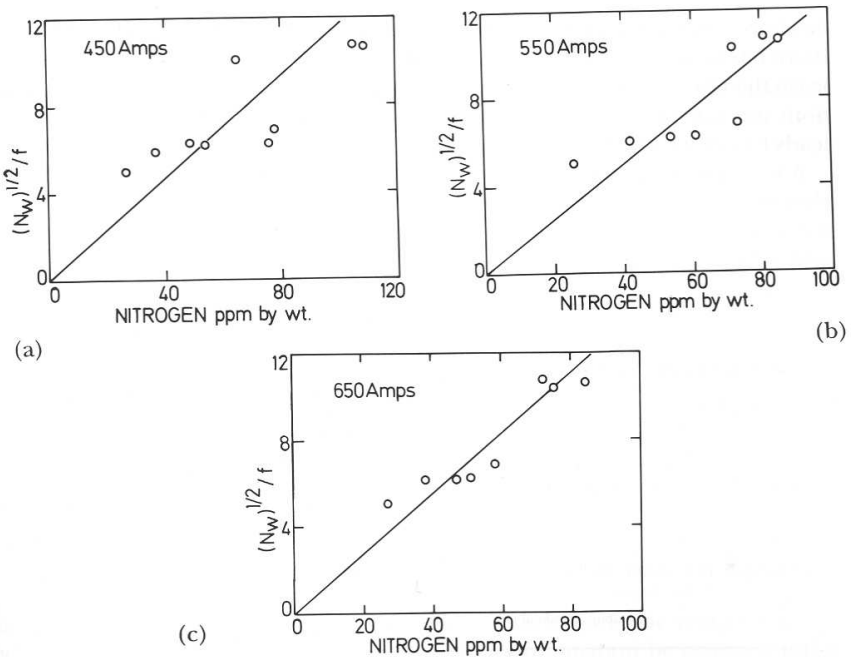

Fig. 22: Correlation of calculated versus experimentally measured nitrogen concentration in submerged arc welds (Bhadeshia *et al.*, 1988). N_w refers to the nitrogen content of the welding wire. (a) 450 A, (b) 550 A and (c) 650 A of welding current.

effect must therefore largely be kinetic, due to for example, the combination of nitrogen with boron (which has a large effect on kinetics at relatively small concentrations).

The difficulties have to a significant extent been resolved recently with a series of careful experiments by Horii *et al.* (1986; 1988) and Lau *et al.* (1987; 1988), who studied titanium, boron, nitrogen phenomena in submerged arc welds. The essence of their conclusions is that nitrogen is not expected to influence the development of microstructure in the absence of boron additions. The situation is found to be quite different when boron is added with the intention of improving hardenability and hence enhancing the opportunity for the austenite to transform into acicular ferrite rather than less desirable phases such as allotriomorphic and Widmanstätten ferrite. Titanium, which is a strong oxide and nitride forming element, is usually added in order to protect the boron from oxidation during transfer across the arc. It also has the key role of preventing the boron from combining with nitrogen in order to form boron nitride. Boron is only effective in improving hardenability if it remains in solid solution in the austenite, since it is a misfitting atom in the austenite lattice and hence segregates to the austenite grain surfaces. This reduces the austenite grain boundary energy thereby making the boundaries less potent heterogeneous ferrite nucleation sites. Boron in the form of nitrides or carbides at the austenite grain surfaces can in fact *reduce* hardenability since the particles seem to induce the nucleation of ferrite. An excess of soluble boron tends to combine with carbon to form boron carbides which are known to be detrimental towards toughness (Dan and Gunji, 1984; Habu, 1978).

It is now recognised that for a given oxygen and boron concentration, the aluminium and titanium concentration (and that of any other oxide former) has to be large enough to combine with all the available oxygen. Furthermore, there has to be enough titanium left over to combine

with any nitrogen so as to leave the boron free to segregate to the austenite grain surfaces. If these conditions are not satisfied, then nitrogen in effect renders the boron useless and leads to a deterioration in microstructure.

A way for making rational decisions during the design of titanium and boron containing deposits could therefore be based on a methodology in which the oxidation reactions are phenomenologically carried out in a sequence consistent with the thermodynamic stability of the elements (Fig. 23).

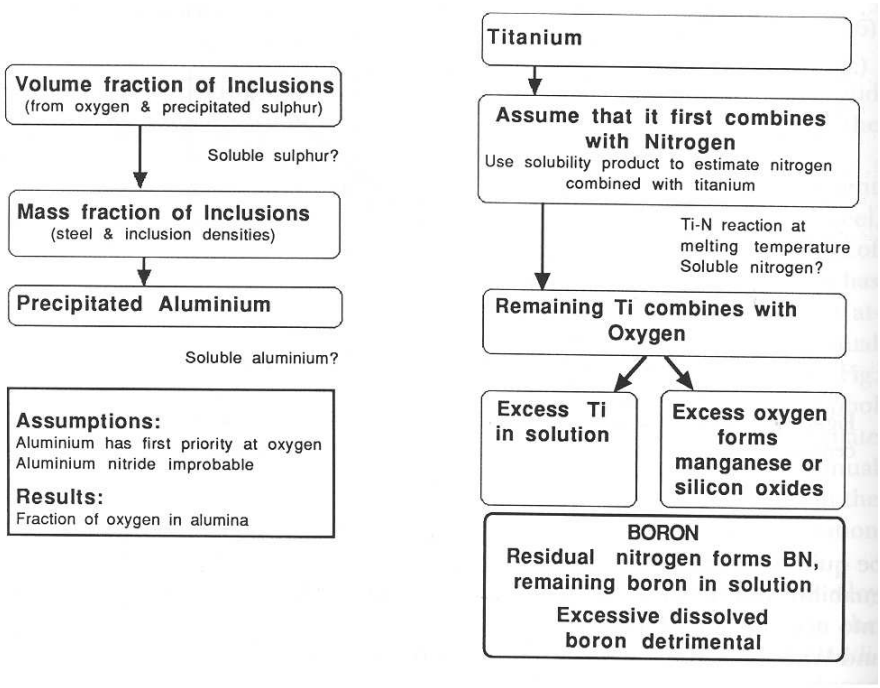

Fig. 23: Flow charts illustrating the procedure for the calculation of inclusion microstructure. The assumptions and difficulties associated with the methods are placed outside of the main boxes.

The difficulties of doing this are illustrated by the work of Kluken and Grong (Kluken and Grong, 1989), whose ideas are reproduced below in a more explicit manner. The total volume fraction V_I of inclusions is given approximately by (Franklin, 1982):

$$V_I \simeq 0.05 w_O + 0.054(w_S - w_S^{sol}) \tag{22}$$

where w_i represents the concentration of element i in units of weight percent and w_S^{sol} the soluble sulphur concentration, usually assumed to be about 0.003 wt.%. The mass fraction of the inclusions is then given by:

$$m_I = V_I \frac{\rho_I}{\rho_S} \tag{23}$$

where ρ_S and ρ_I are the steel and inclusion densities respectively (approximately 7.8 and 4.2 $\mathrm{g\,cm^{-3}}$ respectively). It follows then that the concentration of Al in the inclusions is given by:

$$w_{Al}^{I} = (w_{Al}^{T} - w_{Al}^{sol})/m_I \tag{24}$$

where w_{Al}^{T} and w_{Al}^{sol} represent the total and soluble aluminium concentrations respectively. This relationship assumes that none of the aluminium is present in the form of aluminium nitride, an assumption which is known to be reasonable for most welds. The nitrides however, cause difficulties when considering the next stage in the calculation of inclusion composition, since titanium nitrides are well established to be present in many weld deposits. Lau *et al.* assumed that the titanium first reacts with oxygen, and that any residual titanium can then proceed to react with nitrogen. In the absence of active oxygen, the amount of titanium present as nitride can be estimated by first calculating the amount of nitrogen in solution using well established solubility products (Matsuda and Okumura, 1978):

$$\log\{[w_{Ti}^{sol}][w_{N}^{sol}]\} = \frac{8000}{T} + 0.32 \tag{25}$$

assuming that the concentration of dissolved Ti is known (the temperature at which the calculation is done can to a good approximation be assumed to be close to the melting temperature of the steel). The quantity of titanium in the inclusion, present in the form of nitride (*i.e.,* w_{Ti}^{I-N}), is then given by:

$$w_{Ti}^{I-N} = A_{Ti}(w_{N}^{T} - w_{N}^{sol})/(m_I A_N) \tag{26}$$

where A_i represents the atomic weight of element i. It follows then that the amount of titanium in the inclusions, tied up as oxide (*i.e.,* w_{Ti}^{I-O}) is given by

$$w_{Ti}^{I-O} = (w_{Ti}^{T} - w_{Ti}^{I-N} m_I - w_{Ti}^{sol})/m_I. \tag{27}$$

This differs from equation 13a of Kluken and Grong, which does not seem to take correct account of the titanium combined with nitrogen. The amount of sulphur in the inclusion is calculated in a similar way:

$$w_{S}^{I} = (w_{S}^{T} - w_{S}^{sol})/m_I. \tag{28}$$

Assuming that it is incorporated in the inclusion in the form of manganese sulphide, the concentration of Mn in the inclusion as MnS is given by

$$w_{Mn}^{I-S} = A_{Mn} w_{S}^{I}/A_S. \tag{29}$$

The next step involving the calculation of the SiO_2 and MnO contents of the inclusion requires some assumption about the relative proportions of these two phases. If

$$\theta = \text{wt.\% } SiO_2/\text{wt.\% MnO} \tag{30}$$

and

$$\beta = \frac{(\frac{A_{Mn}}{A_O} + 1)\theta}{(\frac{A_{Si}}{2A_O} + 1) + (\frac{A_{Mn}}{A_O} + 1)\theta} \tag{31}$$

then

$$w_{Si}^I = \beta A_{Si}(w_O^T - m_I w_O^{I-Al} - m_I w_O^{I-Ti})/(2m_I A_O) \tag{32}$$

where w_O^{I-Al} and w_O^{I-Ti} are the concentrations of oxygen in the inclusion, tied up as alumina and titania respectively. It follows that:

$$w_{Mn}^{I-O} = (1-\beta)A_{Mn}(w_O^T - m_I w_O^{I-Al} - m_I w_O^{I-Ti})/(m_I A_O) \tag{33}$$

The calculations presented above cannot be carried out without a knowledge of the Al, Ti and S concentrations in solid solution, and as already pointed out, are subject to numerous approximations. This implicitly includes the assumption that the oxidation state of the titanium is known. Titanium compounds such as TiN, TiC and TiO have similar lattice parameters and crystal structures; they are consequently difficult to distinguish using diffraction methods. Common microanalytical techniques (such as energy dispersive X–ray analysis) clearly identify the presence of titanium, but unless windowless detectors are used, the light elements cannot be detected. Even when oxygen can be detected, the results are difficult to quantify since absorption corrections for the X–rays are difficult due to the shape and unknown thickness of the particles. Therefore, the oxidation state and the factors controlling it, is not well established. Lau *et al.* assumed that the Ti is in the form of TiO_2 whereas Kluken and Grong assumed it to be combined as Ti_2O_3. Abson (1987a) on the other hand, assumes that in weld deposits, the titanium oxide is TiO. The major weakness, however, is the method for the partitioning of oxygen between the different metallic elements. It can for example, easily be demonstrated that manganese and silicon oxides are found in systems where no oxygen is expected to remain after combining with Al and Ti. Furthermore, the silicon concentration has been known to influence the ability of titanium to combine with oxygen (Lee and Pan, 1992a).

The sequence of reactions outlined above should in principle determine the microstructure of the inclusions, with the compounds which form first being located near to the cores of the particles (Fig. 24). Thus, the elements which are least reactive should be concentrated at the inclusion surface. This is consistent with the fact that the nonmetallic particles found in some submerged arc weld deposits consist of titanium nitride cores, surrounded by a glassy phase containing manganese, silicon and aluminium oxides, with a thin layer of manganese sulphide partly covering the surface of the inclusions (Barbaro *et al.*, 1988). Similarly, in a weld containing negligible quantities of aluminium or titanium (< 5 p.p.m), the inclusion core was found to consist of MnO-SiO_2 whereas the addition of some 40 p.p.m. of aluminium led to the presence of some alumina in the core (Es-Souni and Beaven, 1990). On the other hand, both these investigations suggested that in welds containing titanium in addition to Al, Mn and Si, some titanium oxide (or other titanium compounds – the detailed chemistry could not be resolved) could be found at the particle surfaces, a result which is inconsistent with the strong deoxidising potential of titanium, and one which suggests that the titanium oxide

formed at a late stage in the inclusion growth process. This conclusion seems unlikely; an alternative explanation is that the main body of the inclusions (consisting of manganese and silicon oxides) nucleates and grows on the titanium compound, but that the degree of wetting with the substrate is small so that the other oxides do not succeed in engulfing the titanium compounds.

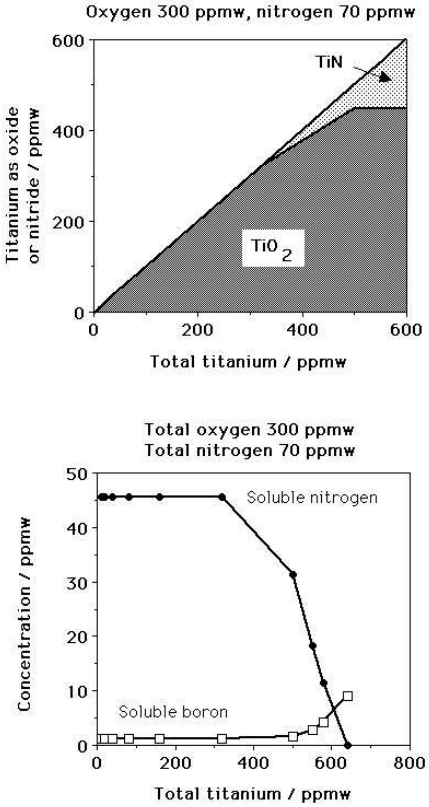

Fig. 24: Calculations showing how the components of inclusions in welds change as the composition is altered. Manganese and silicon oxides are progressively replaced by titanium oxide. When all the oxygen is tied up with the titanium, the latter begins to react with nitrogen and hence helps to liberate boron. For simplicity, aluminium is assumed to be absent.

ACICULAR FERRITE: ROLE OF OTHER PHASES

In weld deposits, acicular ferrite is one of the last transformation products to form after the growth of allotriomorphic and Widmanstätten ferrite. As a consequence, it is bound to be influenced by prior transformation products. Indeed, its volume fraction during continuous cooling transformation of such welds can often be estimated simply from a calculation of the volume fractions of allotriomorphic and Widmanstätten ferrite, and the assumption (in equation 12) that the remainder of the austenite transforms to acicular ferrite (Bhadeshia *et al.*, 1985a). For the same reason, it is found that in wrought alloys with mixed microstructures, the amount of acicular ferrite decreases with the austenite grain size, as grain boundary nucleated phases such as allotriomorphic ferrite become more dominant (Barbaro *et al.*, 1988). The dependence of the volume fraction of acicular ferrite on the austenite grain size becomes less pronounced as the

cooling rate (from the austenite phase field) is increased, since at slow cooling rates, much of the austenite is consumed during the higher temperature formation of allotriomorphic ferrite.

This dependence of the acicular ferrite content on the austenite grain size, in a mixed microstructure of acicular ferrite and allotriomorphic ferrite, can for isothermal reaction be expressed precisely with the help of the following relationship:

$$\ln\{1-i\} \propto S_V \tag{34}$$

where i is the volume fraction of allotriomorphic ferrite divided its equilibrium volume fraction at the temperature concerned and S_V is the amount of austenite grain surface per unit volume of sample. If a number of reasonable assumptions are made (Bhadeshia *et al.*, 1987a) the proportionality can be applied to continuous cooling transformation in low–carbon, low–alloy steels, in which case, $(1-i)$ is approximately equal to the volume fraction of acicular ferrite, thus relating the acicular ferrite content to the austenite grain size.

An interesting observation reported by Dallum and Olson (1989) is that in samples containing mixtures of allotriomorphic ferrite, Widmanstätten ferrite and acicular ferrite, a relatively small austenite grain size leads to a coarser acicular ferrite microstructure. They attributed this to a reduction in the α_w nucleation rate, caused by some unspecified interaction with the prior transformation products (α and α_w). The likely explanation is that with a smaller austenite grain size, the volume fractions of α and α_w that form are correspondingly larger, thereby causing a larger degree of carbon enrichment in the residual austenite. This could lead to a reduction in the acicular ferrite nucleation rate and hence permit the fewer plates that form to develop into larger particles before they collide with each other and stop growing.

Effects like these are of crucial importance in the development of mixed microstructures, but the coarsening of acicular ferrite *per se* is unlikely to lead to any drastic changes in the strength of weld deposits (Bhadeshia *et al.*, 1989a,b). This is because the mean slip distance in a plate does not change very much as the plate becomes larger. Of course, it remains to be demonstrated whether toughness is sensitive to small variations in the size and distribution of acicular ferrite.

We now consider a particular role of allotriomorphic ferrite in influencing the development of acicular ferrite, especially in alloys rich in chromium or molybdenum. At high concentrations of chromium (> 1.5 wt.%) or molybdenum (> 0.5 wt.%), the weld transforms into bainite instead of acicular ferrite. The bainite grows in a classical morphology, with sheaves emanating from the austenite grain surfaces, often with layers of austenite between the platelets of bainitic ferrite. This is in spite of the presence of nonmetallic inclusions which usually serve to intragranularly nucleate the plates of acicular ferrite. This happens because of the reduction in allotriomorphic ferrite content, to a point where the austenite grain boundaries are freed to nucleate bainite. Sneider and Kerrs' (1984) data are consistent with this interpretation. They found that as the chromium concentration is increased, microstructures which are predominantly acicular ferrite are to an increasing extent replaced by bainite, as the fraction of allotriomorphic ferrite decreases. Bainite could not be observed when the allotriomorphic ferrite volume fraction was greater than 0.08, presumably because in their welds, that quantity was sufficient to completely cover the austenite grain surfaces, thereby preventing the grain boundary nucleation of bainite at a lower transformation temperature. It may not in fact be necessary to cover all of the austenite grain surface with allotriomorphs, since the ferrite will first form at the most potent nucleation sites.

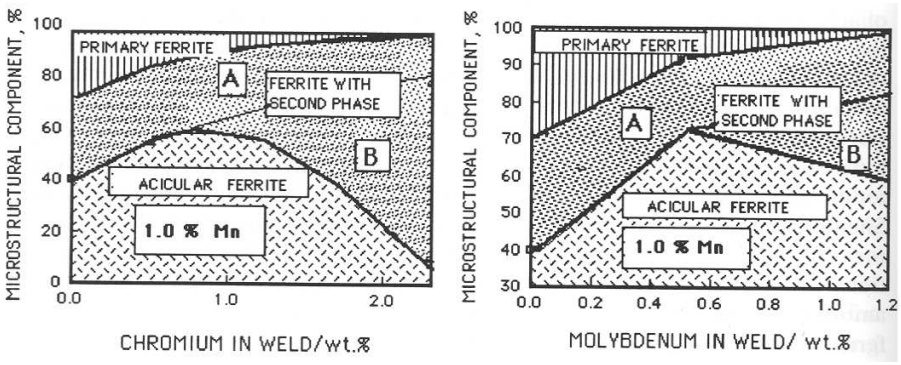

Fig. 25: Changes in the as–deposited microstructure of steel welds as a function of chromium or molybdenum concentration in a series of low–alloy steel weld deposits (after Evans). Notice that in each case, the fraction of acicular ferrite goes through a maximum as the concentration of Cr/Mo increases. The region labelled " ferrite with aligned second phase" by Evans has been subdivided schematically into regions A and B, representing Widmanstätten ferrite and bainitic ferrite microstructures respectively, to indicate that the maximum arises because at high alloy concentrations, acicular ferrite is progressively replaced by bainite.

Evans (1988) showed that the amount of allotriomorphic ferrite decreases steadily with increaseing concentrations of chromium or molybdenum in low–carbon weld deposits. However, the fraction of acicular ferrite peaked as a function of the Cr or Mo concentration. The rest of the microstructure, " ferrite with aligned second phase", therefore increased with solute content (Fig. 25). This latter terminology is used in the welding industry to describe a microstructure in which parallel plates of ferrite are separated by regions of residual phase such as retained austenite. It really refers to packets of parallel Widmanstätten ferrite plates or to sheaves of bainitic ferrite. There is evidence that the Widmanstätten ferrite content of welds actually decreases with increasing Cr or Mo concentration (Bhadeshia *et al.*, 1986b). Hence, the increase in the "ferrite with aligned second phase" noted by Evnas is due to an increase in the fraction of bainite.

That bainite is obtained when the austenite grain boundaries are free from other transformation products explains why Fe–2.25Cr–1Mo wt.% welds used in the power generation industry are bainitic (Klueh, 1974; Wada and Eldis, 1982; Karr and Todd, 1982; Josefsson and Andren, 1989; Vitek *et al.*, 1986; McGrath *et al.*, 1989), with classical sheaves in which the platelets of bainitic ferrite are partially separated by films of retained austenite or martensite. Allotriomorphic ferrite does not form readily in such alloys.

It follows that at high concentrations of chromium and/or molybdenum, acicular ferrite is in increasing proportions, replaced by bainite. The microstructure eventually becomes almost entirely bainitic (Fig. 25). This effect cannot be attributed to any drastic changes in the austenite grain structure, nor to the inclusion content of the weld deposits (Babu and Bhadeshia, 1990). It turns out in fact, that the Cr and Mo alloys have highlighted a more general condition associated with welds containing large concentrations of austenite stabilising alloying additions. Several cases have been reported in the literature, where a similar transition from an acicular ferrite microstructure to one containing a greater amount of bainite is found to occur as the concentration of elements other than Cr or Mo is increased so that the amount of allotriomorphic ferrite is reduced, as summarised in Fig. 26. Horii *et al.* (1986; 1988) found that in a series

of low–alloy steel welds, when the manganese or nickel concentrations exceeded about 1.5 and 2.9 wt.% respectively, the weld microstructure exhibited significant quantities of bainite. Interestingly, in the case of the nickel containing steels, the toughness nevertheless improved since nickel in solid solution has a beneficial intrinsic effect on the toughness of iron. It apparently increases the stacking fault energy of body–centered cubic iron; since the dislocations in such iron are three–dimensionally dissociated, the change in stacking fault energy reduces the stress required for plastic flow at low temperatures, relative to that necessary for cleavage fracture (see Leslie, 1982).

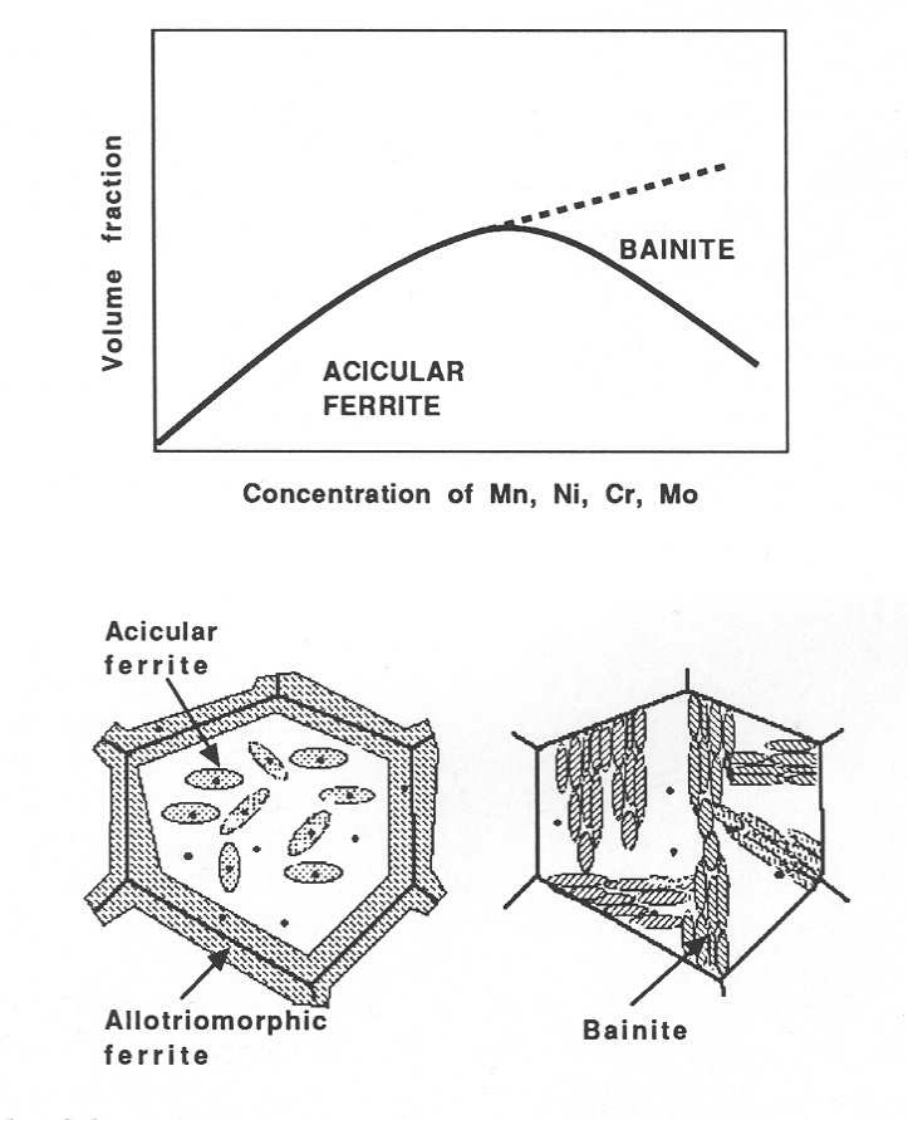

Fig. 26: Schematic summary of the mechanism and data on the transition from an acicular ferrite microstructure to one containing increasing quantities of bainite sheaves.

Direct observations have confirmed the mechanism for the microstructural transition from acicular ferrite to bainite (Babu and Bhadeshia, 1990). The removal of allotriomorphs leads to the growth of grain boundary nucleated bainite (Fig. 27). The allotriomorphic ferrite/austenite boundaries, even when the α/γ orientation is appropriate, cannot develop into bainite because the adjacent austenite is enriched in carbon, to an extent which drastically reduces its bainite

start temperature. A transformation–free zone is therefore found ahead of the allotriomorphic ferrite/austenite interfaces.

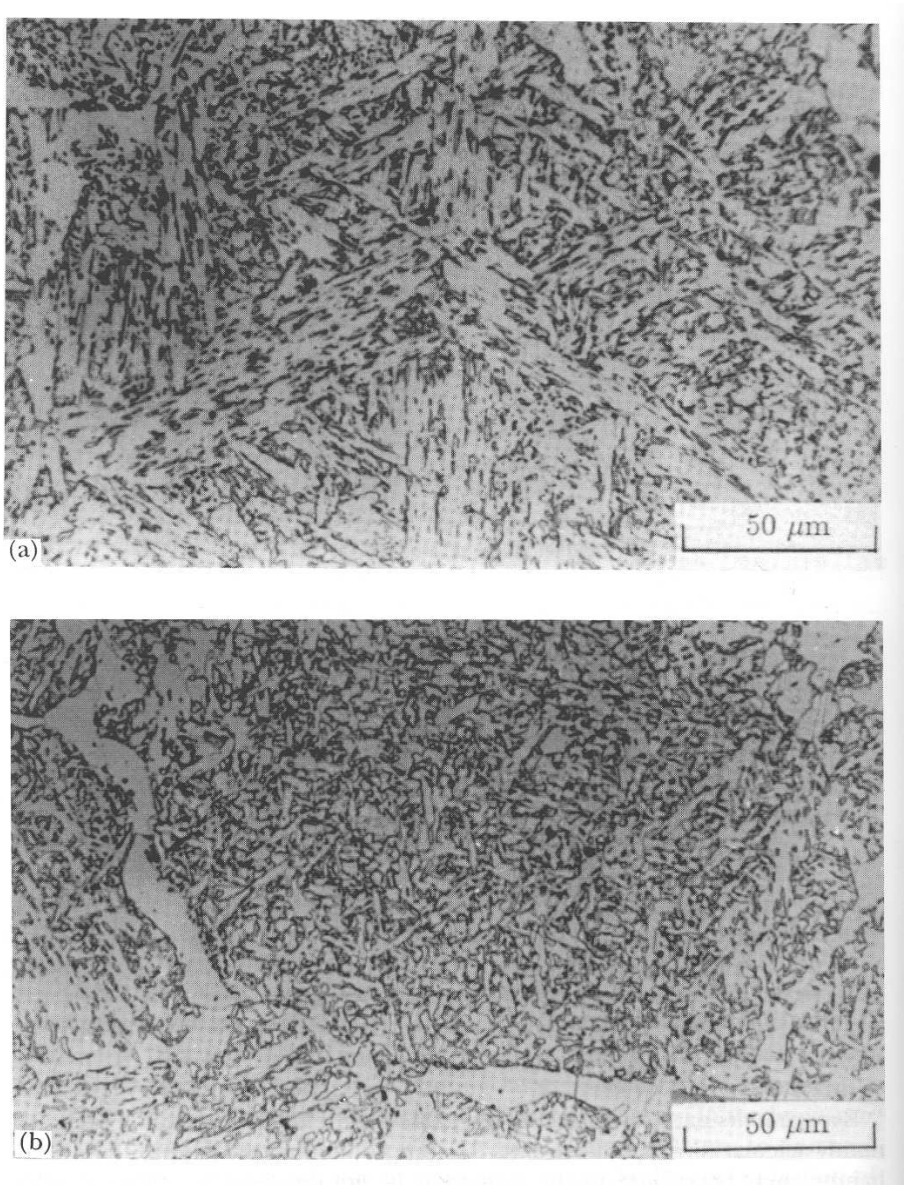

Fig. 27: The change from a bainitic (a) microstructure to one which is predominantly acicular ferrite (b), induced by the introduction of a thin layer of allotriomorphic ferrite at the austenite grain surfaces. Both the acicular ferrite and bainite were otherwise obtained by isothermal transformation under identical conditions.

Recent work by Surian *et al.* (1994) apparently contradict the observations discussed above. The acicular ferrite was found to increase at all concentrations of chromium, rather than to go through a maximum. However, in no case was the allotriomorphic ferrite eliminated completely. Furthermore, their published micrographs reveal continuous allotriomorphs decorating the columnar austenite grains, even in the most concentrated alloy studied. Thus, on the basis of the hypothesis discussed above, bainite is not expected to form at the expense of acicular ferrite.

Wrought Alloys It was pointed out earlier that conventional bainite or acicular ferrite can be obtained under identical isothermal transformation conditions in the same (inclusion–rich) steel; in the former case, the austenite grain size has to be small in order that nucleation from grain surfaces dominates and subsequent growth then swamps the interiors of the austenite grains. For the same reasons, acicular ferrite is not usually obtained in relatively clean wrought steels.

However, significant attempts have recently been made in industry, to inoculate steels with oxide particles in order to induce the formation of acicular ferrite for improved toughness (Nishioka and Tamehiro, 1988). These attempts are driven by the need to develop steels for the offshore oil and gas industries, steels which are required for service in hostile deep and cold environments. This in turn requires unprecedented levels of strength and toughness. These requirements can in principle be met using thermomechanically processed, rapidly cooled bainitic steels. However, when such steels are welded, the resulting thermal cycles induce less desirable microstructures in the heat–affected zones.

The problem can in principle be resolved in an elegant way which takes advantage of the coarsening of the austenite grain structure in the heat–affected zones of weld deposits. Tamehiro and co-workers have developed low alloy steels containing titanium oxides and nitrides, in which these phases help nucleate acicular ferrite during cooling of the heat–affected zone after welding. A typical composition of such a steel is Fe-0.08C-0.20Si-1.4Mn-0.002Al-0.012Ti-0.002N wt.%.

The oxide particles have a diameter of about $2\,\mu$m, and are introduced during steel making. The oxide particles thought to be effective in nucleating acicular ferrite are believed to be Ti_2O_3, although each inclusion is usually a complex combination of the titanium compounds and phases such as MnS, Al_2O_3, (Mn,Si)O, etc., in both crystalline and amorphous conditions. The aluminium concentration of the steel has to be minimal (< 30 p.p.m.) during steelmaking since the formation of Ti–oxides is otherwise prevented (Nishioka and Tamehiro, 1988). This is confirmed by the detailed studies of Imagumbai *et al.* (1985), who measured the microstructure of a large number of wrought steels together with the soluble aluminium concentration and the oxide particle densities. They demonstrated that there is a strong effect of dissolved aluminium on the microstructure; with the volume fraction of acicular ferrite obtained decreasing drastically at concentrations greater than about 70 p.p.m. An interesting result from their work is that the effect of inclusions in enhancing the formation of acicular ferrite was found to saturate at about 120 p.p.m. of oxygen, although this limiting value must also depend on the heat treatment and the details of the other phases present in the steel. For example, it is obvious from their work, that the austenite grain size has to be large to favour the formation of substantial amounts of acicular ferrite, consistent with the results of Yang and Bhadeshia (1987a). The most critical region of the heat affected zone of welds is the region nearest the fusion zone, where the austenite grain structure is very coarse, and in this respect, the inoculated steels are ideal since the coarse grains readily transform to acicular ferrite. It is interesting to note (as pointed out by Imagumbai *et al.*) that the oxygen concentration of these steels at about 120 p.p.m. is comparable with that of normal fully killed steel which usually contains aluminium oxides, so that any detrimental effect of inclusions in helping fracture is not exaggerated for the inoculated steels.

It is always important when considering the role of titanium, to recognise that the nitrogen concentration must be controlled since titanium also forms TiN.

Experimental measurements indicate that the procedure described above is very successful in enhancing the toughness of the critical regions of the HAZ's of welds under both laboratory and commercial conditions. It should be emphasised that the design of such steels also requires that the alloy chemistry be adjusted to avoid the prior formation of phases such as allotriomorphic ferrite, Widmanstätten ferrite, etc., so as to leave enough untransformed austenite available for the formation of an effective quantity of intragranularly nucleated acicular ferrite. As discussed by Nishioka and Tamehiro, this can be accomplished by the careful use of microalloying elements such as Nb, Mo and B, thereby avoiding a large rise in the carbon equivalent of the steel (boron should be avoided for critical applications, since its effects are sometimes difficult to control).

Finally, it is to be noted that prior to the advent of the oxide–inoculated wrought steels just discussed, high–strength low–alloy steels (*e.g.,* Khrishnadev & Ghosh, 1979) were sometimes called "acicular ferrite HSLA" steels. This is because they exhibited a microstructure of heavily dislocated laths; this microstructure is more like the low–carbon bainite in which adjacent laths are in the same crystallographic orientation in space and it is probably not useful to call it an acicular ferrite microstructure, given that the latter nowadays carries the implication of intragranular, heterogeneous nucleation.

It is of interest to examine a recent attempt (Ochi *et al.*, 1988) at inducing the intragranular nucleation of allotriomorphic ferrite using nonmetallic inclusions. The steel concerned had a relatively high sulphur concentration (~ 0.07 wt.%) in order to precipitate a fine dispersion of MnS particles. A small vanadium addition (0.1 wt.%) then led to the precipitation of vanadium nitride on the sulphides, which in turn was found to act as sites for the subsequent formation of vanadium carbides. The carbides were then found to provides the intragranular nucleation sites for ferrite. This particular sequence of events has been thoroughly demonstrated by Ochi *et al.*, although the reason why vanadium carbide is effective in nucleating ferrite is not clear. Whether a similar sequence can be of use in nucleating acicular ferrite remains to be seen, although large concentrations of sulphur are usually not tolerated in steel weld deposits.

LOWER ACICULAR FERRITE

As discussed in the earlier sections, acicular ferrite and bainite seem to have similar transformation mechanisms. The microstructures might differ in detail because bainite sheaves grow as a series of parallel platelets emanating from austenite grain *surfaces*, whereas acicular ferrite platelets nucleate intragranularly at *point* sites so that parallel formations of plates cannot develop. Some of the similarities between bainite and acicular ferrite are (Bhadeshia and Christian, 1990):

1. They both exhibit the invariant–plane strain shape deformations with large shear components, during growth. Consequently, the growth of a plate of acicular ferrite or bainite is confined to a single austenite grain (*i.e.,* it is hindered by a grain boundary) since the coordinated movement of atoms implied by the shape change cannot in general be sustained across a border between grains in different crystallographic orientations. A further implication is that plates of acicular ferrite, like bainite, *always* have an orientation relationship with the parent phase, which is within the Bain region. This is not necessarily the case when the transformation occurs by a reconstructive mechanism.

2. There is no substitutional solute partitioning during the growth of either bainite or acicular ferrite (Strangwood, 1987).

3. Both reactions stop when the austenite carbon concentration reaches a value where it becomes thermodynamically impossible to achieve diffusionless growth (Yang and Bhadeshia, 1987b; Strangwood and Bhadeshia, 1987a). Any redistribution of carbon from the supersaturated ferrite plates occurs after growth. Growth is thus diffusionless, but is followed immediately afterwards by the rejection of carbon into the residual austenite.

4. Acicular ferrite only forms below the bainite–start temperature.

5. There is a large and predictable hysterisis in the temperature at which austenite formation begins from a mixed microstructure of acicular ferrite and austenite, or bainite and austenite (Yang and Bhadeshia, 1987a).

6. The removal of inclusions from a weld deposit, without changing any other feature, causes a change in the microstructure from acicular ferrite to bainite (Harrison and Farrar, 1981).

7. An increase in the number density of austenite grain surface nucleation sites (relative to intragranular sites) causes a transition from acicular ferrite to bainite (Yang and Bhadeshia, 1987a).

8. The elimination of austenite grain surfaces by decoration with inert allotriomorphic ferrite leads to a transition from a bainitic to an acicular ferritic microstructure (Babu and Bhadeshia, 1990).

These and other similarities emphasise the point that bainite and acicular ferrite have the same growth mechanisms. There is one anomaly. Like conventional lower bainite in wrought steels, there ought to exist a *lower* acicular ferrite microstructure, in which the intragranularly nucleated plates of α_a contain plates of cementite inclined at an angle of about 60^o to the habit plane (Bhadeshia & Christian, 1990). The transition from upper to lower bainite is associated with the point where the rejection of carbon from the supersaturated bainitic ferrite into the residual austenite becomes sluggish compared with the precipitation of that carbon as carbides in the ferrite, Fig. 28 (Hehemann, 1970; Takahashi and Bhadeshia, 1990). Consequently, if the carbon concentration of a steel weld is increased sufficiently, then for similar welding conditions, the microstructure should undergo a transition form acicular ferrite to lower acicular ferrite. An experiment designed to test this, using an exceptionally high carbon weld, has successfully detected lower acicular ferrite (Sugden & Bhadeshia, 1989c), supporting the conclusion that acicular ferrite is simply intragranularly nucleated bainite. Lower acicular ferrite is only found when the weld carbon concentration is large enough to permit the precipitation of carbides from the acicular ferrite, before much of the carbon can partition into the residual austenite. This means that in reality, lower acicular ferrite is unlikely to be of technological significance in welds which necessarily have low carbon equivalents. On the other hand, lower acicular ferrite has recently been detected in a high carbon steel fabricated using a high–power laser welding technique (Hall, 1990).

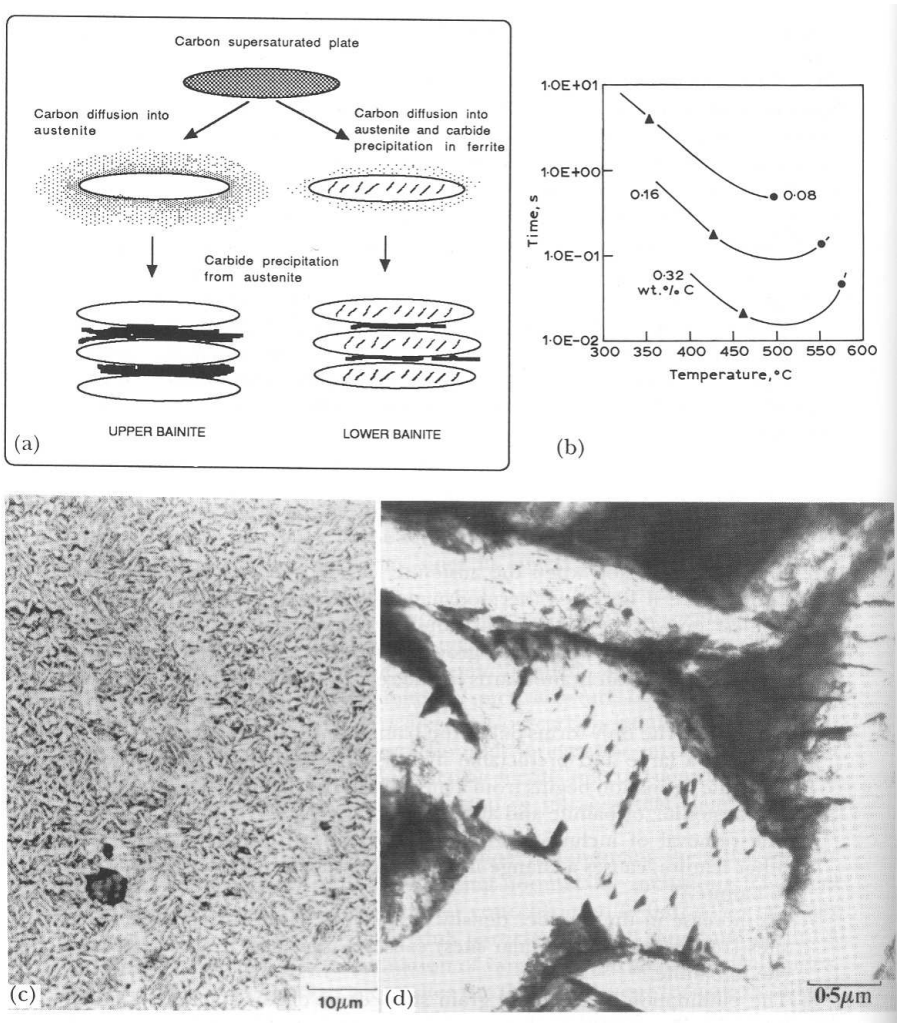

Fig. 28: (a) Schematic illustration of the mechanism of the transition from upper to lower bainite. (b) Calculated times for the decarburisation of ferrite plates, as a function of their initial carbon concentrations. (c) Light micrograph of lower acicular ferrite in an experimental high–carbon steel weld deposit (Sugden and Bhadeshia, 1989c). (d) Corresponding transmission electron micrograph illustrating the carbide particles in the acicular ferrite, in the single crystallographic variant typical of lower bainite in conventional microstructures.

STRESS & THE FORMATION OF ACICULAR FERRITE

Structures which are fabricated during welding usually develop residual stresses which may approach the yield stress of the steel concerned. It is then possible that these stresses have an effect on the development of microstructure during the cooling of the weld to ambient temperature. The development of microstructure may in turn be affected by the influence of external stresses. We have already noted that at free surfaces, both acicular ferrite and bainite cause displacements which are characterised as invariant–plane strains with large shear components. A displacive transformation like this can justifiably be regarded as a mode of deformation of the parent phase. The additional characteristic of the deformation is that the crystallographic structure of that phase is altered in the deformed region (Table 3). Thus,

the permanent strain caused by the transformation is called *transformation plasticity*. Since a phase transformation can be triggered either by cooling below a certain transformation–start temperature, or by the application of a stress in appropriate circumstances, or by a combination of these factors, transformation plasticity can be obtained at stresses which are much smaller than the conventional yield stress of the parent phase, as measured in the absence of transformation.

Just as a combination of a plane and a direction constitutes a deformation system for slip or twinning, the habit plane and displacement vector of the invariant–plane strain accompanying transformation completely describe the deformation system responsible for transformation plasticity. There will in general be 24 of these systems per austenite grain, and they may operate simultaneously to varying extents. Of course, unlike ordinary slip, the different deformation systems within an austenite grain cannot intersect (except in special circumstances where intervariant transformations are possible), so that the ordinary notion of work hardening does not apply. Work hardening nevertheless manifests itself via a different mechanism, in which the stability of the austenite increases as it becomes more finely divided. Given the large number of transformation variants available per grain, the Taylor criterion leads to the conclusion that transformation plasticity can lead to, or accommodate any externally imposed, arbitrary shape change assuming that sufficient parent phase is available. It follows that polycrystalline samples can remain intact at grain boundaries when transformation plasticity is the sole mode of deformation. Furthermore, the transformation plasticity can lead to anisotropic shape changes even in polycrystalline samples transformed without applied stress, if the samples are crystallographically textured in their parent phase.

Table 3: Characteristics of slip, mechanical twinning and displacive transformation.

	Slip	Twin	Displacive
Permanent deformation	Yes	Yes	Yes
IPS shape change	Yes	Yes	Yes
Changes orientation	No	Yes	Yes
Changes lattice type	No	No	Yes
Possible density change	No	No	Yes

Dallum and Olson (1989) studied the microstructure obtained by transformation under the influence of stresses generated during the cooling of constrained samples of reaustenitised steel weld metal. The level of stress therefore varied from zero at the austenitisation temperature to a maximum at ambient temperature, although the absolute magnitude of the stresses involved were not stated. Other tests involving compression were also carried out. It was concluded that with the sort of stresses typical in welding, there was little influence on the volume fraction of acicular ferrite obtained.

A subsequent investigation (Babu and Bhadeshia, 1992) has revealed a large influence of relatively small stresses on the development of the acicular ferrite microstructure.

There are profound changes in microstructure when acicular ferrite grows under the influence of an applied stress, which may be below the yield strength of the austenite (Fig. 6). The stress favours the development of those crystallographic variants which most comply with the applied

stress. This leads to the destruction of the conventional structure in which plates emanating from inclusions point in many different directions. Instead, the austenite tends to transform into a nonrandom microstructure containing just a few variants of intragranularly nucleated plates.

This behaviour is entirely consistent with the displacive mechanism by which acicular ferrite grows, but has further implications as far as welds are concerned. If many variants of acicular ferrite are able to grow, then the shear component of the IPS would tend to cancel out, and the dilatational strain would appear isotropic. However, when the microstructure becomes nonrandom, then the transformation strain ceases to be isotropic. Since the shear component of the IPS shape strain is much larger than the dilatational component (0.22 versus 0.03 – see Bhadeshia and Christian, 1990), it dominates the transformation strains as only the variants favoured by the stress form. As Magee (1966) has pointed out, this must have implications on the calculation of residual stresses. There are, however, no models of residual stress calculation which take anisotropic transformation plasticity into account. They all assume a uniform volume expansion on the decomposition of austenite.

ACICULAR FERRITE IN QT STEELS

Quenched and tempered (QT) martensitic steels are used in applications such as the fabrication of submarine hulls. Many largely unsuccessful attempts have been made to laser weld such steels, without using any filler metal (*i.e.,* autogenous welds). The resulting fusion zone consists of untempered martensite with a hardness which is far in excess of the unaffected plate steel. It consequently exhibits poor mechanical properties, particularly toughness.

THE MICROPHASES

"Microphase" is the term used to describe the small amount of martensite/austenite/degenerate–pearlite which forms after all the other phases (allotriomorphic ferrite, Widmanstätten ferrite, acicular ferrite) have formed. The fraction of the microstructure which is left untransformed after the major phases have formed is very small in most low–alloy low–carbon steels; hence the term microphases. Microphases are also found in the heat–affected zones of welded steels.

The chemical composition of the microphases is for the substitutional solutes, identical to that of the alloy as a whole, but is substantially enriched with respect to the carbon concentration (Komizo and Fukada, 1989; Matsuda *et al.*, 1990; Fig. **??**). The excess carbon is due to partitioning as the major phases grow. It is interesting (Fig. **??**) that the degree of carbon enrichment is found to increase as the cooling rate decreases. This can be attributed to the fact that as the cooling rate decreases, the volume fraction of ferrite that grows prior to microphase formation is larger. Hence, by mass balance, the carbon concentration of the residual austenite is expected to be larger.

Fracture due to Microphases It is generally recognised that microphases occur in two main morphologies, those originating from films of austenite which are trapped between parallel plates of ferrite, and others which are blocky in appearance.

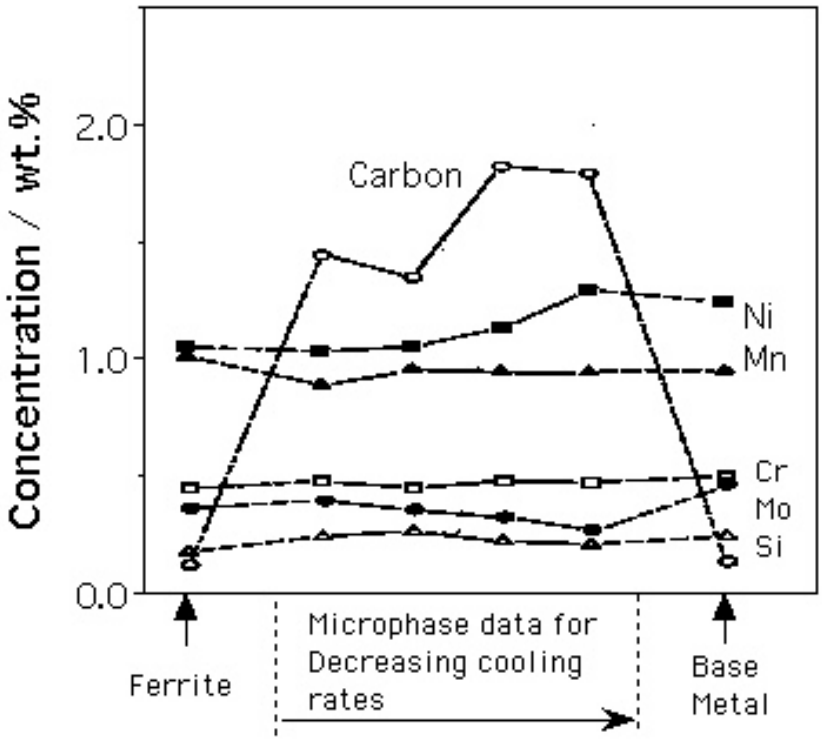

Fig. 29: The distribution of alloying elements in ferrite, the base metal and in the microphases, as a function of the cooling conditions (after Matsuda *et al.*, 1990).

The mechanism by which the microphases influence toughness in low–alloy steels (strength about 800 MPa) have been studied in detail by Chen *et al.* (1984). The effects vary with the test temperature. The films of hard phases tend to crack readily when loaded along their longest dimensions, often splitting into several segments. The blocks of microphases, on the other hand, tend to remain uncracked. At high temperatures, the cracks in the films initiate voids and hence lead to a reduction in the work of ductile fracture. The ferrite, which is softer and deforms first, has a relatively low strength at high temperatures and cannot induce fracture in the blocky microphases. The latter only come into prominence at low temperatures, where their presence induces stresses in the adjacent ferrite, stresses which peak at some distance ahead of the microphase/ferrite interface. This induces cleavage in the ferrite. Larger blocks are more detrimental in this respect because the peak stress induced in the adjacent ferrite is correspondingly larger.

SENSITIVITY TO CARBON

It is striking that small variations in carbon concentration can have a major influence on the microstructure of welds, especially since the average carbon concentration $\overline{x}$ of a weld is usually kept very small. It is apparent from Figs. 7 & 9 that the sensitivity of growth kinetics to carbon becomes larger as the concentration of carbon decreases. These are important observations given that the general trend is to lower the carbon concentrations even for wrought steels, sometimes to levels approaching the solubility of carbon in ferrite. The difference in the solubility of carbon in ferrite ($x^{\alpha\gamma}$) and $\overline{x}$ is therefore small, and the kinetics of transformation increase rapidly as the difference decreases, for two reasons. Firstly, the supersaturation term which appears in most kinetic equations is given by:

$$\Omega = [x^{\gamma\alpha} - \overline{x}]/[x^{\gamma\alpha} - x^{\alpha\gamma}]. \tag{35}$$

It follows that supersaturation increases as $\overline{x}$ tends towards $x^{\alpha\gamma}$. Secondly, during carbon *diffusion–controlled* growth, for example for α and α_w, the amount of carbon that has to diffuse ahead of the interface varies with the difference $\overline{x} - x^{\alpha\gamma}$, and as the latter tends to decrease to zero, the growth velocity increases sharply.

Hence, the effect of carbon is seen to be largest (Figs. 6,10) when $\overline{x}$ changes from 0.03 $\rightarrow$ 0.05 wt.%, when compared with the change from 0.09 $\rightarrow$ 0.11 wt.%. Changes in mechanical properties are found to mimic this behaviour, the strength of low–carbon steels being particularly sensitive to the carbon concentration (Wilson *et al.*, 1988). This increased sensitivity of the austenite to ferrite transformation to carbon at lower concentrations leads to a decreased sensitivity to substitutional alloying elements.

It is interesting that the sensitivity of transformation kinetics to carbon at low concentrations explains the need recognised widely in industry, for two carbon equivalent formulae to cover the high and low carbon steels. This analysis also illustrates how physical models can help ratify empirical experience, and consequently engender confidence in the utilisation of such experience.

$$\text{IIW} \quad > 0.18\,\text{wt.\% C}$$

$$\text{CE} = \text{C} + \frac{\text{Mn} + \text{Si}}{6} + \frac{\text{Ni} + \text{Cu}}{15} + \frac{\text{Cr} + \text{Mo} + \text{V}}{5} \quad \text{wt.\%}$$

$$\text{Ito} - \text{Besseyo} \quad < 0.18\,\text{wt.\% C}$$

$$\text{CE} = \text{C} + \frac{\text{Si}}{30} + \frac{\text{Mn} + \text{Cu} + \text{Cr}}{20} + \frac{\text{Ni}}{60} + \frac{\text{Mo}}{15} + \frac{\text{V}}{10} + 5\text{B} \quad \text{wt.\%}$$

The IIW formula shows much smaller tolerance to substitutional alloying elements than the Ito–Besseyo equation, because at low carbon concentrations the kinetics of transformations become so rapid as to permit increased alloying without unduly increasing the hardenability. Fig. 30 illustrates again that the microstructure and mechanical properties change more rapidly at low carbon concentrations; the calculations are for manual metal arc welds, carried out according to Bhadeshia *et al.*, 1985a.

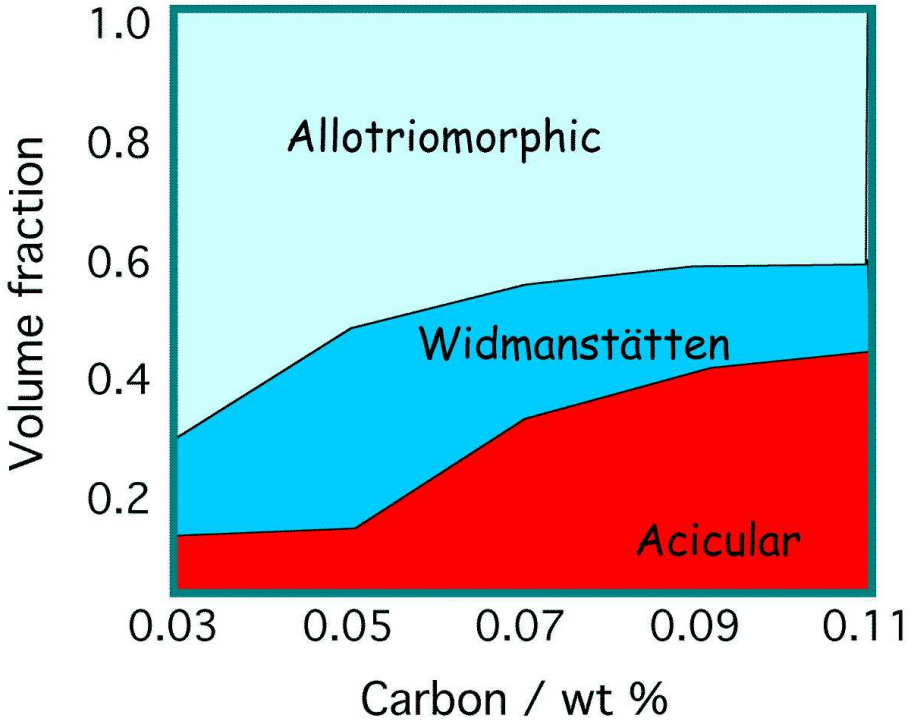

Fig. 30: Calculated variations in microstructure and mechanical properties as a function of carbon concentration in Fe–1Mn–C wt.% steels deposit using manual metal arc welding (1 kJ/mm).

ELEMENTARY MECHANICAL PROPERTIES

Progress in the modelling of mechanical properties has been painfully slow, especially if the modelling is not empirical. The vast majority of investigators seem to be satisfied with regression equations relating chemical composition to mechanical properties. This can be dissatisfying since any regression analysis is limited to the experimental dataset on which it is based, and indeed may not be based on sound physical metallurgy principles. The usual procedure of relating the strength to chemical composition is obviously incorrect, since tempering alters the strength without changing the chemistry.

It has been demonstrated that some reasonable assumptions can be made to simplify the calculation of the strength of multirun weld deposits on a more fundamental basis (Sugden and Bhadeshia, 1988b). A volume fraction V_P is defined to include both the primary microstructure, and the reheated regions which are *fully* reaustenitised, on the grounds that these regions are mechanically similar to the as–deposited regions. The remainder $V_S = 1 - V_P$, includes all the regions which have been tempered or partially reaustenitised, and which have lost most of the microstructural component of strengthening. V_P can be estimated from the alloy chemistry since this in turn influences the extent of the austenite phase field via the Ae_3 temperature (Svensson *et al.*, 1988a,b). It is emphasised that V_P and V_S do not refer to the volume fractions of the primary and secondary microstructures respectively, but are defined in a peculiar way to simplify the task of estimating the strength of multirun welds. Thus, V_P includes the primary microstructure and regions which are fully reaustenitised by the deposition of further material, and V_S includes all the other regions which have essentially lost most of the microstructural component of strength (Svensson *et al.*, 1988a,b).

The yield strength σ_Y of a multirun MMA weld deposit is given by:

$$\sigma_Y = V_P\sigma_P + V_S\sigma_S \tag{36}$$

where σ_P is the yield strength of the primary microstructure, assumed to equal that the reheated regions which are fully reaustenitised. σ_S is the yield strength of regions which have largely lost the microstructural component of strength, and which are either partially reaustenitised or tempered. Recent work has resolved σ_P into components due to the strength of pure, annealed iron σ_{Fe}, solid–solution strengthening components σ_{SS} and microstructural strengthening components σ_α, σ_{α_w} and σ_{α_a}, due to α, α_w and α_a respectively (Sugden and Bhadeshia, 1988b). Similarly, σ_S has been resolved into σ_{Fe}, σ_{SS} and a component due to microstructural strengthening. Hence, both σ_P and σ_S can be estimated from a knowledge of the volume fractions of phases, alloy chemistry and readily available data on the strength of iron.

The solid solution strengthening term discussed above includes the effect of nitrogen concentration. In the calculations that follow, the nitrogen concentration is in the absence of experimental data calculated using methods developed recently (Svensson *et al.*, 1988b; Bhadeshia *et al.*, 1988). It is recognised that these methods are crude, especially for manual metal arc welds, where factors such as arc length and iron powder content have not yet been taken into account. Furthermore, the effects of dilution are not accounted for, although for all–weld metal deposits of the kind considered here, this should not be an important factor. In spite of these difficulties, it is certainly possible to obtain a rough estimate of the nitrogen concentration (Bhadeshia *et al.*, 1988) of MMA weld deposits, as a function of weld chemistry and heat input.

There is a major difficulty in formulating general models for the strength of multirun weld deposits, stemming from the inability to take secondary hardening effects (due to elements like Mo, Cr) into account in estimating σ_S. While in ordinary welds, the secondary microstructure loses most of its microstructural strength, that is clearly not the case for secondary hardening alloys, and this leads to an underestimation of strength (Fig. 31). It is important to realise that precipitation of alloys carbides is not necessary for secondary hardening effects to manifest themselves in hardness data, since preprecipitation phenomena can cause significant strengthening in the reheated regions. There is as yet, no systematic methodology for taking such effects into account.

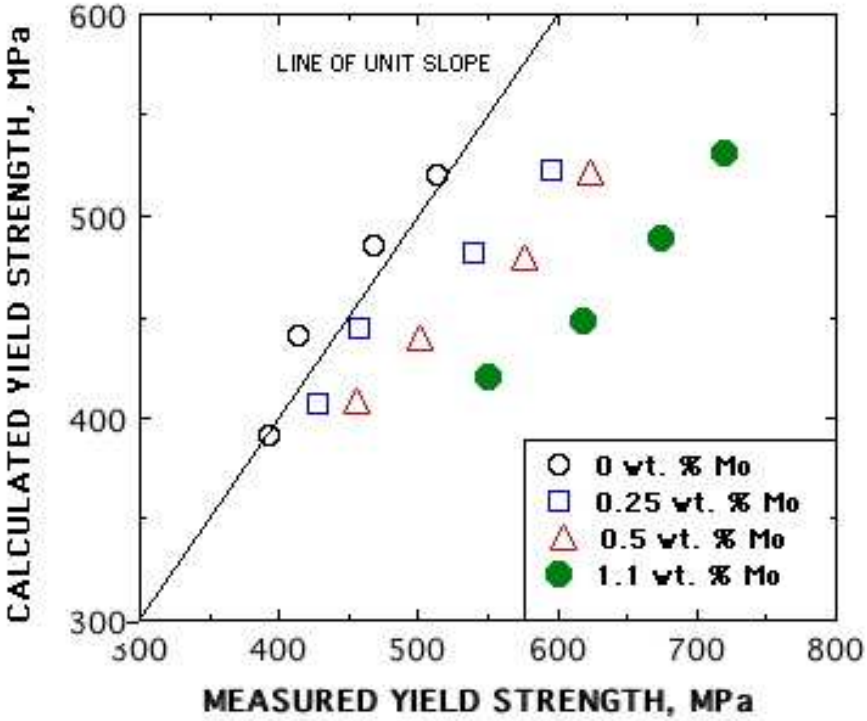

Fig. 31: Plot of the yield strength as calculated using the theory presented by Svensson *et al.* (1988b), versus experimental data due to Evans. Perfect agreement with theory is indicated by the line. The degree of underestimation of strength is clearly seen to increase as the molybdenum concentration of the welds increases.

Ductility There has been a limited amount of progress in the modelling of tensile ductility of the as–deposited microstructure of steel welds (Sugden and Bhadeshia, 1989a). The ductility can to a good approximation be divided into two main components whose magnitudes are assumed to be controlled by different physical processes. These components are the uniform plastic strain, as recorded prior to the onset of macroscopic necking in the tensile specimen, and the nonuniform component which is the remainder of the plastic strain.

By factorising the ductility into these components, it is possible to express the nonuniform component in terms of the inclusion content of the weld deposit, after taking into account variations in specimen cross–sectional area (A_O) and gauge length (L_O):

$$\text{nonuniform elongation}, \% = 100 \times \beta \frac{A_O^{0.5}}{L_O} \tag{37}$$

where β is Barba's constant, but now expressed as a function of the inclusion content:

$$\beta \simeq 1.239 - 9.372 \times (\text{wt.\% O}) + (\text{wt.\% S}). \tag{38}$$

There is as yet no model for estimating the uniform component of strain, but such a model would require a detailed knowledge of the strain hardening behaviour of the individual phases of the microstructure, together with some theory for multiphase deformation. Note that the equation emphasises the role of particles in reducing ductility.

Acicular Ferrite: Mechanism of Toughening An acicular ferrite microstructure is usually assumed to be good for the achievement of a high cleavage toughness. This is because the plates of ferrite point in many different directions, and hence are able to frequently deflect cracks. This should give better toughness when compared with allotriomorphic ferrite, or even Widmanstätten ferrite or bainite, which tends to form in packets of parallel plates (across which cracks can propagate with relative ease). However, good evidence to this latter effect has been lacking. An example is illustrated in Fig. **??**, where the fracture assessed impact transition temperature is plotted as a function of the strength and microstructure (Horii and Okita, 1992). It is obvious that the progressive replacement of a coarse allotriomorphic ferrite microstructure with acicular ferrite, even though the strength increases in the process.

As acicular ferrite is then replaced with bainite, the toughness deteriorates, but the cause of this is not straightforward to interpret because the strength increases at the same time (Fig. 32).

Knott and co–workers have suggested that once a crack is initiated at an inclusion, it propagates without hinderance by acicular ferrite. Recent work by Ishikawa and Haze (1994) has demonstrated that whilst this must be true when the general level of toughness is small, the gradient of stress at any poisition in the vicinity of a crack decreases as the toughness increases. Hence, the propagation behaviour changes, and cleavage cracks are then arrested in an acicular ferrite microstructure but not in one which is dominated by Widmanstätten ferrite.

Scatter in Mechanical Properties Fracture mechanics are widely applied in the design of engineering structures, but difficulties arise when repeated tests of the kind used in characterising toughness, on the same material, yield significantly different results. Such scatter in toughness is a common feature of relatively brittle materials such as ceramics, where it is a key factor limiting their wider application even when the average toughness may be acceptable. Steel users have become increasingly aware in recent years that scatter in toughness data can also be of concern in wrought and welded steels. Apart from the difficulties in adopting values for design purposes, the tests necessary for the characterisation of toughness as a material

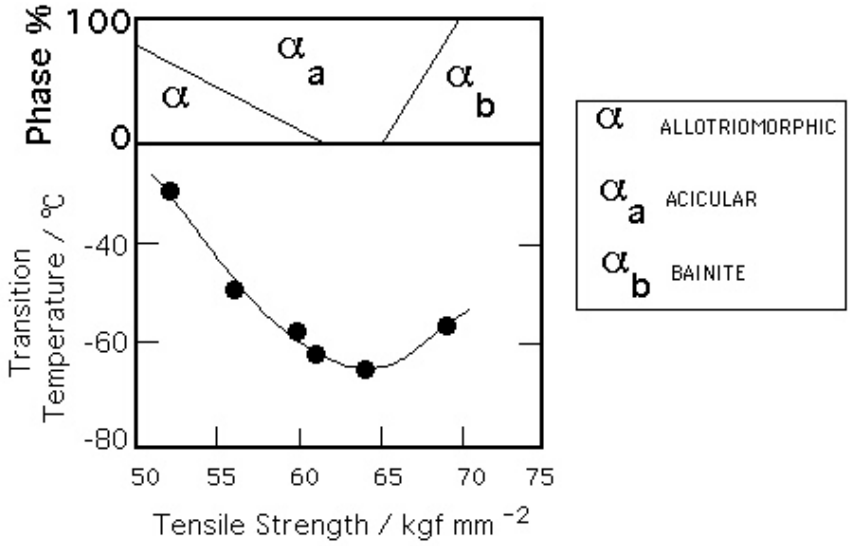

Fig. 32: Variation in the fracture assessed impact transition temperature as a function of the strength of the weld, and of the microstructure (Horii and Ohkita, 1992).

property are rather expensive, the number of experiments needed to establish confidence being larger for less unreliable materials.

A major factor responsible for variations in toughness in welds is likely to be the inclusion population which consists mainly of large oxides originating from the slags used to control the weld pool stability and composition. The inclusions are neither uniform in size, nor are they uniformly distributed in the weld. There is also mounting evidence that variations in microstructure can also be an important factor in influencing scatter in toughness data (Tweed & Knott, 1983, 1987; Bowen *et al.*, 1986; Neville and Knott, 1986; Hagiwara and Knott, 1980). Neville (1985) noted that microstructural inhomogeneities such as hard pearlite islands, can lead to a significant variations in measured fracture toughness values during repeat tests on specimens of the same material.

The two quantities that need to be defined in order to assess variations in mechanical properties are the degree of scatter, and the heterogeneity of microstructure. The definitions have to be of a kind amenable to alloy design techniques, while at the same time being physically meaningful.

Representation of Scatter Consider the scatter commonly observed in impact toughness data. The three most frequently used ways of rationalising variations in results from the toughness testing of weld metals are to take an average of the Charpy readings obtained at a given temperature, measure the standard deviation (Drury, 1984), or plot the lowest Charpy readings obtained in order to focus attention on the lower ends of the scatter bands (Taylor, 1982).

An alternative to this was suggested by (Smith, 1983) who proposed a scatter factor SF to quantify any spread obtained in Charpy values, where

$$SF = \frac{MaximumEnergy - MinimumEnergy}{AverageEnergy} \times 100(\%) \tag{39}$$

This is essentially a definition of *range*. As such, it has the disadvantage of giving excessive weight to the extreme values, taking account of all intermediate results only via the mean in the denominator. The relation is in general an unpredictable function of test temperature.

None of the methods discussed above are completely suitable for alloy design purposes, where the aim is to minimise scatter over the whole of the impact transition curve (the plot of impact energy versus test temperature). An idealised impact energy–temperature curve should be sigmoidal in shape, and the scatter of experimental data can in principle be measured as a root–mean–square deviation about a such a curve, obtained by best–fitting to the experimental data. This gives a representation of scatter in which one value of scatter is defined for each complete impact transition curve. It has the advantage that the value represents the entire dataset used in generating the transition curve.

Representation of Microstructural Heterogeneity Since it is believed that the scatter in Charpy data is amongst other factors, dependent on the nonuniformity of weld microstructure, the degree of inhomogeneity needs to be quantified. This can be done by calculating the entropy H of a given microstructure (Lange, 1967; Karlin and Taylor, 1975).

If X is a random variable assuming the value i with probability p_i, $i = 1, \ldots, n$, the entropy of X, as a logarithmic measure of the mean probability, is computed according to

$$H\{X\} = -\sum p_i \ln\{p_i\}. \tag{40}$$

It should be noted that for $p_i = 1$, $H\{X\} = 0$. Conversely, the entropy is a maximum value $\ln\{n\}$ when $p_1 = \ldots = p_n = \frac{1}{n}$.

The primary microstructure of most common welds can be taken as having three principal constituents: acicular, allotriomorphic and Widmanstätten ferrite. It is important to emphasise that although α_a and α_w have similar strengths, the weld metal microstructure cannot be treated as a two–phase microstructure (with α_a and α_w grouped together), since the *toughnesses* of the two phases are quite different. Therefore, the entropy of a given weld metal microstructure

$$H = -[V_\alpha \ln\{V_\alpha\} + V_a \ln\{V_a\} + V_w \ln\{V_w\}] \tag{41}$$

where V_α, V_a and V_w are the volume fractions of allotriomorphic, acicular and Widmanstätten ferrite respectively.

The entropy of the distribution quantifies the heterogeneity of the microstructure. H will vary from zero for an homogeneous material to $\ln\{3\}$ (*i.e.* 1.099) for a weld with equal volume fractions of the three phases. By multiplying by $1/\ln\{3\}$, the heterogeneity of the three phase microstructure of a weld may be defined on a scale from zero to unity, *i.e.*

$$Het_3 = H \times 0.910. \tag{42}$$

Another scale of heterogeneity can also be addressed, to see if the primary and secondary regions of multipass welds could be treated similarly. Here, the secondary region is taken to comprise that part of the microstructure consisting of partially reaustenitised and significantly tempered regions (Svensson *et al.*, 1988b). It follows that the heterogeneity of the assumed two-phase microstructure is given by

$$Het_2 = -[V_p \ln\{V_p\} + V_s \ln\{V_s\}] \times \frac{1}{\ln\{2\}} \tag{43}$$

where V_p and V_s are the volume fractions of the primary and secondary regions respectively.

It is evident from (Fig. 34a) that there is a strong relationship between the scale parameter, and microstructural heterogeneity for low–alloy steel all–weld metals. Consequently, a significant part of the observed scatter in weld metal Charpy results is attributable to the inhomogeneity of the microstructure, with larger scatter being associated empirically with more heterogeneous microstructures. This result can be compared with the common feature of fracture toughness experiments where the positioning of the fatigue crack is found to be an important factor in CTOD testing of weldments.

The relatively poor correlation for the multipass welds (Fig. 34b) highlights a limitation of this technique. The failure of the method for multirun welds might be attributed to the small range of microstructural entropy in the data analysed, so that the major differences in scatter are attributable to factors such as inclusions rather than microstructure. Secondly, the microstructural entropy term does not weight the phases involved in terms of their mechanical properties, but rather in terms of their volume fractions. This is a significant weakness of the method, since it would predict heterogeneity in a multiphase system even when all the phases exhibit identical mechanical properties. For multirun welds, it is known that the strength of the reheated regions scales with that of the as–deposited regions, so that differences in mechanical properties in such welds should be less than expected intuitively.

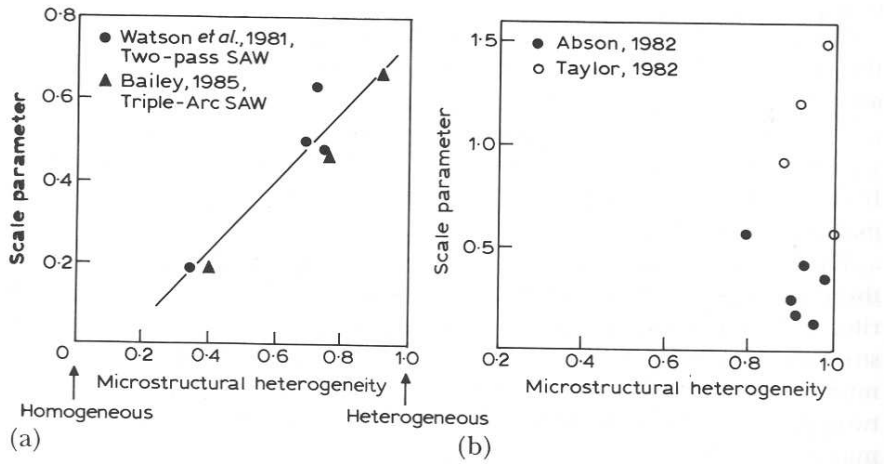

Fig. 33: (a) The relationship between microstructural heterogeneity and scatter, as measured by the scale parameter. Each point corresponds to a calculation using a complete Charpy impact transition curve. (b) Microstructural heterogeneity versus scatter for the manual metal arc, multirun welds, illustrating rather poor correlation.

Effect of Copper on the Mechanical Properties Copper has two primary effects, firstly to retard the transformation of austenite (since it is an austenite stabilising element), and secondly to strengthen ferrite via the precipitation of ϵ–Cu. **Comment somewhere on the role of nickel in copper bearing steels.

In manual metal arc welds, copper is not surprisingly found to lead to an increase in strength, but at concentrations in excess of about 0.7 wt.% to a deterioration in toughness in both the as–welded and stress–relieved states (Es-Souni *et al.*, 1990). There may be a simple explanation for this, in that an increase in strength should indeed lead to a deterioration of toughness, since the comparisons are never at constant strength.

Kluken *et al.* (1994) showed that in submerged arc welds, the yield strength is less sensitive to copper additions than the ultimate tensile strength, perhaps because the copper precipitates cause a greater rate of work hardening. On the other hand, Es–Souni *et al.* (1990) found the rate of change, as a function of the copper concentration, to be identical for both the yeild and tensile strengths, in manual metal arc welds.

The austenite stabilising effect of copper seems to cause either an increase in the microphase content, or changes the nature of the microphases from cementite and ferrite to mixtures of retained austenite and high–carbon martensite (Es–Souni *et al.*, 1990; Alekssev *et al.*, 1991). The presence of copper has not been found to influence either the distribution or the nature of the usual non–metallic inclusions found in steel weld deposits (Es–Souni *et al.*, 1990).

SUGGESTIONS FOR FUTURE RESEARCH

The research reviewed above is limited in some important aspects. The amount of work that needs to be done in order to produce a reliable description of a complete welded joint is daunting. It is hoped that the ideas formulated below stimulate specific investigations in the field of microstructure modelling of welds. A possible form of a coordinated programme of research is illustrated in Fig. 34. It consists of the following major elements, discussed in detail in the sections that follow:

1. The primary microstructure, where trace element effects, nucleation mechanism and a treatment of the kinetics of the acicular ferrite transformation is essential to complete and strengthen existing microstructure models.

2. Kinetics of the reverse transformation to austenite on heating. It is not yet possible to predict the microstructure of multirun welds and of their heat–affected zones because of a lack of knowledge in this area.

3. Constrained welds inevitably develop stresses during cooling, which our preliminary experiments prove have a significant influence on the development of microstructure. This work should lead naturally to the calculation of residual stresses in transforming assemblies.

4. The application of the research to a novel idea on high–strength steel welds.

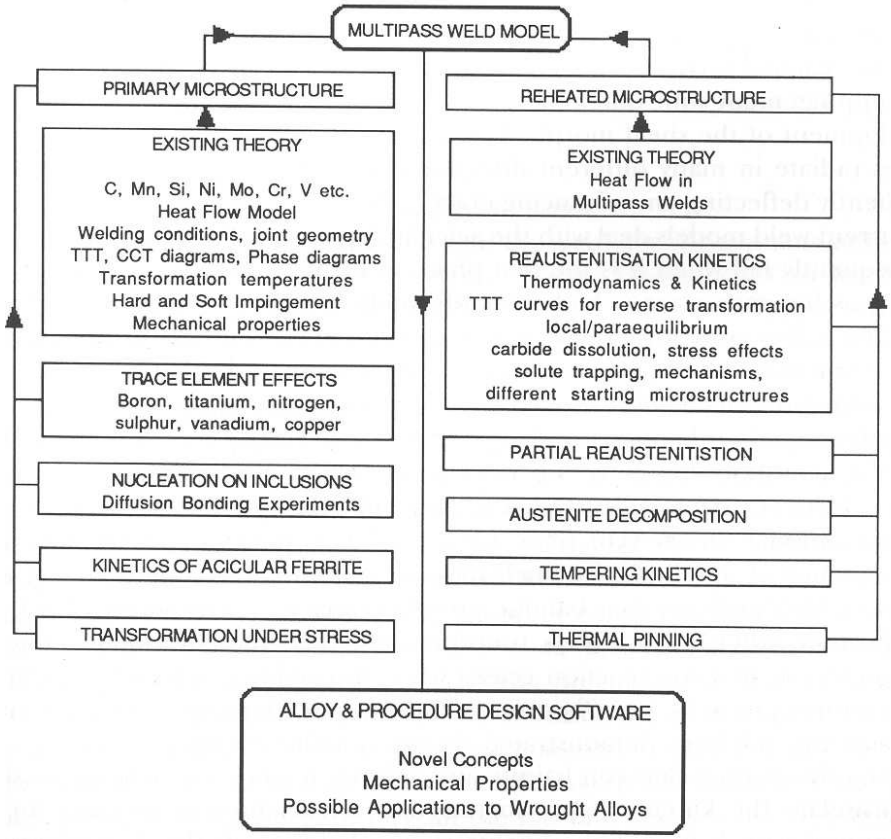

Fig. 34: Flowchart defining future research.

Aspects of the Primary Microstructure Kinetics of the Acicular Ferrite Reaction: Acicular ferrite is beneficial in welds because of its ability to deflect cleavage cracks. There is growing evidence that the mechanism of transformation of acicular ferrite is similar to that of bainite. The microstructures look different because acicular ferrite nucleates intragranularly from point sites (inclusions), and impingement with other plates growing from adjacent sites prevents the development of the sheaf morphology associated with bainite. Acicular ferrite plates radiate in many different directions from their point nucleation sites, frequently deflecting any advancing crack.

Current weld models deal with the acicular ferrite content by difference, and consequently fail when it is the first phase to form during the cooling of austenite, as happens in many high–strength welds. There is therefore, a pressing need for a first principles theoretical treatment of the kinetics of the acicular ferrite reaction. This has never before been attempted, probably because the transformation mechanism has only recently been clarified. Kinetic theory has been developed for bainitic transformations (Bhadeshia, 1981a). This theory accounts for the fact that the activation energy G^* for nucleation varies linearly with the chemical driving force (*i.e.,* $G^* \propto \Delta G^{\gamma\alpha}$) rather than the inverse square relationship found in conventional theory (*i.e.,* $G^* \propto (\Delta G^{\gamma\alpha})^{-2}$). This peculiar dependence is a consequence of the displacive nucleation mechanism. The kinetic theory also includes the condition that bainitic growth ceases in circumstances far from equilibrium, when diffusionless transformation becomes thermodynamically impossible,

so that the reaction ceases when the residual austenite reaches a composition given by the T'_O curve on the phase diagram. This particular characteristic has been demonstrated also for acicular ferrite.

Given the analogy between bainite and acicular ferrite, it should be possible to formulate the kinetic theory for acicular ferrite after accounting for its intragranular nucleation. Experiments are needed to verify the dependence of the activation energy for the nucleation of acicular ferrite on inclusions, on the chemical driving force. In particular, it is necessary to design and study samples in which the ratio of grain surface to intragranular nucleation densities varies. Monitoring the onset of a detectable degree of acicular ferrite formation then enables the free energy dependence to be deduced. It should be necessary to cover a range of alloys to give sufficient variation in the driving force at constant temperature. The theory should then be tested against experimental kinetic data on acicular ferrite in low–alloy steels.

Nucleation–Diffusion Bonding Experiments: The complex microstructure and constitution of the nonmetallic inclusions responsible for acicular ferrite nucleation makes it difficult to conduct controlled experiments to assess their nucleation potencies. Some feasibility studies have been conducted using a new technique designed to overcome these problems (Strangwood, 1987). Pure ceramics of well defined composition, purity, crystallinity and structure were diffusion bonded to steels which were then heat treated. By comparing the events at the ceramic/steel interface with those within the steel at a distance from this interface, it is possible to deduce conclusively whether the ceramic *stimulates* ferrite nucleation. These experiments were limited by the equipment then available. Modern thermomechanical simulators should enable the study of the heterogeneous nucleation of acicular ferrite on ceramics rather than the allotriomorphic ferrite obtained in earlier experiments (Strangwood & Bhadeshia, 1988).

Inclusion Microstructure: It is currently assumed in calculations that the weld deposit contains sufficient intragranular nucleation sites for acicular ferrite formation. This has been shown to be reasonable for typical arc welds which contain sufficient levels of impurity elements, and for those welds in which the acicular ferrite content depends largely on the major alloying additions. There is nevertheless, a considerable body of evidence that in certain welds, quantities of boron, titanium, aluminium, sulphur, nitrogen, and other trace elements can alter the evolution of the microstructure. To deal with these important cases, it is necessary to be able to predict and control the *inclusion* microstructure and chemistry.

The modelling of inclusions from a knowledge of the trace elements has relied on the assumption of chemical equilibrium and a phenomenological sequence of reactions, carried out in an order consistent with the perceived thermodynamic stability of the individual elements. This leads to anomalies, such as the incorrect prediction of TiN/TiO precipitation. There is also the doubtful assumption that the relative stabilities of the compounds that form can be assessed using free energy data which are standardised for the reaction of each metallic element with one mole of oxygen, the oxide and the pure element have unit activities. In fact, all the reactant and product activities are far from unity, so that the ranking of the oxide stabilities can change significantly as a function of the actual concentrations involved. It is necessary to investigate a more rigorous method based on solution thermodynamics and growth kinetics. The activities of the individual trace elements will be computed using Wagner interaction parameters (some of which will have to be deduced from an assessment of the appropriate phase diagrams and

thermochemical data), so that the oxidising or nitriding potentials, and the reaction states, of the individual elements can be ranked correctly.

Reverse Transformation to Austenite Past efforts at the prediction of the microstructure in the heat affected zones of steel welds, consist essentially of heat flow and austenite grain growth theory, combined with highly empirical microstructural estimates. There remain major hurdles in the modelling of *multirun* welds and their heat–affected zones. Such welds are fabricated by sequentially depositing many layers of metal in order to fill the weld gap; this procedure is adopted where quality is of paramount importance. The completed layers are therefore reheated each time a new layer is deposited. This causes them to undergo partial or complete reverse transformation to austenite which on subsequent cooling retransforms to a different *secondary* microstructure. Other regions of this secondary microstructure which do not reach high enough peak temperatures are tempered during reheating.

The theory for the rate of the reverse transformation to austenite, and hence for predicting the secondary microstructure hardly exists in any useful form, making it impossible to predict a TTT diagram for reaustenitisation, let alone partial reaustenitisation. The subsequent decomposition of the austenite cannot be modelled with any confidence; nor can the changes in the tempered regions. The ideas for developing such theory are discussed below.

Conditions at the transformation interface: Austenite in welds grows by reconstructive transformation because the high temperatures involved permit a closer approach to equilibrium. Unlike the $\gamma \rightarrow \alpha$ reaction, both the driving force for transformation and the diffusivity increase with superheat, so that the reaction rate increases indefinitely with temperature. The mechanism of reconstructive transformation is complicated by the multicomponent constitution of most steels. Several species of atoms therefore diffuse during growth, at very different rates, and it is not a trivial matter to match the fluxes of all the elements in a manner consistent with the velocity of the interface, while at the same time, retain local equilibrium exists at the interface. When Fe–C–X alloys (X being a metallic solute) are transformed at low supersaturations, there is bulk partitioning of the slow diffuser, the activity gradient of the fast diffuser being reduced to a negligible level. At larger supersaturations, there is negligible partitioning of the slow diffuser, so that its activity gradient in the parent phase is large enough to allow it to keep pace with the faster diffusing element. Paraequilibrium transformation involves zero partitioning of substitutional elements during transformation, the ratio of substitutional solute to iron atoms being constant everywhere, even on the finest conceivable scale.

There is no satisfactory theory for the transition from local equilibrium to paraequilibrium. The conjecture that the transition occurs when the calculated extent of the diffusion field of the slow diffuser becomes comparable to atomic dimensions is known to be incorrect. For austenite growth, the task is rather more complicated in that the transition from local to paraequilibrium is expected to occur as the transformation temperature increases. The transition is therefore not stimulated by a lack of atomic mobility, but by an increase in the interface velocity.

Concentration profiles at the transformation interfaces have to be characterised in detail, firstly to establish the local equilibrium assumption, and secondly to provide direct experimental data on the conditions under which local equilibrium gives way to paraequilibrium during reaustenitisation. It may even be the case that the paraequilibrium condition does not exist when the

mechanism of transformation is reconstructive. These characterisations require chemical and spatial resolution on an atomic scale for all the relevant elements and will be carried out using a specially designed field–ion microscope/atom probe.

Solute Trapping Although it is usual to assume the existence of some kind of equilibrium or constrained equilibrium at the transformation interface, there is in principle not reason why the transformation should not occur with some partitioning of solute species, and some *solute trapping*. Trapping implies that the chemical potential of the species increases on transfer across the interface, and represents a nonequilibrium event. There could thus be an infinite number of possible kinetic conditions between the states of local equilibrium and paraequilibrium.

It is possible to obtain unique solutions for the relation between interface velocity, transformation temperature and carbon supersaturation by solving simultaneously, three separate interface response functions which are descriptions of interface mobility, diffusion field velocity and solute trapping velocity. We propose to develop this theory for reaustenitisation. A major advantage here is that the partially transformed sample can be configurationally frozen by quenching for subsequent examination in an atom–probe. The research should help resolve many fundamental issues on nonequilibrium transformations.

Overall Kinetics of Reaustenitisation: Quantitative studies of the degree of isothermal austenite formation as a function of time, temperature and alloy chemistry will form an essential database for the kinetic theory. Initial experiments will be conducted on samples already containing some austenite so that the growth phenomenon can be studied in isolation. Further work will compare against the growth experiments to reveal clearly the role of austenite nucleation. TTT and continuous–heating–transformation diagrams for reaustenitisation as a function of different starting microstructures will be measured for the analysis discussed below. In this context, it is noteworthy that attempts at predicting the austenite grain size are based entirely on coarsening theory. This ignores the fact that the grain size prior to the onset of coarsening is determined by the austenite to ferrite *transformation* kinetics. The work proposed here is an ideal basis for a fresh look at austenite grain size prediction, including the alloy carbide/nitride solution and precipitation kinetics.

Kinetic Model for Reaustenitisation: The aim here would be to produce a model capable of calculating the TTT diagrams for reaustenitisation as a function of alloy chemistry and starting microstructure. This is probably a very ambitious aim – it has never before been attempted, and the number of variables is very large indeed. For this reason, initial work should focus on starting microstructures important in the welding problems, consisting mainly of allotriomorphic ferrite, Widmanstätten ferrite and acicular ferrite. Overall reaction kinetics will be treated in terms of the theory of nucleation and growth in multicomponent systems. The diffusion during growth (unusually) takes place in the growing phase (austenite). Since the austenite particles are at first very small, soft–impingement (overlap of diffusion fields) effects occur early in the transformation. Consequently, finite difference methods will have to be used in the prediction of kinetic behaviour and in the treatment of the transformation behaviour of partially reaustenitised microstructures.

Transformation under the Influence of Stress None of the weld microstructure models to date take any account of the influence of stress on transformation kinetics, even though the residual stresses in constrained welds can be limited only by yielding. Displacive transformations such as acicular ferrite should be particularly sensitive to stress since the invariant–plane strain (IPS) shape deformation has a large shear component. Its interaction with the applied stress (or that of the lattice deformation during nucleation) adds a " mechanical" driving force, which may complement or oppose the chemical driving force. For acicular ferrite, the stored energy due to the IPS shape deformation is a large fraction of the typically available chemical driving force.

Any response to stress for transformations like acicular ferrite, is complicated by the partitioning of carbon either after or during growth. There is no quantitative treatment in this respect, probably because the reported experiments are incomplete from the point of view of theoretical analysis. The transformation strains have been never been monitored along more than one direction; in fact, they are not expected to be isotropic, given the IPS shape change and the inevitable fact that polycrystalline specimens are textured. Consequently, uniaxial data are of little use in deconvoluting the total strain into transformation plasticity and dilatational strain.

It is necessary to study of both the bainite and acicular ferrite reactions with the samples under tensile or compressive stresses. The bainite to acicular ferrite transition will be induced by altering the relative number densities of austenite grain to intragranular nucleation sites. Stress well below the austenite yield strength will be applied at first, during isothermal transformation, to avoid complications due to plastic deformation prior to transformation. The kinetics of the transformation and the transformation plasticity must be deduced as a function of time at temperature using radially symmetrical samples.

The absolute dilatational strains can be converted directly to the extent of reaction. For the growth process, it is likely that the stress effect can be modelled from the interaction of the macroscopic shape strain with the applied stress. Additional factors that may have to be considered include any changes in the level of intervariant–accommodation as the microstructure complies with the imposed stress, and any consequent changes in the degree of plastic accommodation of the shape strain. Differential scanning calorimetry experiments can be conducted to measure the amount of energy stored in the sample after ordinary transformation, and that after transformation under stress. The nucleation–stress interaction is more complicated by virtue of the fact that it is less understood. The nucleation behaviour of bainite (and perhaps that of acicular ferrite) can be rationalised using martensitic nucleation theory but allowing the partitioning of carbon at the nucleation stage. The free energy needed to obtain a detectable rate of nucleation has to exceed a level specified by the universal function G_N (a unique function for all steels) which varies linearly with temperature. Experiments will be conducted on acicular ferrite to verify this behaviour in zero stress experiments, followed by the application of finite stresses.

The nucleation and growth phenomena can then be combined into an overall transformation kinetics model to cover anisothermal transformation kinetics, beginning with the pragmatic approximation of additivity.

The measured strains can form the basis of a model for calculating the residual stress developed in welds as they cool. Some classic experiments by Jones and Alberry illustrated clearly that displacive reactions alter radically the nature of the residual stresses. However, the usual

assumption that the effect arises due to transformation plasticity caused by volume changes is bound to be incorrect, because the stress favours compliant crystallographic variants so that the transformation plasticity may be dominated by the much larger shear strains.

Some samples will be metallographically polished prior to transformation under stress in the environmental chamber of the thermomechanical simulator, giving unique data on the stress / crystallography interaction, data of importance in choosing variant selection criteria, and hence in calculating the mechanical driving force. Experimental data will be collected for a number of designed alloys, including those giving carbide–free transformations, and others in which mixed allotriomorphic/bainite microstructures are obtained. In this way, the effects of mixed reactions (which inevitably happen in "real" situations can also be characterised.

A Novel Application Mechanically Homogeneous, High–Strength Multirun Welds: There is growing evidence that mechanical and microstructural inhomogeneity of the type associated with multirun welds leads *scatter* in mechanical properties. For toughness, the lower bound within the scatter has to be accepted for design, leading to a less than optimum exploitation of material properties. The problem can be circumvented in single–run welds but the high heat input required leads to poorer quality. Tempering treatments or weld refinement techniques can also lead to mechanical homogeneity but at the expense of mean strength. Here we suggest a novel method designed to produce homogeneous multirun welds of high strength and toughness, with a microstructure of acicular ferrite and ductile martensite by simultaneously satisfying four conditions:

1. The Ae3 temperature of the weld metal should be reduced, so that the effect of depositing a new layer is to reaustenitise as much of the adjacent substrate as possible.

2. The hardenability must be adjusted to permit the reaustenitised regions to transform back on cooling, to a microstructure consisting of the required mixture of acicular ferrite and ductile martensite.

3. A low Ae3 also ensures that reheated regions which are not reaustenitise, are not excessively tempered (to avoid a loss of strength). The alloy concerned must be designed to be resistant to tempering.

4. The strength of acicular ferrite is limited and must be enhanced by the presence of martensite. A low average carbon concentration is essential to ensure ductile martensite. Unusually, the fraction of acicular ferrite must be kept small ($\simeq 0.5$) to avoid excessive austenite carbon–enrichement which could embrittle the martensite. These interactions need to be fully modelled before embarking on any experimental programme.

Widmanstätten ferrite – MECHANICAL PROPERTIES

There are many investigations which suggest that Widmanstätten ferrite can be detrimental to toughness (Owen *et al.*, 1957; Gulyaev and Guzovskaya, 1977; Koval'chuk *et al.*, 1979; Chilton and Roberts, 1979, 1980; Otterberg *et al.*, 1980; Stenbacka, 1980; Morrison and Preston, 1984; Glover *et al.*, 1984; Huang *et al.*, 1989). Recent work involving controlled experiments has,

however, established that when the microstructure is changed from one which is predominantly allotriomorphic ferrite, to one containing Widmanstätten ferrite, there is an improvement in both the toughness and strength (Bodnar and Hansen, 1994). This might be expected since large fractions of Widmanstätten ferrite are usually associated with refined microstructures.

It is sometimes claimed that the presence of Widmanstätten ferrite changes the deformation behaviour by inducing continuous yielding during tensile deformation, whereas discontinuous yielding is characteristic of microstructures dominated by allotriomorphic ferrite. However, some careful studies by Bodnar and Hansen (1994) show that even microstructures containing Widmanstätten ferrite often show discontinuous yielding behaviour. They suggested that in cases where continuous yielding has been reported, the microstructures contained sufficient quantities of bainite or martensite to mask the deformation behaviour of Widmanstätten ferrite.

APPENDIX 1

Key Characteristics of Transformations in Steels Table 4 lists the key characteristics of phase transformations in steels. The nomenclature used for the transformation products is as follows: martensite (α'), lower bainite (α_{lb}), upper bainite (α_{ub}), acicular ferrite (α_a), Widmanstätten ferrite (α_w), allotriomorphic ferrite (α), idiomorphic ferrite (α_i), pearlite (P), substitutional alloying elements (X). Consistency of a comment with the transformation concerned is indicated by ($=$), inconsistency by ($\neq$); cases where the comment is only sometimes consistent with the transformation are indicated by a bullet ($\bullet$). The term *parent* γ implies the γ grain in which the product phase grows. Note that it is not justified to distinguish massive ferrite from α.

Notes Related to Table 4 Nucleation and growth reactions are of first order in the Ehrenfest classification; in all such reactions, the parent and product phases can coexist, and are separated by well–defined interfaces. Martensitic transformations, although they can be rapid, still involve a nucleation and growth process.

It is significant that all of the ferrite crystals which grow in the form of plates cause an invariant–plane shape deformation which is dominated by shear. The ferrite within pearlite does not have a plate morphology; Hillert showed some time ago that it is wrong to consider pearlite as alternating layers of ferrite and cementite – instead a colony of pearlite is an interpenetrating bicrystal of ferrite and cementite.

Reconstructive diffusion is the flow of matter necessary to avoid the strains characteristic of displacive transformations. A diffusional transformation may phenomenologically be regarded as a combination of a lattice change and a recrystallisation of the product phase, reconstructive diffusion being the flow necessary for the recrystallisation process.

In diffusionless transformations, it is possible to specify (in a localised region at least) how particular vectors, planes and unit cells of one structure (defined by an imaginary labelling of the individual atoms) are derived from *corresponding* vectors, planes and unit cells of the other structure. This is termed a lattice correspondence and it defines a pure lattice deformation which carries the original lattice points, or some fraction of these points into points of the new lattice. When interstitial atoms are present, they may move over large distances during transformation

Table 4: Characteristics of solid–state transformations in steels.

Comment	α'	α_{lb}	α_{ub}	α_a	α_w	α	α_i	P
Nucleation and growth reaction	$=$	$=$	$=$	$=$	$=$	$=$	$=$	$=$
Plate shape	$=$	$=$	$=$	$=$	$=$	$\neq$	$\neq$	$\neq$
IPS shape change with large shear	$=$	$=$	$=$	$=$	$=$	$\neq$	$\neq$	$\neq$
Diffusionless nucleation	$=$	$\neq$	$\neq$	$\neq$	$\neq$	$\neq$	$\neq$	$\neq$
Only carbon diffuses during nucleation	$\neq$	$=$	$=$	$=$	$=$	$\neq$	$\neq$	$\neq$
Reconstructive diffusion during nucleation	$\neq$	$\neq$	$\neq$	$\neq$	$\neq$	$=$	$=$	$=$
Often nucleates intragranularly on defects	$=$	$\neq$	$\neq$	$=$	$\neq$	$\neq$	$=$	$\neq$
Diffusionless growth	$=$	$=$	$=$	$=$	$\neq$	$\neq$	$\neq$	$\neq$
Reconstructive diffusion during growth	$\neq$	$\neq$	$\neq$	$\neq$	$\neq$	$=$	$=$	$=$
Atomic correspondence (all atoms) during growth	$=$	$=$	$=$	$=$	$\neq$	$\neq$	$\neq$	$\neq$
Atomic correspondence only for atoms in substitutional sites	$=$	$=$	$=$	$=$	$=$	$\neq$	$\neq$	$\neq$
Bulk redistribution of X atoms during growth	$\neq$	$\neq$	$\neq$	$\neq$	$\neq$	$\otimes$	$\otimes$	$\otimes$
Local equilibrium at interface during growth	$\neq$	$\neq$	$\neq$	$\neq$	$\neq$	$\otimes$	$\otimes$	$\otimes$
Local paraequilibrium at interface during growth	$\neq$	$\neq$	$\neq$	$\neq$	$=$	$\otimes$	$\otimes$	$\neq$
Diffusion of carbon during transformation	$\neq$	$\neq$	$\neq$	$\neq$	$=$	$=$	$=$	$=$
Carbon diffusion-controlled growth	$\neq$	$\neq$	$\neq$	$\neq$	$=$	$\otimes$	$\otimes$	$\otimes$
Co-operative growth of ferrite and cementite	$\neq$	$\neq$	$\neq$	$\neq$	$\neq$	$\neq$	$\neq$	$=$
High dislocation density	$=$	$=$	$=$	$=$	$\otimes$	$\neq$	$\neq$	$\neq$
Incomplete reaction phenomenon	$\neq$	$=$	$=$	$=$	$\neq$	$\neq$	$\neq$	$\neq$
Necessarily has a glissile interface	$=$	$=$	$=$	$=$	$=$	$\neq$	$\neq$	$\neq$
Always has an orientation within the Bain region	$=$	$=$	$=$	$=$	$=$	$\neq$	$\neq$	$\neq$
Grows across austenite grain boundaries	$\neq$	$\neq$	$\neq$	$\neq$	$\neq$	$=$	$=$	$=$
High interface mobility at low temperatures	$=$	$=$	$=$	$=$	$=$	$\neq$	$\neq$	$\neq$
Displacive transformation mechanism	$=$	$=$	$=$	$=$	$=$	$\neq$	$\neq$	$\neq$
Reconstructive transformation mechanism	$\neq$	$\neq$	$\neq$	$\neq$	$\neq$	$=$	$=$	$=$

without affecting the lattice correspondence; this is sometimes loosely expressed by stating that there is an atomic correspondence for the solvent and substitutional solute atoms but not for the interstitial atoms. A further relaxation of the condition is to allow the solvent and substitutional solute atoms to be displaced during transformation among the sites specified by the lattice correspondence, but not to create new sites or to destroy any specified sites; in this way the lattice correspondence is preserved but there is no longer an atomic correspondence. Note that in the classification presented above, the single atomic jumps of interstitial atoms needed to destroy Zener ordering (which is produced automatically by the Bain correspondence) are not taken into account.

Even though two crystals may have an identical *bulk* composition, it may not be concluded that their compositions at the transformation interface are identical. There are modes of transformation (*e.g.,* negligible partitioning local equilibrium) where the bulk compositions are predicted to be identical but where the phases differ in the vicinity of the transformation interface. For plain carbon steels, there is no difference between equilibrium and paraequilibrium.

The incomplete reaction phenomenon implies that when a reaction can be studied in isolation, it stops before the phases reach their equilibrium or paraequilibrium compositions when stored energy terms have been accounted for.

An orientation within the Bain region means a reproducible relation which may be irrational but is close to the rational NW or KS relations.

Massive ferrite is not classified as a separate morphology since it can be included within allotriomorphic or idiomorphic ferrite.

ACKNOWLEDGMENTS

We are grateful to ESAB AB (Sweden) for financing some of this research, and to Professor Colin Humphreys for the provision of research facilities at the University of Cambridge. The Science and Engineering Research Council also provided financial support via several CASE awards. It is a particular pleasure to acknowledge the numerous contributions made by members of the Phase Transformations Group at Cambridge. Our discussions with Suresh Babu have been particularly stimulating. Some of this work has been carried out under the auspices of the "Atomic Arrangements: Design and Control Project", which is a collaboration between the University of Cambridge and the Japan Research and Development Corporation.

REFERENCES

.

Abson, D. J., (1987a) Nonmetallic Inclusions in Ferritic Steel Weld Metals – A Review, IIW Doc. IX–1486–87.

Abson, D. J., (1987b) *Welding Institute Research Report 7931.01/86/544.3.* The Welding Institute, Cambridge, U. K., 1–30.

Abson, D. J., (1988) Welding Institute Research Report 376/1988, Cambridge, UK.

Abson, D. J. and Pargeter, R. J., (1986) *Int. Met. Rev.,* **31,** 141–194.

Akselsen, O. M., Grong, ϕ., Ryum, N. and Christensen, N., (1986) *Acta Metallurgica,* **34,** 1807–1815.

Alberry, P. J. and Jones, W. K. C., (1979) CEGB report R/M/R282, Marchwood Engineering Laboratories, Marchwood, Southampton, U. K.

Alberry, P. J. and Jones, W. K. C., (1982) *Metals Technology,* **9,** 419–427.

Alberry, P. J., Brunnstrom, R. R. L. and Jones, K. E., (1983) *Metals Technology,* **10,** 28–38.

Alekseev, A. A., Shevchenko, G. A., Pokhodnya, I. K. and Yurlov, B. V., (1991) Effect of copper on structure and properties of multilayer C–Mn–Ni weld metal *IIW Document II–A–845–91,* 1–7.

Ashby, M. F. and Easterling, K. E., (1982) *Acta Metallugica,* **30,** 1969–1978.

Atkinson, C., (1967) Numerical Solutions to Planar Growth where the Diffusion Coefficient is Concentration Dependent, *Acta Metallurgica,* **16,** 1019–1022.

Babu, S. S. and Bhadeshia, H. K. D. H., (1990) *Materials Science and Technology,* **6,** 1005-1020.

Babu, S. S., Bhadeshia, H. K. D. H. and Svensson, L.–E., (1991) *J. of Materials Science Letters,* **10,** 142–144.

Babu, S. S. and Bhadeshia, H. K. D. H., (1992) *Materials Science and Engineering,* **A156,** 1–9.

Bailey, E. F., (1954) *Transactions ASM,* **46,** 830–850.

Baker, R. G. and J. Nutting, (1959) *Journal of the Iron and Steel Institute,* **192,** 257–268.

Barbaro, F. J., Edwards, R. H. and Easterling, K. E., (1988) The Composition and Morphology of Nonmetallic Inclusions in HSLA Steel Weld Metals, *Proc. 7th Australian X–Ray Analysis Association AXAA–88, University of Western Australia,* 1–14.

Barbaro, F. J., Krauklis, P. and Easterling, K. E., (1989) *Materials Science and Technology,* **5,** 1057–1068.

Barritte, G. S. and Edmonds, D. V., (1982) Advance in the Physical Metallurgy and Applications of Steels, The Metals Society, London, 126–135.

Barritte, G. S., Ricks, R. A. and Howell, P. R., (1982) *Quantitative Microanalysis with High Spatial Resolution,* The Metals Society, London. 112–118.

Bhadeshia, H. K. D. H., (1981a) *Acta Metallurgica,* **29,** 1117–1130.

Bhadeshia, H. K. D. H., (1981b) *Metal Science,* **15,** 477–479.

Bhadeshia, H. K. D. H., (1982) *Metal Science,* **16,** 159–165.

Bhadeshia, H. K. D. H., (1985a) *Progress in Materials Science,* **29,** 321–386.

Bhadeshia, H. K. D. H., (1985b) *Mat. Science and Technology,* **1,** 497–504.

Bhadeshia, H. K. D. H., (1987) *Geometry of Crystals,* Institute of Metals, London, p.55.

Bhadeshia, H. K. D. H., (1988a) *Scripta Metallurgica,* **22,** I–IV.

Bhadeshia, H. K. D. H., (1988b) Phase Transformations '87, Ed. G. W. Lorimer, Institute of Metals, London, 309–314.

Bhadeshia, H. K. D. H., (1989) Recent Trends in Welding Science and Technology, eds. S. A. David and J. M. Vitek, ASM International, Ohio, U. S. A., 189–198.

Bhadeshia, H. K. D. H., (1990) *Metallurgy, Welding and Qualification of Microalloyed (HSLA) Steel Weldments,* American Welding Society, Florida, U.S.A., 1–35, in press.

Bhadeshia, H. K. D. H. and D. V. Edmonds, (1980) *Acta Metallurgica,* **28,** 1265–1273.

Bhadeshia, H. K. D. H., Svensson, L.–E. and Gretoft, B., (1983) Acta Universitatis Ouluensis, Series C, No.26, University of Oulu, Finland (Proc. of the 3rd Scandanavian Symposium on Materials Science), 73–78.

Bhadeshia, H. K. D. H., Svensson, L.–E. and Gretoft, B., (1985a) *Acta Metallurgica,* **33,** 1271–1283.

Bhadeshia, H. K. D. H., Svensson, L.–E. and Gretoft, B., (1985b) *J. of Materials Science Letters,* **4,** 305–308.

Bhadeshia, H. K. D. H., Svensson, L.–E. and Gretoft, B., (1986a) *J. Mat. Science,* **21,** 3947–3951.

Bhadeshia, H. K. D. H., Svensson, L.–E. and Gretoft, B., (1986b) 4th Scand. Symp. on Mat. Science, Norwegian Institute of Technology, Norway, 153–158.

Bhadeshia, H. K. D. H., Svensson, L.–E. and Gretoft, B., (1986c) Prediction of the Microstructure of Submerged–Arc Linepipe Welds, *Proceedings of the Third International Conference on Welding and Performance of Pipelines,* ed. P. M. Hart, Welding Institute, Cambridge, 1–10.

Bhadeshia, H. K. D. H., Svensson, L.–E. and Gretoft, B., (1987a) *Welding Metallurgy of Structural Steels,* ed. J. Y. Koo, AIME, Warrendale, Penn. 517–530.

Bhadeshia, H. K. D. H., Svensson, L.–E. and Gretoft, B., (1987b) Advances in the Science and Technology of Welding, ASM, Metals Park, Ohio, 225–229.

Bhadeshia, H. K. D. H., Svensson, L.–E. and Gretoft, B., (1988) *J. Materials Science Lett.,* **7,** 610–612.

Bhadeshia, H. K. D. H. and Svensson, L.–E, (1989a) Effect of Alloying Additions on the Microstructure and Properties of Vertical–Up MMA Welds, Part I, *Joining and Materials,* **2,** 182R–187R.

Bhadeshia, H. K. D. H. and Svensson, L.–E, (1989b) Effect of Alloying Additions on the Microstructure and Properties of Vertical–Up MMA Welds, Part II, *Joining and Materials,* **2,** 236R–238R.

Bhadeshia, H. K. D. H., and Svensson, L.–E., (1989c) *J. Materials Science,* **24,** 3180–3188.

Bhadeshia, H. K. D. H. and Christian, J. W., (1990) *Metallurgical Transactions A,* **21A,** 767–797.

Bodnar, R. L. and Hansen, S. S., (1994) *Metallurgical and Materials Transactions A,* **25A,** 763–773.

Bowen, P., Druce, S. G. and Knott, J. F., (1986) *Acta Metallurgica,* **34,** 1121–1131.

Briant, C. L. and Banerji, S. K., (1978) *International Metals Reviews,* **232,** 164–199.

Bramfitt, B. L. and Marder, A. R., (1973) *Metallurgical Transactions,* **4,** 2291.

Bronshtein, I. N. and Semendyayev, K. A., (1973) *A Guide Book to Mathematics,* Verlag Harri Deutsch, Frankfurt, Germany, 106–107.

Buchmayr, B. and Cerjak, H., (1988) "Weld Quality: Role of Computers" Pergamon Press, Oxford, 43–50.

Buki, A. A., (1992) Calculating the chemical composition of deposited metal when welding with coated electrodes *Welding International,* **6,** 818–820.

Calvo, F. A., Bently, K. P. and Baker, R. G., (1963) Studies of the Welding Metallurgy of Steels, BWRA, Abingdon, Cambridge, 71.

Chandrasekharaiah, M. N., Dubben, G. and Kolster, B. H., (1994) An atom probe study of retained austenite in ferritic weld metal *American Welding Journal,* **71,** 247s–252s.

Chart, T. G., Counsell, J. F., Jones, G. P., Slough, W., Spencer, P. J., (1975) *Int. Met. Rev.,* **20,** 57–82.

Chen, J. H., Kikuta, Y., Araki, T., Yoneda, M. and Matsuda, Y., (1984) *Acta Metallurgica,* **32,** 1779–1788.

Chijiiwa, R., Tamehiro, H., Hirai, M., Matsuda, H. and Mimura, H., (1988) *Offshore Mechanicas and Arctic Engineering Conference,* Houston, Texas.

Chilton, J. M. and Roberts, M. J., (1979) *Vanadium in High Strength Steels,* Vanitec, London, 11–21.

Chilton, J. M. and Roberts, M. J., (1980) *Metallurgical Transactions A,* **11A,** 1711–1721.

Christian, J. W., (1975) Theory of Transformations in Metals and Alloys, 2nd ed., Part I, Pergamon Press, Oxford.

Christian, J. W. and Edmonds, D. V., (1984) Phase Transformations in Ferrous Alloys, Eds. Marder and Goldstein, TMS–AIME, Pennsylvania, USA, 293–326.

Coates, D. E., (1973) Diffusional Growth Limitation and Hardenability, *Metallurgical Transactions,* **4,** 2313–2325.

Court, S. and Pollard, J., (1987) *Welding Metallurgy of Structural Steels,* ed. J. Y. Koo, TMS–AIME, Pennsylvania, 335–349.

Dadian, M., (1986) Advances in the Science and Technology of Welding, Ed. S. A. David, ASM, Metals Park, OH 44073, 101–117.

Daigne, J., Guttman, M. and Naylor, J. P., (1982) *Materials Science and Engng.,* **56,** 1–10.

Dallum, C. B. and Olson, D. L., (1989) Stress and Grain Size Effects on Weld Metal Ferrite Formation, *American Welding Journal,* 198s–205s.

Dan, T. and Gunji, K., (1984) *Transactions Nat. Res. Inst. for Metals (Japan),* **26,** 8.

Davenport, E. S. and Bain, E. C., (1930) *TMS AIME,* **90,** 117–154.

Davies, G. J. and Garland, J. G., (1975) *Int. Metallurgical Rev.,* **20,** 83–106.

Deb, P., Challenger, K. D. and Therrien, A. E., (1987) Structure–property correlation of SA and GMA weldments in HY100 steel, *Metallurgical Transactions A,* **18A,** 987–999.

Dowling, J. H., Corbett, J. H. and Kerr, H. W., (1986) *Metallurgical Transactions A,* **17A,** 1611–1623.

Drury, B. G., (1984) *Welding and Metal Fabrication,* **53,** 250–252.

Dubé, C. A., Aaronson, H. I. and Mehl, R. F., (1958) *Rev. Met.,* **55,** 201.

Es-Souni, M. and Beaven, P. A., (1990) Microanalysis of inclusion/matrix interfaces in weld metals, IIW Doc. IIA–815–90.

Es-Souni, M., Beaven, P. A. and Evans, G. M., (1990) Microstructure and mechanical properties of Cu–bearing MMA C–Mn weld metal *Oerlikon Schweibmitteilungen,* **No. 123,** 15–31.

Evans, G. M., (1981) IIW Document IIA–529–81.

Evans, G. M., (1986) *Metal Construction,* **18,** 139.

Evans, G. M., (1988) IIW Doc.II–A–739–88.

Evans, G. M., (1990) IIW Document II–1146–90.

Farrar, R. A. and Harrison, P. L., (1987) Review: acicular ferrite in carbon–manganese weld metals, *J. Mat. Science,* **22,** 3812–3820.

Fleck, N. A., Grong, ϕ., Edwards, G. R. and Matlock, D. K., (1986) *Welding Research Supplement to the Welding Journal,* 113s–121s.

Franklin, A. G., (1982) *J. Iron & Steel Institute,* **207,** 181–186.

Fredriksson, H., (1976) *Scand. J. Metallurgical,* **5,** 27–32.

Fredriksson, H., (1983) Acta Universitatis Ouluensis, Series C, No.26, University of Oulu, Finland (Proc. of the 3rd Scandanavian Symposium on Materials Science) 1–25.

Glover, G., Oldland, R. B. and Voight, G., (1984) *High–Strength, Low–Alloy Steels,* eds. D. P. Dunne and T. Chandra, South Coast Printers, New South Wales, Australia, 271–275.

Gretoft, B., Bhadeshia, H. K. D. H. and Svensson, L.–E., (1986) *Acta Stereologica,* **5,** 365–371.

Goldak, J., Chakravarti, A. and Bibby, M., (1984) *Metallurgical Transactions B,* **15B,** 299–305.

Goldak, J., Bibby, M., Moore, J., House, R. and Patel, B., (1986) *Metallurgical Transactions B,* **17B,** 587–600.

Grong, O. and Matlock, D. K., (1986) *Int. Met. Rev.,* **31,** 27–48.

Grong, O., Kluken, A. O. and Bjornbakk, B., (1988) *Joining and Materials,* **1,** 164–169.

Gulyaev, A. P. and Guzovskaya, M. A., (1977) *Met. Sci. Heat Treat.,* **19,** 1020–1024.

Habu, R., (1978) *Transactions I. S. I. J.,* **18,** 492.

Hagiwara, Y. and Knott, J. F., (1980) *Advances in Fracture Research,* ed. D. Francois, Pergamon Press, Oxford, U. K. 707.

Hall, B., (1990) Ph.D. Thesis, University of Cambridge.

Harrison, P. L. and Farrar, R. A., (1981) *J. Mater. Science,* **16,** 2218–2226.

Harrison, P. and Farrar, R., (1987) *Metal Construction,* **19,** 392–446, 447–450.

Heckel, R. W. and Paxton, H. W., (1961) *Transactions ASM,* **53,** 539.

Hehemann, R. F., (1970) *Phase Transformations, ASM, Metals Park, Ohio, U. S. A.,* 397–432.

Hillert, M., (1952) *Jernkontorets Ann.,* **136,** 25–37.

Horii, Y., Ohkita, S., Wakabayashi, M. and Namura, M., (1986 and 1988) "Welding Materials for Low Temperature Service", and, "Study on the Toughness of Large Heat Input Weld Metal for Low Temperature Service TMCP Steel", *Nippon Steel Reports.*

Horii, Y. and Ohkita, S., (1992) *Welding International,* **6,** 761–765.

Huang, Z. and Yao, M., (1989) *Mateirals Science and Engineering A,* **A119,** 211–217.

Hultgren, A., (1951) *Jernkontorets Ann.,* **135,** 403.

Hyam, E. D. and Nutting, J., (1956) *Journal of the Iron and Steel Institute,* **184,** 148–165.

Ichikawa, K., Horii, Y., Funaki, S., Ohkita, S. and Yurioka, N., (1994a) *Quarterly Journal of the Japan Welding Society,* in press.

Ichikawa, K., Horii, Y., Motomatsu, R., Yamaguchi, M. and Yurioka, N., (1994b) *Quarterly Journal of the Japan Welding Society,* in press.

Ion, C., Easterling, K. E. and Ashby, M. F., (1984) *Acta Metallurgica,* **32,** 1949–1962.

Imagumbai, M., Chijiiwa, R., Aikawa, N., Nagumo, M., Homma, H., Matsuda, S. and Mimura, H., (1985) "HSLA Steels: Metallurgy and Applications", eds. J. M. Gray, T. Ko, Z. Shouhua, W. Baorong and X. Xishan, ASM International, Ohio, U. S. A., 557–566.

Ishikawa, T. and Haze, T., (1994) *Materials Science and Engineering A,* **A176,** 385–391.

Ito, Y. and Nakanishi, M., (1975) *International Institute of Welding Document XII–113–75.*

Ito, Y. and Nakanishi, M., (1976) *Sumitomo Search,* **15,** 42–62.

Iezawa, T., Inoue, T., Hirano, O., Okazawa, T. and Koseki, T., (1993) *Tetsu to Hagane,* **79,** 96–102.

Jingsheng, Y., Zongsen, Y. and Chengjian, W., (1988) *J. of Metals,* **40,** 26–31.

Josefsson, B. J. and Andren, H.–O., (1989) *Recent Trends in Welding Science and Technology,* eds. S. A. David and J. M. Vitek, ASM International, Ohio, U.S.A., 243–248.

Judson, P. and McKeown, D., (1982) *2nd Int. Conf. on Offshore Welded Structures,* London, The Welding Institute, Abington, Cambridge.

Kar R. J. and Todd, J. A., (1982) Discussion to Wada and Eldis, 1982.

Karlin, S. and Taylor, H. M., (1975) *A First Course in Stochastic Processes,* Academic Press, New York, U. S. A., 495–502.

Kawabata, F., Matzuyama, J., Nishiyama, N. and Tanaka, T., (1986) *Transactions I. S. I. J.,* **26,** 395–402.

Kayali, E. S., Corbett, J. M. and Kerr, H. W., (1983) *J. Materials Science Letters,* **2,** 123–128.

Kayali, E. S., Pacey, A. J. and Kerr, H. W., (1984) *Canadian Metallurgical Quarterly,* **23,** 227–236.

Keown, S. R., Smaill, J. S. and Erasmus, L. A., (1976) *Metals Technology,* **3** 194.

Klueh, R. L., (1974) *J. Nuclear Mats.,* **54,** 55–63.

Kluken, A. O. and Grong, ϕ., (1989) *Metallurgical Transactions A,* **20A,** 1335–1349.

Kluken, A. O., Grong, ϕ. and Rorvik, G., (1990) *Metallurgical Transactions A,* **21A,** 2047–2058.

Kluken, A. O., Grong, ϕ. and Hjelen, J., (1991) *Metallurgical Transactions A,* **20A,** 657–663.

Kluken, A. O. and Grong, ϕ, (1992) Temper embrittlement in steel weld metals containing titanium and boron *International Trends in Welding Science and Technology* eds. S. A. David and J. M. Vitek, ASM International, Metals Park, Ohio, U. S. A., 569–574.

Kluken, A. O., Siewert, T. A. and Smith, R., (1994) Effects of copper, nickel and boron on mechanical properties of low–alloy steel weld metals deposited at high heat input *American Welding Journal,* **73,** 193s–199s.

Kobayanshi, T., Kuwana, T. and Kiguchi, R., (1972) *J. Japan Welding Society,* **41,** 308.

Komizo, Y. and Fukada, Y., (1989) CTOD properties and MA constituent in the HAZ of C–Mn Microalloyed Steel, *The Sumitomo Search,* **No. 40,** 31–40.

Konkol, P. J., (1987) *Welding Metallurgy of Structural Steels,* ed. J. Y. Koo, T.M.S.–A.I.M.E., Warrendale, Pennsylvania, U.S.A., 367–380.

Koval'chuk, G. Z., Geichenko, V. N., Yarmosh, V. N. and Podobedova, L. V., (1979) *Met. Sci. Heat Treat.,* **21,** 114–117.

Krauss, G. and McMahon Jr., C. J., (1992) *Martensite,* eds. G. B. Olson and W. S. Owen, ASM International, Materials Park, Ohio, U.S.A., 295–322.

Krishnadev, M. R. and Ghosh, R., (1979) *Metallurgical Transactions A,* **10A,** 1941–1944.

Kubaschewski, O. and Evans, E. Ll., (1950) Metallurgical Thermochemistry, Pergamon Press, Oxford, U. K.

Lancaster, J. F., (1987) *Metallurgy of Welding,* 4th edition, Allen and Unwin, London.

Lange, F. H., (1967) *Correlation Techniques,* Iliffe Books Ltd., London, U. K. 76–77.

Lau, T. W., Sadowsky, M. M., North, T. H. and Weatherly, G. C., (1987) *Welding Metallurgy of Structural Steels,* ed. J. Y. Koo, T.M.S.–A.I.M.E., Warrendale, Pennsylvania, U.S.A., 349–365.

Lau, T. W., Sadowsky, M. M., North, T. H. and Weatherly, G. C., (1988) *Materials Science and Technology,* **4,** 52–61.

Lazor, R. B. and Kerr, H. W., (1980) Pipeline and Energy Plant Piping: Design and Technology, Pergamon Press, Toronto, Canada, 141–149.

Lee, J.–Y. and Pan, Y.–T, (1992a) Effect of silicon content on the microstructure and toughness of simulated heat affected zone in titanium killed steels, *Materials Science and Technology,* **8,** 236–244.

Lee, J.–Y. and Pan, Y.–T., (1992b) Effect of sulphur content on the microstructure and toughness of simulated HAZ in Ti–killed steels, *Submitted to Materials Science and Technology.*

Leslie, W. C., (1982) *Physical Metallurgy of Steels,* McGraw–Hill Kogakusha, Tokyo, Japan.

Lundin, C. D., Kelly, S. C., Menon, R. and Kruse, B. J., (1986) Welding Research Council Bulletin 315, New York, USA.

Mabuchi, H., Uemori, R. and Fujioka, M., (1996) *ISIJ International,* **36,** 1406–1412.

Mack, C., (1956) *Proc. Cambridge Phil. Soc.,* **52,** 246.

Magee, C. L., (1966) *Ph.D. Thesis,* Carnegie Mellon University, Pittsburgh, USA.

Matsuda, F., Li, Z., Bernasovsky, P., Ishihara, K. and Okada, H., (1990) An Investigation of the Behaviour of M–A constituent in Simulated HAZ of HSLA steels, IIW Document IX–B–1591–90.

Matsuda, S. and Okamura, N., (1978) *Transactions I. S. I. J.,* **18,** 198–205.

McGrath, J. T., Chandel, R. S., Orr, R. F. and Gianetto, J. A., (1989) *Canad. Metallurgical Quarterly,* **28,** 75–83.

McMahon Jr., C. J., Cianelli, A. K., Feng, H. C. and Ucisik, A. H., (1977) *Metallurgical Transactions A,* **8A,** 1059.

McMahon Jr., C. J. and Qu Zhe, (1983) *Metallurgical Transactions A,* **14A,** 1101.

McMahon Jr., C. J., (1987) *Innovations in ultrahigh–strength steel technology,* eds. G. B. Olson, M. Azrin and B. S. Wright, Sagamore Army Research Conference, Northwestern University, U.S.A., 597–618.

Mehrotra, V., Bibby, M., Goldak, J. and Moore, J., (1985) "Welding for Challenging Environments" Pergamon Press, Oxford.

Mills, A. R., Thewlis, G. and Whiteman, J. A., (1987) *Mat. Science and Technology,* **3,** 1051.

Mori, N., Homma, H., Okita, S. and Wakabayashi, M., (1981) Mechanism of Notch Toughness Improvement in Ti–B bearing Weld Metals, IIW Doc. IX–1196–81.

Mori, N., Homma, H., Wakabayashi, M. and Ohkita, S., (1982) Characteristics of Mechanical Properties of Ti–B bearing Weld Metals, IIW Doc. II–980–82, IX–1229–82.

Morrison, W. B. and Preston, R. R., () Proc. Int. Symp. on Niobium, edited by H. Stuart, TMS–AIME, Warrendale, PA, 939–966.

Murza, J. C. and McMahon Jr., C. J., (1980) *ASME Journal of Engineering Materials Technology,* **102** 369.

Myers, E. J., (1953) First Int. Cong. in Stereology, Vienna Medical Academy, **15/1, 15/7.**

Nakanishi, M., Komizo, Y., Seta, I, Nakamura, M. and Saitoh, Y., (1983) Development of High Toughness Steel Plates for Low Temperature Service by Dispersion with Nitride Particles and Oxide Particles, International Institute of Welding Document IX–1281–83.

Neville, D., (1985) Ph.D. Thesis, University of Cambridge, U. K.

Neville, D. and Knott, J. F., (1986) *J. Mechanics and Physics of Solids,* **34,** 243–291.

Nishioka, K. and Tamehiro, H., (September 1988) *Microalloying '88,* **ASM Int., Chicago.**

North, T. H., Mao, X. and Nakagawa, H., (November 1990) *International Conference "The Metallurgy, Welding and Qualification of Microalloyed (HSLA) Steel Weldments",* American Welding Society, eds. J. T. Hickey, D. G. Howden and M. D. Randall, 219–248.

Ochi, T., Takahashi, T. and Takada, H., (1988) 30th Mechanical Working and Steel Processing Conference, *Iron and Steel Society, Warrendale, USA.*

Oh, D. W., Olson, D. L. and Frost, R. H., (1991) *Journal of Engineering for Industry,* in press.

Okabe, R., Koshizuka, N., Tanaka, M. and San–Nomiya, Y., (1983) *Transactions I. S. I. J.,* **23,** B–390.

Oldland, R. B., (December 1985) *Australian Welding Research,* 31–43.

Otterberg, R., Sandrom, R. and Sandberg, A., (1980) *Metals Technology,* **7,** 397–408.

Owen, W. S., Whitmore, D. H., Cohen, M. and Averbach, B. L., (1957) *Welding Journal Research Supplement,* **November,** 503s–511s.

Pehlke, R. D. and Eliott, J. F., (1960) *Transactions A. I. M. E.,* **218,** 1088.

Ricks, R. A., Howell, P. R. and Barritte, G. S., (1982) *J. Materials Science,* **17,** 732–740.

Ringer, S. R., Barbaro, F., Krauklis, P. and Easterling, K. E., (1990) Coarsening Phenomena in the Microstructures of Titanium Microalloyed Steels, *Microstructure Control to Achieve Properties in Modern Steels,* Institute of Metals and Materials, Australasia.

Rudberg, E., (1952) *Jernkontorets Ann.,* **136,** 91.

Savage, W. F., Lundin, C. D. and Aaronson, A. H., (1965) *Weld. J.,* **44,** 175.

Savage, W. F. and Aaronson, A. H., (1966) *Weld. J.,* **45,** 85.

Schulz, B. J. and McMahon Jr., C. J., (1972) *Temper Embrittlement of Alloy Steels,* STP 499, American Society for Testing and Metals, 104.

Smith, E., (1983) *Welding and Metal Fabrication,* **51,** 210–204.

Sneider, G. and Kerr, H. W., (1984) *Canadian Metallurgical Quarterly,* **23,** 315–325.

Stenbacka, N., (1980) *Scandanavian Journal of Metallurgy,* **9,** 225–236.

Steven, W. and Balajiva, K., (1959) *J. Iron and Steel Institute,* **193,** 141.

Still, J. R. and Rogerson, J. H., (1978) *Metal Construction,* **10,** 339–342.

Still, J. R. and Rogerson, J. H., (1980) *Metal Construction,* **12,** 120–123.

Strangwood, M., (1987) Ph.D. Thesis, University of Cambridge.

Strangwood, M. and Bhadeshia, H. K. D. H., (1987a) *Advances in Welding Science and Technology, ed. S. A. David, ASM International, Ohio, U.S.A.,* 209–213.

Strangwood, M. and Bhadeshia, H. K. D. H., (1987b) Welding Metallurgy of Structural Steels, Ed. J. Y. Koo, AIME, Warrendale, 495–504.

Strangwood M. and Bhadeshia, H. K. D. H., (1988) Phase Transformations '87, Ed. G. W. Lorimer, Institute of Metals, London, 466–470.

Sugden, A. A. B. and Bhadeshia, H. K. D. H., (1988a) The Non–Uniform Distribution of Inclusions in Low–Alloy Steel Welds, *Metallurgical Transactions A,* **19A,** 669–674.

Sugden, A. A. B. and Bhadeshia, H. K. D. H., (1988b) A Model for the Prediction of Strength in Steel Welds, *Metallurgical Transactions A,* **19A,** 1597–1602.

Sugden, A. A. B. and Bhadeshia, H. K. D. H., (1989a) *J. Materials Science,* **25,** 613–618.

Sugden, A. A. B. and Bhadeshia, H. K. D. H., (1989b) *Recent Trends in Welding Science and Technology,* eds. S. A. David and J. M. Vitek, ASM International, Ohio, U. S. A., 745–748.

Sugden, A. A. B. and Bhadeshia, H. K. D. H., (1989c) Lower Acicular Ferrite *Metallurgical Transactions A,* **20A,** 1811–1818.

Surian, E., Trotti, J., Cassanelli, A. and de Vedia, L. A., (1994) Influence of Chromium on the Mechanical Properties and Microstructure of Weld Metal from a High–Strength SMA Electrode *Welding Journal,* **73,** 45s–53s.

Svensson, L.–E., (1986) The Effect of Alloy Chemistry on Vertical–up Arc Welds, Internal Report, ESAB AB.

Svensson, L.–E., Gretoft, B. and Bhadeshia, H. K. D. H., (1986) *Scandanavian J. of Metallurgy,* **15,** 97–103.

Svensson, L.–E. and Bhadeshia, H. K. D. H., (1988a) Improved Weldment Control using Computer Technology, Vienna, Austria, Pergamon Press, Oxford, 71–78.

Svensson, L.–E., Gretoft, B., Sugden, A. A. B. and Bhadeshia, H. K. D. H., (1988b) *Computer Technology in Welding II, Welding Institute, Abingdon, UK,* **paper 24.**

Takahashi, M. and Bhadeshia, H. K. D. H., (1990) *Materials Science and Technology,* **6** 592–603.

Takayama, S., Ogura, T., Fu, S. C. and McMahon Jr., C. J., (1980) *Metallurgical Transactions A,* **11A,** 1513.

Taylor, D. S., (1982) *Welding and Metal Fabrication,* **50,** 452–460.

Thewlis, G., (January 1989a) *Joining and Materials,* 25–31.

Thewlis, G., (March 1989b) *Joining and Materials,* 125–129.

Thewlis, G., (May 1990) Transformation kinetics of submerged arc weld metal, *British Steel Corporation Report IXJ 165 90,* 1–11.

Trivedi, R., (1970) *Metallurgical Transactions,* **1,** 921–927.

Trivedi, R. and Pound, G. M., (1969) *J. Appl. Phys.,* **38,** 3569–3576.

Tuliani, S. S., (1973) Ph.D. Thesis, University of Southampton.

Tweed, J. H. and Knott, J. F., (1983) *Metal Science,* **17,** 45–54.

Tweed, J. H. and Knott, J. F., (1987) *Acta Metallurgica,* **35,** 1401–1414.

Ueshima, Y., (1989) *Tetsu to Hagane,* **75** 501–508.

Umemoto, M., Furuhara, T. and Tamura, I., (1986) *Acta Metallurgica,* **34,** 2235–2245.

Underwood, E. E., (1970) Quantitative Stereology, Addison–Wesley, Reading MA.

Vander Vroot, G. F., (1984) *Metallography, Principles and Practice,* McGraw–Hill Book Company, London, 219–223.

Vandermeer, R. A., Vold, C. L. and King, W. E., Jr., (1989) Recent Trends in Welding Science and Technology, eds. S. A. David and J. M. Vitek, ASM International, Ohio, U. S. A., 223–228.

Vitek, J. M., Packan N. H. and David, S. A., (1986) Advances in the Science and Technology of Welding, Ed. S. A. David, ASM International, Ohio, U. S. A. 203–208.

Wada T. and Eldis, G. T., (1982) ASTM STP 7, American Soc. for Testing Materials, 343–362.

Wagner, C., (1952) *Thermodynamics of Alloys,* Addison Wesley, Cambridge, Massachusetts, 51.

Watson, M. N., (1980) Ph.D. Thesis, University of Southampton.

Wilson, A. D., Hamburg, E. G., Colvin, D. J., Thompson, S. W. and Krauss, G., (1988) Properties and Microstructures of Cu Precipitation Aged Plate Steels, *"Microalloyed HSLA Steels", ASM International, Metals Park, Ohio, USA,* 259–279.

Yamamoto, K., Matsuda, S., Haze, T., Chijiiwa, R. and Mimura, H., (1988) *Residuals and Unspecified Elements in Steel,* ASM International, Ohio, U.S.A..

Yang, J. R. and Bhadeshia, H. K. D. H., (1987a) *Advances in Welding Science and Technology, ed. S. A. David, ASM International, Ohio, U. S. A.,* 187–191.

Yang, J. R. and Bhadeshia, H. K. D. H., (1987b) Welding Metallurgy of Structural Steels, Ed. J. Y. Koo, AIME, Warrendale, 549–563.

Yang J. R. and Bhadeshia, H. K. D. H., (1989a) *Materials Science and Technology,* **5,** 93–97.

Yang, J. R. and Bhadeshia, H. K. D. H., (1989b) *Materials Science and Engineering A,* **A118,** 155–170.

Yang J. R. and Bhadeshia, H. K. D. H., (1990) The Dislocation Density of Acicular Ferrite in Steel Welds, *Welding Journal Research Supplement,* **69,** 305s–307s.

Yu, J. and McMahon Jr., C. J., (1980) *Metallurgical Transactions A,* **11A,** 291.

Yu–Qing, W. and McMahon Jr., C. J., (1986) *Supplement to Trans. Japan Inst. Metals,* **27,** 579.